

**APPLICATION OF THE UNIT STEP FUNCTION
TO TRANSIENT FLOW PROBLEMS WITH
TIME-DEPENDENT BOUNDARY CONDITIONS**

**A DISSERTATION
SUBMITTED TO THE DEPARTMENT OF PETROLEUM ENGINEERING
AND THE COMMITTEE ON GRADUATE STUDIES
OF STANFORD UNIVERSITY
IN PARTIAL FULFILLMENT OF THE REQUIREMENTS
FOR THE DEGREE OF
DOCTOR OF PHILOSOPHY**

By

Antonio Claudio de Franca Corrêa

February 1988

I certify that I have read this thesis and that in my opinion **it** is fully adequate, in scope and quality, as a dissertation for the degree of Doctor of Philosophy.

(Principal Adviser)

I certify that I have read this thesis and that in my opinion it is fully adequate, in scope and quality, **as** a dissertation for the degree of Doctor of Philosophy.

I certify **that** I have read this thesis and that in my opinion it is fully adequate, in scope and quality, **as** a dissertation **for** the degree of Doctor of Philosophy.

Approved for the University Committee
on Graduate Studies:

Dean of Graduate Studies

ABSTRACT

Determination of reservoir parameters by the analysis of wellbore pressure data obtained from variable rate tests requires the use of superposition. However, because implementation of superposition requires a flow model to be known a priori, then the results obtained ~~from~~ the analysis of test data may ~~be~~ affected by the model choice. This may be a serious drawback when information on reservoir flow geometry is sought from well tests. Furthermore, flow rate monitoring is not always performed, in which case the use of superposition may not be practical ~~or~~ even possible.

This work describes a general procedure ~~to~~ solve transient flow problems with boundary conditions which depend upon time. The method uses combinations of unit step functions to write a boundary condition which is valid for all times. Solution is then obtained by Laplace transformation. The procedure does not involve superposition.

The method ~~is~~ applied to solve two classical transient flow problems: pressure buildup following either constant-rate or constant-pressure production. Both wellbore storage and a skin effect are included, even though production for the latter problem is at constant pressure.

Solution to the drillstem test problem is discussed in detail. An original approach was used to model the drillstem test as a "slug test" with a step change in wellbore storage. During production, the effect of fluid accumulation inside the drill string ~~is~~ described by a changing liquid level wellbore storage coefficient. Upon shut-in, wellbore storage becomes compressibility dominated due to fluid compression below the shut-in point. The solutions are used to develop practical methods for analysis of drillstem test pressure data. Applications to field data will provide the initial reservoir pressure, the formation permeability and the skin effect. The methods are also extended to include multiple production and shut-in phases.

The procedure described here is not restricted to solution of the diffusivity equation. It may ~~be~~ applied to a variety of other interesting and useful problems. New transforms and operational rules to be used with the unit step function are also presented.

ACKNOWLEDGEMENTS

The author wishes to acknowledge **Dr.** Henry J. Ramey, Jr. for his support and guidance throughout **the course** of this work.

Sincere **thanks** are also due to **Dr.** Irwin Remson, **Dr.** William E. Brigham, **Dr.** Roland N. Home, and **Dr.** Younes Jalali for serving on **the** examination committee. **Thanks are** also extended to the rest of the Petroleum Engineering Department faculty for the valuable training they provided the author during **his stay** at Stanford.

Special **thanks** are due to the Brazilian people who through PETROBRAS (Petroleo Brasileiro SA) provided the financial support for **this** project.

To my parents
Darcy and Maria

To my wife
Roseana

To our children
Marcio, Claudio, Darcy, Flavio, and Barbara

Table of Contents

Abstract	iii
Acknowledgements	iv
Table of Contents	vi
List of Figures	ix
List of Tables	xI
1. Introduction	1
2. Pressure Transient Testing	4
3. Statement of the Drillstem Test Problem	8
3.1. Drillstem Test Description	8
3.2. Reservoir Problem	12
3.2.1. Reservoir Equation	12
3.2.2. Reservoir Initial Condition	13
3.2.3. Outer Boundary Condition	13
3.3. Wellbore Problem	14
3.3.1. Wellbore Initial Condition	14
3.3.2. Flowing Phase	15
3.3.3. Shut-in Phase	16
3.3.4. Coupling Conditions	17
3.4. Normalized Equations	18
4. Solution Method	21
4.1. Laplace Transformation	21

4.2. Operational Rules for the Unit Step Function	22
4.8. Application of the Unit Step Function Method	27
4.3.1. Pressure Buildup Following Constant-Rate Production	27
4.3.2. Pressure Buildup Following Constant-Pressure Production	31
5. Pressure Analysis of Drillstem Tests	36
5.1. Solution of the Drillstem Test Problem	36
5.1.1. Late-Time Approximation	39
5.1.2. Results	42
5.1.3. Damage Ratio	45
5.2. Solution of the General DST Problem	46
5.2.1. Change in Pipe Diameter	52
5.2.2. Second DST Cycle	54
5.3. Field Cases	55
5.3.1. High Productivity Well	56
5.3.2. Low Productivity Well	62
6. Discussion	68
6.1. Integrated Material Balance Method	68
6.2. DST with Constant-Pressure Flow	73
6.3. Homer Analysis	80
6.3.1. High Productivity Well	81
6.3.2. Low Productivity Well	85
6.4. Radius of Investigation	87
6.4. Homer Graphs for Slug Test Solutions	87
7. Conclusions and Recommendations	92

8. Nomenclature	93
9. References	96
Appendix A. Fundamental Solutions to the Diffusivity Equation	101
A.1 Specified Sandface Flow Rate	101
A.2 Constant-Rate Production with Skin and Wellbore Storage	105
A.3 "Slug Test" Solution	108
Appendix B. Computer Program	112

List of Figures

	<u>Page</u>
Figure 3.1 Schematic of a basic DST tool (After Earlougher (1977))	9
Figure 3.2 DST Pressure-Time Chart	10
Figure 4.1 Unit Step Function and its Complement	23
Figure 4.2.1 Graph of a piecewise continuous function.....	26
Figure 4.2.2 Segment of a piecewise continuous function.....	26
Figure 4.3.1 Use of the unit step function to provide a translation in time	32
Figure 4.3.2 $F(t)$ and the product of $F(t)$ and the unit step function	33
Figure 5.1 Influence of Skin on Pressure Buildup	43
Figure 5.2 Influence of Shut-in Storage Factor on Pressure Buildup	44
Figure 5.3 DST General Case	47
Figure 5.4 Pressure-Time Behavior for DST	48
Figure 5.5 Combination of Unit Step Functions	50
Figure 5.6 DST with Change in Pipe Diameter	53
Figure 5.7 DST Chart for Well A	57
Figure 5.8 Pressure Buildup Analysis for Well A	59
Figure 5.9 Flow Analysis for Well A	60
Figure 5.10 DST Chart for Well 7-APR-10-BA	63
Figure 5.11 Pressure Buildup Analysis for Well 7-APR-10-BA	65
Figure 6.1 Increasing Wellbore Storage Constant-Rate Solution	71
Figure 6.2 Decreasing Wellbore Storage Constant-Rate Solution	72
Figure 6.3 Influence of Production Time on Pressure Buildup	74
Figure 6.4 Influence of Wellbore Storage on Pressure Buildup	75
Figure 6.5 Influence of Skin Effect on Pressure Buildup	76
Figure 6.6 Normalized Pressure Drop in the Reservoir	79

Figure 6.7	Homer Graph for Well A with Actual Production Time	82
Figure 6.8	Homer Graph for Well A with Equivalent Production Time	84
Figure 6.9	Homer Graph for Well 7-APR-10-BA	86
Figure 6.10	Homer Graph for DST Model -Influence of Skin	88
Figure 6.11	Homer Graph for DST Model -Effect of Flowing Wellbore Storage	89
Figure 6.12	Homer Graph for DST Model -Influence of Production Time	90
Figure A.1	Constant-Rate Drawdown Type Curve	107
Figure A.2	"Slug Test" Type Curve	110

List of Tables

	<u>Page</u>
Table 3.1 Definitions of Dimensionless Variables	20
Table 4.1 Operational Rules for the Unit Step Function	28
Table 5.1 DST Data for Well A	58
Table 5.2 DST Data for Well 7-APR-10-BA	64
Table A.1 Laplace Transformed Solutions for Radial Flow	104

1. INTRODUCTION

Pressure transient testing in wells has been studied extensively during the past five decades. A number of methods based on solutions to the diffusivity equation have been proposed to analyze field data. Most methods are based upon constant-rate production. However, production rates are usually difficult to control. Flow rate monitoring is not always performed (or even possible), despite the fact that constant-rate test interpretations have become standard in the industry.

Analytical interpretation methods may be based upon the superposition of fundamental constant rate solutions to the diffusivity equation. A pressure buildup **is** one type of test which is most likely to result in a constant rate, in this case a zero rate. In many cases the production phase is better represented by a constant-pressure flow, and the use of superposition may not be practical. In general, the effect of a variable rate is more important **in** short time tests. A drillstem test (**DST**) is a typical example of a test where both the flow rate and the bottom-hole pressure are uncontrolled and variable. Interpretation of **DST** pressure-time data by methods based on the solution to the constant-rate case may produce uncertain results.

Practical use of well test analysis requires knowledge obtained from analysis of solutions to the diffusivity equation considering a wide range of boundary conditions. A well is often subject to physical conditions which may be best represented by a time-dependent boundary condition. If there is a change in the flow process in the wellbore, then a different boundary condition may be required to model the results of the test thereafter. Analytical solutions to these **types** of problems are usually difficult to obtain, and as a result such problems are often handled by finite difference methods.

An example of a time-dependent boundary condition is found in a pressure buildup test. If the well is produced at a constant rate, on shut in there is a change in the numerical value of the flow rate, but the boundary condition conserves its form. In **this** case the solution is simple and may be promptly obtained by superposition. However if the well is produced at constant

pressure, the conditions describing the sandface flow are considerably different for both the production and shut-in phases of the test. This is not a trivial problem.

A drillstem test represents another important problem in pressure transient testing. Analysis of pressure response obtained from a drillstem test provides important additional information for deciding whether it is economical to complete a well. Again, interpretation of DST pressure buildup data has classically been based on methods where the basic assumption is that the well has been produced at a constant rate. However, solution to the diffusivity equation for a constant rate production gives a declining flowing pressure with time, yet most DST's show an increasing flowing pressure during production. This apparent paradox suggests that application of the Homer (1951) method to analysis of DST pressure buildup data may lead to uncertain results.

An original approach was used to model the DST problem. A **DST** can be characterized as a changing wellbore storage problem following an instantaneous pressure drop at the well. During production, the wellbore storage coefficient is given by the rate of fluid accumulation inside the wellbore. On shut in, the wellbore storage mechanics change to a process of fluid compression below the bottom hole valve. **This** concept is useful to model both the flowing and pressure buildup phases with a single inner boundary condition.

According to the previous discussion, there is a need to develop a procedure to solve the diffusivity equation with time-dependent boundary conditions. Such procedure could be applicable to important problems in well testing.

This work describes a general procedure for solution of transient flow problems with time-dependent boundary conditions. The method uses the unit step function, or combinations of unit step functions, to write a boundary condition which is valid for all times. Applications to pressure buildup produce analytical solutions correct for both the flowing and shut-in periods. These solutions are obtained by solving the diffusivity equation with a single inner boundary condition which includes the mixed conditions for flow and buildup. Both a skin effect and wellbore storage may be considered. The solution is obtained by Laplace

transformation. The method can be used to solve a variety of other significant problems. Thus, another purpose is to present new transforms and operational rules useful for other problems.

This work is organized in sections with the object of describing a comprehensive approach to solutions of transient testing problems. Section 2 discusses briefly the history of well test analysis. Section 3 presents a description of the drillstem test. It also describes the formulation of the governing partial differential equations and appropriate boundary conditions for the drillstem test problem. A general method of solution to transient flow problems with time dependent boundary conditions is described in Section 4. The method is applied to solution of two classical problems; pressure buildup following either constant-rate or constant-pressure production.

Section 5 presents a solution to the drillstem test problem. The solution is used to develop interpretation methods for drillstem test pressure data. Solutions for drillstem tests with multiple cycles **of** production and shut-in are also presented. Two field cases are discussed in detail. Section 6 discusses the implications of the theory developed in this study with respect to previous analysis methods of drillstem test pressure data.

Conclusions and recommendations are presented in Section 7. A review of useful solutions to the diffusivity equation is presented in Appendix A. Finally, Appendix B presents the computer program used to calculate pressure buildup curves for drillstem tests.

2. PRESSURE TRANSIENT TESTING

The literature on pressure transient testing is extensive. Because the diffusivity equation also describes the process of conduction of heat in solids, there have been similar advances in both well testing and heat conduction theory. Interest in solutions to the difisivity equation has also been shared with hydrologists in the study of groundwater flow, and important advances have also been made in that field of technology.

Pressure buildup testing has been the most widely used method to evaluate oil and gas wells. Historically, equations for pressure buildup analysis have been obtained through the application **of** superposition or Duhamel's theorem.

Measurements of stabilized pressure in closed-in wells have been described since the early **1920's**. Moore, Schilthuis and Hurst (**1933**) suggested that the rise in the bottom-hole pressure in closed-in wells could be used to determine formation permeability. The authors described an oil well test in which annulus liquid levels were measured sonically to permit calculation of the sandface flow rate. It appears that the authors presented the first clear description of the mechanics of well bore storage.... a changing sandface flow rate.

Muskat (**1937**) presented an equation to describe pressure buildup in wells. He suggested a trial and error graphical procedure to determine both formation permeability and reservoir pressure **from** pressure buildup data.

Theis (**1935**) suggested a graphical method to determine aquifer transmissivity from field measurements of recovery in water wells.

The problem of constant rate production including wellbore storage was first presented in the petroleum engineering industry by van Everdingen and Hurst (**1949**). They used the Laplace transform method described in Carslaw and Jaeger (**1941**) to obtain a general solution in terms of a Mellin integral. They evaluated the integral and presented the results in graphical form. A long time approximation for the wellbore pressure was also described. Later, van Everdingen (**1953**) and Hurst (**1953**) extended this solution to include a skin effect. It is some-

times overlooked that van Everdingen and Hurst (1949) presented the zero skin type curve in their classic study.

Horner (1951) applied superposition to the constant terminal rate solution to obtain a pressure buildup equation similar to the one described by Theis (1935). Horner (1951) used this solution to propose a method to estimate both the formation permeability and the static reservoir pressure from pressure buildup data. He also studied the effect of closed reservoirs on pressure buildup in wells. He did not include the effect of wellbore storage in his theoretical model.

Apparently the first study of constant-pressure production followed by shut-in was presented by Jacob and Lohman (1952). An analytical solution to the problem of radial heat conduction with constant temperature at the inner boundary had already been presented by Jaeger (1942). He also presented an asymptotic expansion for the surface heat flux for large values of time. Later, Jaeger (1955) used that solution to evaluate the transient radial temperature distribution. The author also computed the temperature change on the internal cylindrical surface after shutting off the supply of heat required to maintain a constant internal temperature. This problem is analogous to pressure buildup following constant pressure production, including wellbore storage effects. In another study, Jaeger (1956) presented the solution to a heat conduction problem which is analogous to the constant-rate skin and wellbore storage problem. The author also considered a problem which was later identified to be equivalent to the flow period of a drillstem test,

The drillstem test has been used as a primary tool for formation evaluation since its introduction in the petroleum industry in 1926. According to Olson (1967), in the early stages of its development a DST was mainly used to identify reservoir fluids. It was not until the early 1950's that drillstem tests were properly designed to obtain reliable pressure buildup data. Saldana-Cortez (1983) presents a comprehensive literature review on drillstem tests.

The flowing phase of a drillstem test is conceptually similar to a "slug test" in water well testing practise, which was introduced by Ferris and Knowles (1954) as a means of

determining aquifer transmissivity. The authors presented their solution based on the instantaneous point source described in Carslaw and Jaeger (1947). They used the asymptotic nature of the solution to propose a graphical method to estimate aquifer transmissivity from long time data. The Fems and Knowles (1954) solution did not match both short and intermediate time responses of observed "slug test" data adequately.

Jaeger (1956) presented a rigorous solution to an analogous heat conduction problem. He showed the difference between solutions for either positive or zero skin effect. Jaeger also presented short and late time approximations for the equivalent "slug test" problem. Cooper *et al* (1967) applied Jaeger's (1956) solution to develop a "slug test" type curve for estimating aquifer transmissivity. The authors did not consider a skin effect, however.

Dolan *et al* (1957) discussed the application of the Horner equation to pressure buildup in drillstem tests. They concluded that in the case of a gradual change in the flow rate, the average flow rate should be used to compute the formation permeability. From their results, it was apparent that the correct Homer straight line would not develop for practical values of shut-in time.

Matthews and Russell (1967) compiled and organized the information on pressure transient testing. Their monograph included a chapter on drillstem tests.

Agarwal *et al* (1970) presented a review of literature on heat conduction problems which included wellbore storage effects. They computed Jaeger's (1956) integral for the constant rate solution and presented the results as families of **type** curves. Ramey (1970) used those curves to describe the use of type curve matching in analysis of short term tests.

Agarwal and Ramey (1972) showed that the wellbore pressure solution for the flowing phase of a drillstem test is proportional to the time derivative of the wellbore pressure solution for constant rate production with skin and wellbore storage effects. The authors also described an approximate solution for the problem of constant rate production with **an** abrupt change in wellbore storage. Earlougher *et al* (1973) discussed the effects of changing wellbore storage on injection well testing.

Ramey *et al* (1975) computed and correlated the "slug test" solution given by Jaeger (1956). The authors presented their results in terms of type curves which include both wellbore storage and skin effect combined into a correlating parameter.

Earlougher (1977) presented a monograph on advances in well test analysis which included a chapter on drillstem testing.

Ehlig-Economides and Ramey (1979) used the superposition integral to compute the shut-in pressure after production at constant pressure. They concluded that the correct Horner straight line could be obtained by using an equivalent production time based on material balance. They also concluded that the flow rate at the time just prior to shut-in should be used to compute the reservoir permeability.

Uraiet and Raghavan (1979) solved the same problem using a **finite** difference technique. They concluded that the Homer time ratio should be computed with the correct production time, and the average production rate should be used to determine reservoir permeability.

Soliman (1981) used the unit step function to represent the inner boundary condition for pressure buildup following constant-rate production. He also derived an expression for the shut-in pressure after a very short production period.

There are other pertinent and important references on pressure transient testing. During the past **ten** years the Stehfest (1970) algorithm has been widely used to compute pressure transient solutions from the inversion of Laplace transform solutions. With the advances in digital computing power, it is now possible to compute solutions for very complex models. Also, automated interpretation of well test data using non-linear regression techniques is now practical. Recent developments in measurement of bottom hole rates enable the use of deconvolution methods in analysis of well test data. However, analytical solution methods will still play an important role in the future trend of well test analysis.

3. STATEMENT OF THE DRILLSTEM TEST PROBLEM

A description of the drillstem test is presented in this section. The physical processes and fluid flow mechanisms taking place both in the reservoir and in the wellbore are discussed in order to establish a mathematical model for the drillstem test problem. The partial differential equation describing radial flow in the reservoir **and** appropriate boundary conditions for the drillstem test problem are presented. Wellbore storage mechanics are discussed for both the production and shut-in phases of a drillstem test.

3.1. DRILLSTEM TEST DESCRIPTION

Basically a drillstem test may be considered to be a temporary completion of a well. A **DST** tool, which is connected to the lower end of the drill string, is run into a mud-filled borehole in order to isolate the interval of interest from the surrounding zones. A sequence of production and shut-in phases is then performed.

The basic equipment comprising a modern **DST** tool, from bottom to top, are;

- 1) pressure gauges
- 2) perforated pipes
- 3) by-pass valve
- 4) tester valve
- 5) drill string

A schematic of the operation of a basic **DST** tool for the several phases of a test is presented in Fig. 3.1. Bottom hole charts connected to the pressure gauges record the pressure history of the test. A typical pressure-time chart is presented in Fig. 3.2.

The following discussion refers to the fluid mechanics in and around the tool as displayed in Fig. 3.1 and to the **DST** chart presented in Fig. 3.2. The base line (line A-H) in Fig. 3.2 is drawn before the pressure gauge is assembled into the drill string, and it shows a record of the

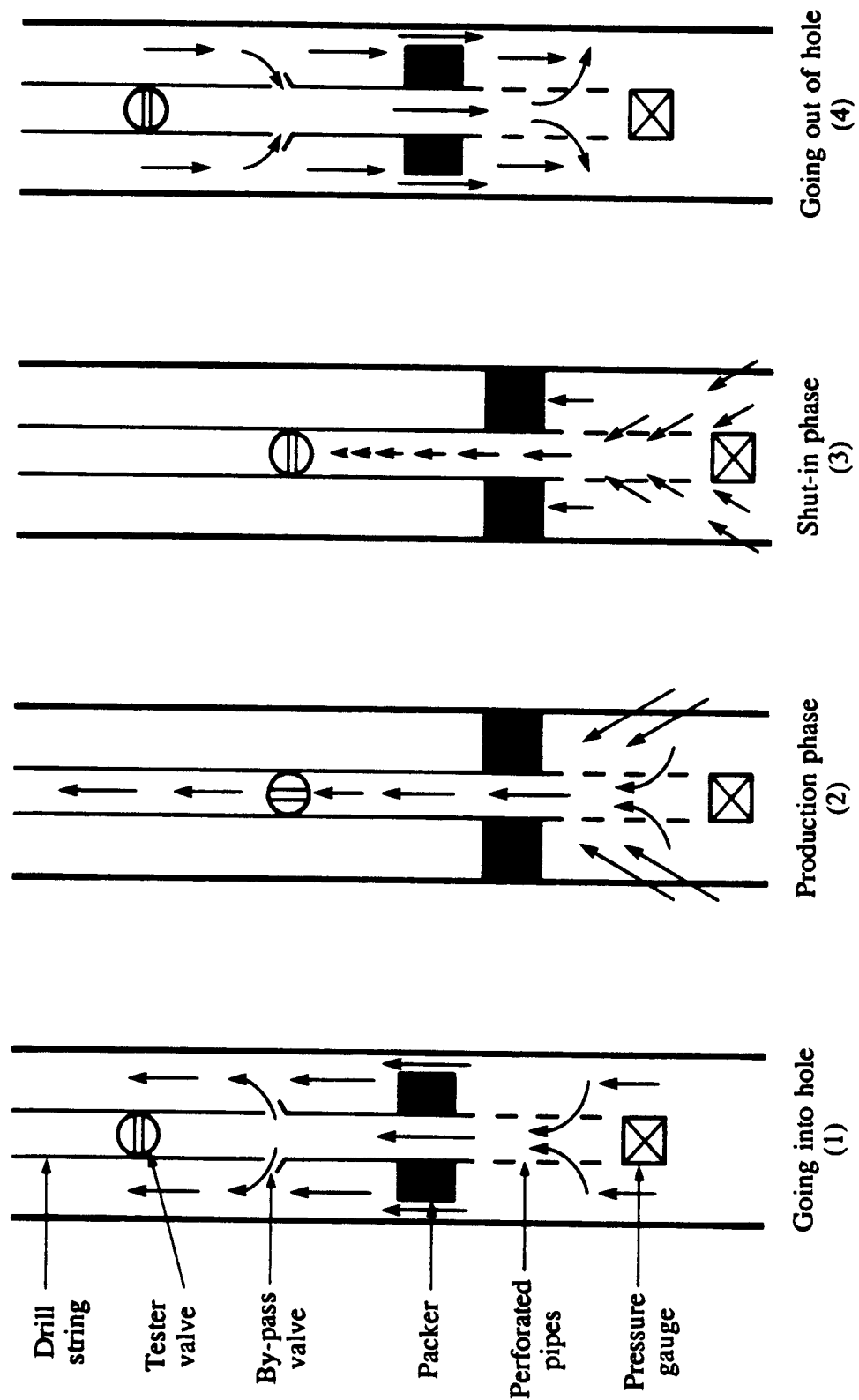


Figure 3.1 Schematic of a basic DST tool (After Earlougher, 1977)

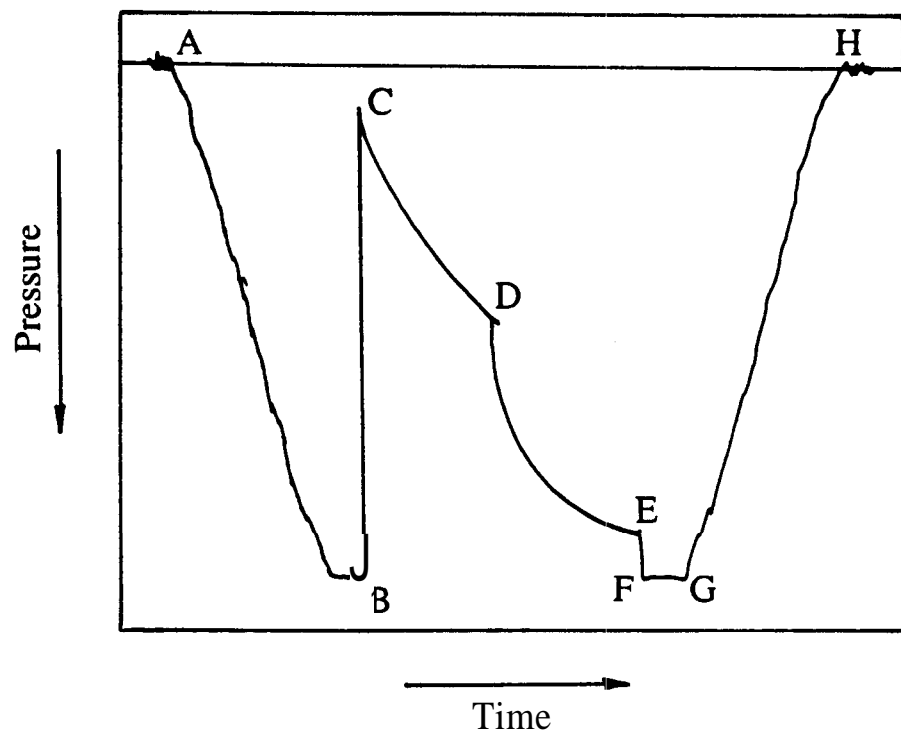


Figure 3.2. DST pressure-time chart

atmospheric pressure at the well location. During the trip down the borehole (line A-B in Fig. 3.2), the pressure gauge records the increase in the hydrostatic mud pressure. The opened by-pass valve (Fig. 3.1-1) avoids pressure surges into the formation.

As the DST tool reaches the testing depth, the pressure gauge records the hydrostatic mud pressure (point B, Fig. 3.2), while the wellhead flow equipment is being assembled. The packer is then set, the by-pass valve is closed, and a complete isolation of the testing interval is obtained. Compression of the DST tool after setting the packer activates a hydraulically operated time-delay mechanism which controls the opening of the tester valve.

By the time the tester valve is opened, a sudden pressure drawdown is imposed on the formation (line B-C in Fig. 3.2), because the pressure immediately above the tester valve is either atmospheric or controlled by any liquid or gas cushion used in the test. During the following production phase, formation fluids flow into the drill string (Fig. 2.1-2). The fluid accumulation inside the drill string causes an increasing back pressure on the formation (line C-D in Fig. 3.2), which is typical of liquid production wells.

At point D (Fig. 3.2) the tester valve is closed (Fig. 3.1-3), and line D-E (Fig. 3.2) reflects the pressure buildup taking place at the sandface. During this phase, the fluid in the storage chamber between the packer and the bottom of the hole is continuously compressed, as the reservoir fluid approaches a new equilibrium state represented by the static reservoir pressure.

At the end of the pressure buildup phase, the packer is released (Fig. 3.1-4 and line E-F in Fig. 3.2), and the final hydrostatic mud pressure is recorded (line F-G in Fig. 3.2). Finally, the DST tool is pulled out of the hole (line G-H in Fig. 3.2) and the test is completed,

Pressure-time data obtained from drillstem tests are used with methods of interpretation to provide estimates of reservoir parameters and well condition.

RESERVOIR PROBLEM

In order to use DST pressure data for determining reservoir properties, a mathematical model is required to describe the physical processes occurring during the test. Fluid production and wellbore pressure response reflect the characteristics **of** the reservoir. Reservoir pressure is considered to **be** a function of position and time. Fluid flow in the reservoir may be described by a partial differential equation, and we seek a solution satisfying the conditions of a drillstem test.

3.2.1. Reservoir Equation

Flow **of** fluids through porous media may be modeled by the diffusivity equation, which is derived from the principle **of** mass conservation and Darcy's law, with an appropriate equation of state for the fluid. See Matthews and Russell (1967) for a more detailed derivation of this governing equation. Because the drillstem test may be viewed as a short term test, and due to the cylindrical geometry of the well, the flow in the reservoir may be described by the radial form of the diffusivity equation, which is:

$$\frac{\partial^2 p}{\partial r^2} + \frac{1}{r} \frac{\partial p}{\partial r} = \frac{\phi \mu c_t}{k} \frac{\partial p}{\partial t}, \quad (3.1)$$

where:

- r = radial distance from the center of the well, [L],
- t = elapsed time, [T],
- $p(r, t)$ = reservoir pressure, $[M] [L]^{-1} [T]^{-2}$,
- ϕ = reservoir porosity, fraction **of** bulk volume,
- c_t = total compressibility of the system, $[M]^{-1} [L] [T]^2$,
- μ = fluid viscosity at reservoir conditions, $[M] [L]^{-1} [T]^2$,
- k = reservoir permeability, $[L]^2$.

In the derivation of the diffusivity equation, the following assumptions were made:

- (1) radial horizontal flow,
- (2) isotropic and homogeneous porous medium,
- (3) single phase flow,
- (4) constant fluid viscosity,
- (5) constant fluid compressibility,
- (6) small enough pressure gradients everywhere in the reservoir such that the pressure gradient squared term in the rigorous equation can be neglected.

3.2.2. Reservoir Initial Condition

The reservoir **is** assumed to have a homogeneous pressure distribution before the start of the test. **The** initial reservoir condition may be represented by:

$$p(r, 0) = p_i, \quad r > r_w, \quad (3.2)$$

where:

p_i = initial reservoir pressure, $[M] [L]^{-1} [T]^{-2}$,

r_w = wellbore radius, $[L]$.

This condition may be obtained if the testing interval is properly isolated from the surrounding zones. Furthermore this condition assumes no "super-charge" forces in the reservoir. "Super-charge" is caused by a pressure gradient near the wellbore resulting from the invasion of the porous zone to be tested by water loss from the drilling fluid. "Super-charge" effects may be eliminated if the radius of investigation during the flowing phase of the test is greater than the invaded zone. This usually can be achieved with a relatively short flow period.

3.2.3. Outer Boundary Condition

Due to the short term nature of a drillstem test, the wellbore pressure response is not likely to be affected by the external reservoir boundaries during the test period. Therefore, the outer boundary condition for the drill stem test problem may be represented by assuming a reservoir of infinite extent in the radial direction, which is given by:

$$\lim_{r \rightarrow \infty} p(r, t) = p_i . \quad (3.3)$$

For the case of a well located either close to a reservoir boundary or in a highly transmissive formation, boundary effects may play an important role in the late: time wellbore pressure response. These cases will not be considered in this work, however.

3.3. WELLBORE PROBLEM

As the reservoir energy drives formation fluids towards the surface, fluid flow in the drill string must be considered in order to establish the equation for the wellbore pressure. The general wellbore problem should include both frictional and inertial effects due to possible multiphase flow in the drill pipe. However, if the production rate is small as in the case of low productivity wells, the wellbore problem may be simplified to the equation for a material balance on the produced fluids.

3.3.1. Wellbore Initial Condition

Fluid production in a DST begins by imposing an instantaneous pressure drawdown at the sandface due to opening of a bottom hole valve. It may be described by the following wellbore initial condition:

$$p_w(0_+) = p_0 , \quad (3.4)$$

where:

$p_w(t)$ = wellbore pressure, $[M] [L]^{-1} [T]^{-2}$,

p_0 = initial flowing pressure, $[M] [L]^{-1} [T]^{-2}$.

Drillstem tests may be run with a liquid cushion inside the drill string. In this case, the initial flowing pressure p_0 is given by the product of the height and the average density of the liquid cushion, plus any existing gas pressure at the top of the liquid column.

Another point to be considered is that the wellbore initial condition is based on the idea that the tester valve is opened instantaneously. Because these valves are mechanical devices, they usually require a finite time to be fully opened. However, this effect should only be important for very short flow periods, and thus they would affect short-time pressure data analysis only for highly productive wells.

3.3.2 Flowing Phase

In liquid-producing wells, the flow period of a DST is characterized by a continuous accumulation of reservoir fluids inside the drill string. As production time increases, the bottom hole wellbore pressure increases due to the increasing liquid level of produced fluids. Because the flow period is usually short and no liquid is produced at the surface, the rate of fluid accumulation in the wellbore must equal the sandface flow rate. Thus, a material balance for the produced fluid yields:

$$q_w(t) - C_F \frac{dp_w}{dt} = 0, \quad 0 < t < t_p, \quad (3.5)$$

where:

$$C_F = \frac{\pi r_p^2}{\rho g B}, \quad (3.6)$$

and:

B = formation volume factor, dimensionless,

g = gravity acceleration constant, $[L] [T]^{-2}$,

$p_w(t)$ = bottom-hole wellbore pressure, $[M] [L]^{-1} [T]^{-2}$,

$q_w(t)$ = instantaneous flow rate at sandface, $[L]^3 [T]^{-1}$.

r_p = internal radius of the drill string, $[L]^2$,

$$\begin{aligned}\rho &= \text{average density of the liquid in the wellbore, } [\text{M}] [\text{L}]^{-3}, \\ C_F &= \text{flowing-phase wellbore storage factor, } [\text{M}]^{-1} [\text{L}]^4 [\text{T}]^2, \\ t_p &= \text{production time, } [\text{T}].\end{aligned}$$

The **DST** flow period condition is similar to the "slug test" condition, where a change in pressure may be obtained by instantaneously removing a column of water from a well with an initial hydrostatic level. Because the amount of liquid initially in the borehole is maximized in a "slug test", inertial effects are important and oscillations in the fluid level may occur. An oilfield **DST** with a gas cushion tends to minimize inertial effects in the wellbore. However, because of the mass of liquid in the formation, inertial effects may affect fluid flow in the reservoir. **This** problem has not yet been studied , and it may be important when testing high rate inflow wells,

3.3.3. Shut-in Phase

After a well is closed by means of a bottom-hole valve, the reservoir fluid reaching the wellbore during the pressure recovery phase is compressed below the shut-in point. **This** may be described by:

$$q_w(t) - C_S \frac{dp_w}{dt} = 0, \quad t > t_p, \quad (3.7)$$

where:

$$C_S = c_w V_w, \quad (3.8)$$

and:

$$\begin{aligned}V_w &= \text{wellbore volume below the shut-in point, } [\text{L}]^3, \\ c_w &= \text{compressibility of the fluid in the wellbore, } [\text{M}]^{-1} [\text{L}] [\text{T}]^2, \\ C_S &= \text{shut-in phase wellbore storage factor, } [\text{M}]^{-1} [\text{L}]^4 [\text{T}]^2.\end{aligned}$$

Similarities between Eq. (3.5) and Eq. (3.7) suggest that the **DST** problem may be viewed as a "slug test" with a changing wellbore storage coefficient. During the production

phase, the wellbore storage mechanism is controlled by a changing liquid level, and after the shut-in of the well, wellbore storage becomes compressibility dominated. The compressibility-dominated wellbore storage coefficient may be orders of magnitude smaller than the changing liquid level wellbore storage factor. This may be observed by a sharp change in a DST pressure-time curve after the shut-in time.

3.3.4. Coupling Conditions

So far the reservoir and wellbore pressures have been treated independently. However the two pressures may be coupled by a condition which considers a skin effect at the wellbore and by the definition of the sandface flow rate.

The instantaneous flow rate at the sandface is given by Darcy's law. For the case of radial flow, it is given by:

$$q_w(t) = \frac{2\pi k h}{\mu} \left[r \frac{\partial p}{\partial r} \right]_{r=r_w}, \quad (3.9)$$

where:

h = formation thickness, [L].

As described by van Everdingen (1953) and Hurst (1953), the assumption of an infinitesimal skin around the sandface leads to the following condition:

$$p_w(t) = p(r_w, t) - q_w(t) S, \quad S > 0, \quad (3.10)$$

where:

S = skin effect.

The case of a negative skin effect may be handled by the effective wellbore radius concept as defined in Matthews and Russell (1967), which yields:

$$p_w(t) = p(r'_w, t), \quad S \leq 0, \quad (3.11)$$

and the effective wellbore radius r'_w is defined as:

$$r_w' = r_w e^{-S} . \quad (3.12)$$

In practice, Eqs. (3.10) and (3.11) are applicable for cases where the extent of either a damaged or stimulated region around the wellbore is of the order of a few wellbore radii. If the extent of the altered region is large, the coupling condition should be modified to consider both the radius of the altered zone and its transmissivity, using the composite reservoir concept.

3.4. NORMALIZED EQUATIONS

For the sake of simplicity, the equations describing the drillstem test problem can be normalized by introducing the dimensionless variables defined in Table 3.1. The DST problem is then summarized by the following equations:

Reservoir Equation:

$$\frac{\partial^2 p_D}{\partial r_D^2} + \frac{1}{r_D} \frac{\partial p_D}{\partial r_D} = \frac{\partial p_D}{\partial t_D} , \quad (3.13)$$

Reservoir Initial Condition:

$$p_D(r_D, 0) = 0 , \quad (3.14)$$

Reservoir Outer Boundary Condition:

$$\lim_{r_D \rightarrow \infty} p_D(r_D, t_D) = 0 , \quad (3.15)$$

Wellbore Initial Condition:

$$p_{wD}(0_+) = 1 , \quad (3.16)$$

Wellbore Flowing Equation:

$$q_{wD}(t_D) + C_{FD} \frac{dp_{wD}}{dt_D} = 0 , \quad 0 < t_D < t_{pD} , \quad (3.17)$$

Wellbore Shut-in Equation:

$$q_{wD}(t_D) + C_{SD} \frac{dp_{wD}}{dt_D} = 0, \quad t_D > t_{pD}, \quad (3.18)$$

Sandface Flow Rate:

$$q_{wD}(t_D) = - \left[r_D \frac{\partial p_D}{\partial t_D} \right]_{r_D=1}, \quad (3.19)$$

Skin Effect:

$$p_{wD}(t_D) = p_D(1, t_D) + S q_{wD}(t_D), \quad S > 0, \quad (3.20)$$

$$p_{wD}(t_D) = p_D(e^{-S}, t_D), \quad S \leq 0. \quad (3.21)$$

time	$t_D = \frac{k t}{\phi \mu c_t r_w^2}$
radius	$r_D = \frac{r}{r_w}$
reservoir pressure	$p_D(r_D, t_D) = \frac{p_i - p(r, t)}{p_i - p_0}$
wellbore pressure	$p_{wD}(t_D) = \frac{p_i - p_w(t)}{p_i - p_0}$
sandface flow rate	$q_{wD}(t_D) = \frac{q_w(t) \mu}{2 \pi \phi h c_t (p_i - p_0)}$
cumulative recovery	$Q_{wD}(t_D) = \frac{Q_w(t) \mu}{2 \pi \phi h c_t (p_i - p_0)}$
wellbore storage factor	$C_D = \frac{C}{2 \pi \phi h c_t r_w^2}$

TABLE 3.1 - Definitions of Dimensionless Variables

4. SOLUTION METHOD

This section describes the use of the Laplace transform and the unit step function to solve transient fluid flow problems with time-dependent boundary conditions. Operational rules for the unit step function are also derived. The proposed solution method has been applied to solve the problems of pressure buildup following either constant-rate or constant-pressure production.

4.1. LAPLACE TRANSFORMATION

The method of Laplace transformation has been used extensively to solve transient fluid flow problems. The Laplace transform of a function $g(t)$ is defined as:

$$L[g(t)] = \bar{g}(s) = \int_0^{\infty} e^{-st} g(t) dt , \quad (4.1)$$

where:

- s = complex Laplace transform variable, $[T]^{-1}$,
- $g(t)$ = original function to be transformed,
- $\bar{g}(s)$ = Laplace-transformed function,
- $L[]$ = Laplace transform operator notation.

Laplace transformation is useful in solving transient problems described by linear differential equations. When the transformation is applied to an ordinary differential equation it reduces the original problem to an algebraic problem. A partial differential equation can be reduced to an ordinary differential equation in Laplace space. Once the transformed problem is solved, in many cases the real time solution may be found directly from tables of Laplace transforms. A summary of some useful operational rules and a table of Laplace transforms are presented by Churchill (1944).

If the inverse Laplace transform can not be found directly, it may be determined by the

use of the inversion formula, which is given by the Mellin inversion integral:

$$g(t) = \frac{1}{2\pi i} \int_{a-i\infty}^{a+i\infty} e^{st} \bar{g}(s) ds , \quad (4.2)$$

where:

i = complex number, $\sqrt{-1}$,

a = real number lying to the right of the singularities of $\bar{g}(s)$.

The use of the inversion formula may sometimes lead to solution forms which are difficult to compute. However, several methods have been developed to invert the Laplace transform numerically. Among them, the Stehfest (1970) algorithm has proven to be efficient in the computation of inverse Laplace transforms obtained from well test problems.

The Laplace transform method is also useful in determining both early and late time limiting analytical forms of solutions to transient flow problems. For late time, the transformed solution is evaluated as the transform variable, s , approaches zero. For early time, the transform is evaluated as $s \rightarrow \infty$.

42. OPERATIONAL RULES FOR THE UNIT STEP FUNCTION

The unit step function is defined by Churchill (1944), as:

$$\begin{aligned} S_k(t) &= 0 , \quad 0 < t < k , \\ &= 1 , \quad t > k , \end{aligned} \quad (4.3)$$

and its Laplace transform is:

$$L[S_k(t)] = \frac{e^{-ks}}{s} . \quad (4.4)$$

The unit step function and its complement are presented graphically in Figure 4.1. This function is useful in expressing boundary conditions which depend upon time. Often this procedure leads to forms requiring the transform of a product of the step function and some other function of time, i.e., $S_k f(t)$.

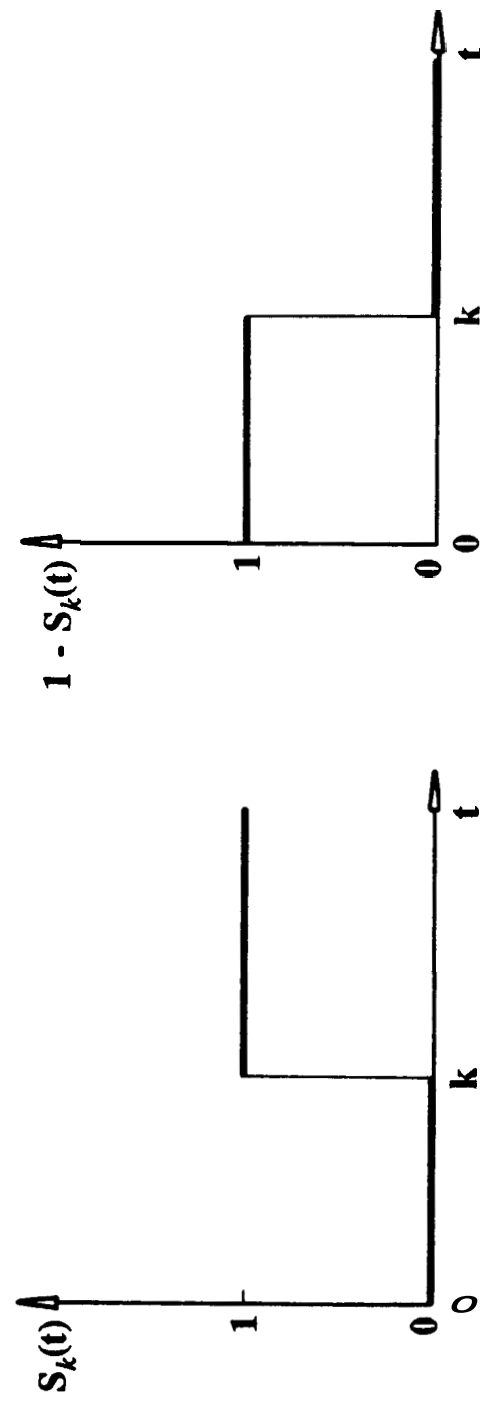


Figure 4.1 Unit Step Function and its Complement

Due to the nature of the unit step function, the Laplace transform of $S_k f(t)$ is given by:

$$L[S_k f(t)] = \int_k^\infty e^{-st} f(t) dt , \quad (4.5)$$

Note in Eq. (4.5) that the lower limit of integration is k rather than zero, since S_k is zero for $0 < t < k$. Equation (4.5) can also be expressed as an ordinary Laplace transform integral from 0 to ∞ as follows:

$$L[S_k f(t)] = \bar{f}(s) - \int_0^k e^{-st} f(t) dt . \quad (4.6)$$

Also, according to the uniqueness of the Laplace transform, the following inversion formula can be obtained from Eq. (4.6):

$$L^{-1} \left[\int_0^k e^{-st} f(t) dt \right] = (1 - S_k) f(t) . \quad (4.7)$$

The Laplace transform of the product of the unit step function and the time derivative of $f(t)$ is:

$$L[S_k f'(t)] = \int_k^\infty e^{-st} f'(t) dt , \quad (4.8)$$

or, following the logic leading to Eq. (4.6):

$$L[S_k f'(t)] = \int_0^\infty e^{-st} f'(t) dt - \int_0^k e^{-st} f'(t) dt , \quad (4.9)$$

which may be integrated by parts to yield:

$$L[S_k f'(t)] = s \bar{f}(s) - f(k_-) e^{-ks} - s \int_0^k e^{-st} f'(t) dt . \quad (4.10)$$

Because the function $f(t)$ may be discontinuous at $t = k$, the notation $f(k_-)$ in Eq. (4.10) refers to the limit of $f(t)$ as t approaches k from the left. Similarly, $f(k_+)$ represents the limit as t approaches k from the right. From Eq. (4.7) and Eq. (4.10):

$$L[S_k f'(t)] = s L[S_k f(t)] - f(k) e^{-ks} . \quad (4.11)$$

Another application of the unit step function is to find the Laplace transform of time-derivatives of sectionally continuous functions. Let $f(t)$ be a sectionally continuous function as presented in Figure 4.2.1, with discontinuities at t_1, t_2, \dots, t_n . This may be represented as:

$$\begin{aligned} f(t) &= f_0(t) , \quad 0 < t < t_1 , \\ &= f_1(t) , \quad t_1 < t < t_2 , \\ &\quad \vdots \\ &= f_n(t) , \quad t > t_n , \end{aligned} \quad (4.12)$$

where $f_k(t)$ are piecewise continuous functions defined in the intervals $t_k < t < t_{k+1}$, $k = 0, 1, \dots, n$, with $t_0 = 0$. For times greater than t_n , the sectionally continuous function $f(t)$ may be represented by a combination of unit step functions, or:

$$f(t) = \sum_{k=0}^{n-1} (S_k - S_{k+1}) f_k(t) + S_n f_n(t) , \quad (4.13)$$

and a typical segment of $f(t)$ is presented in Figure 4.2.2.

The Laplace transform of the derivative of this piecewise continuous function, $f(t)$, is given by:

$$L[f'(t)] = \int_0^\infty e^{-st} \left[\sum_{k=0}^{n-1} (S_k - S_{k+1}) f'_k(t) + S_n f'_n(t) \right] dt , \quad (4.14)$$

which results in:

$$L[f'(t)] = \sum_{k=0}^{n-1} \int_{t_k}^{t_{k+1}} e^{-st} f'_k(t) dt + \int_{t_n}^\infty e^{-st} f'_n(t) dt . \quad (4.15)$$

Each integral term in Eq. (4.15) may be integrated by parts to yield:

$$\begin{aligned} L[f'(t)] &= \sum_{k=0}^{n-1} \left[f_k(t) e^{-st} \right]_{t_k}^{t_{k+1}} - s \sum_{k=0}^{n-1} \int_{t_k}^{t_{k+1}} e^{-st} f_k(t) dt + \\ &\quad \left[f_n(t) e^{-st} \right]_{t_n}^\infty - s \int_{t_n}^\infty e^{-st} f_n(t) dt . \end{aligned} \quad (4.16)$$

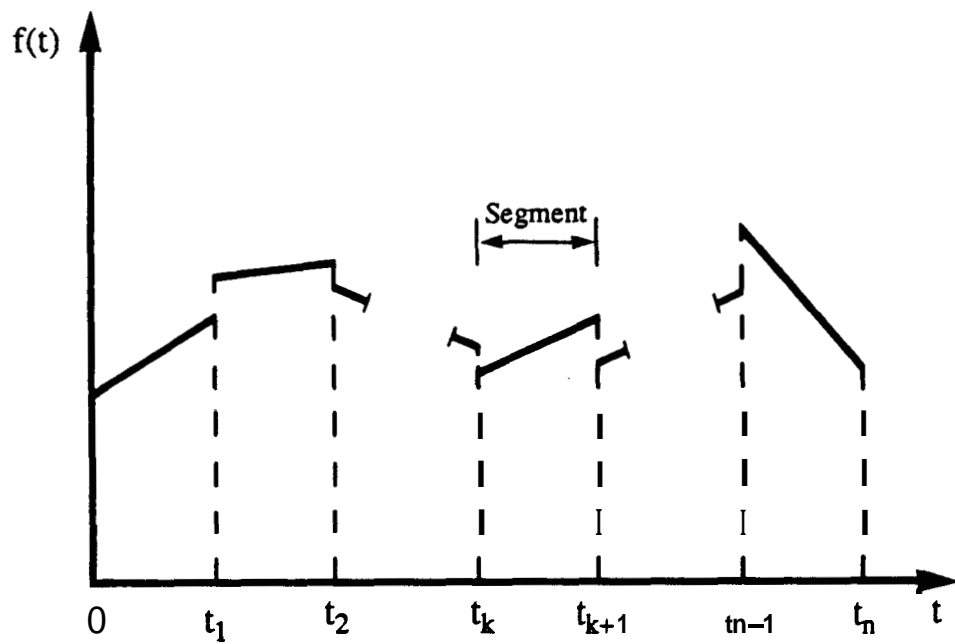


Figure 4.2.1. Graph of a piecewise continuous function

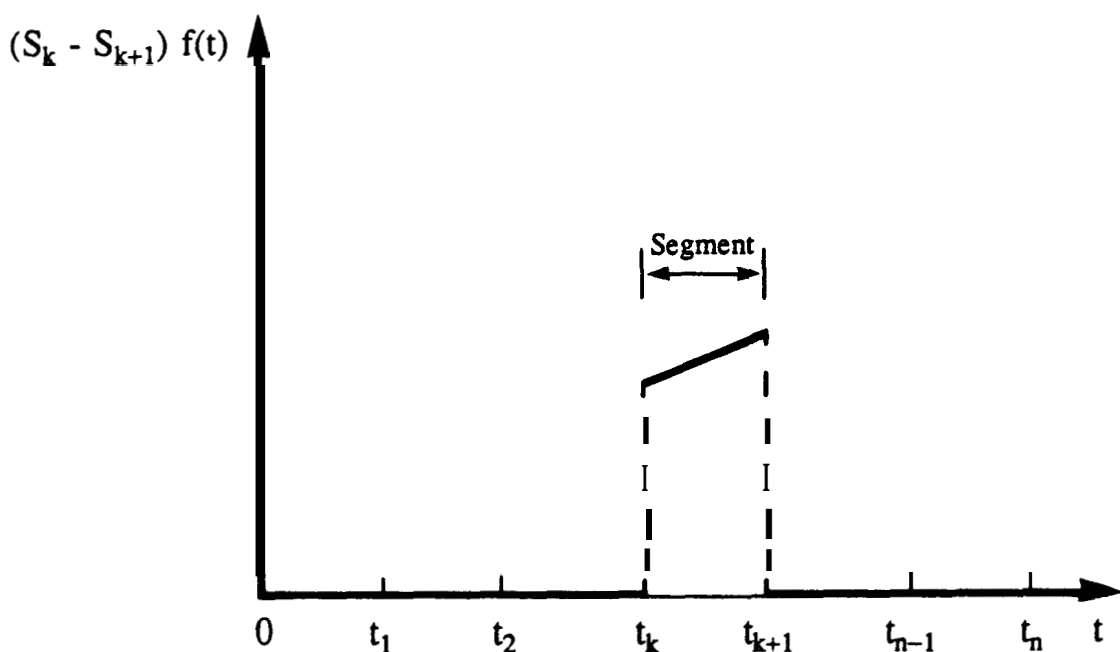


Figure 4.2.2. Segment of a piecewise continuous function

Because a continuous interval may be divided into a finite number of subintervals, integration of a function along a given interval may be expressed as a series of integrals along the subintervals. Hence, the Laplace transform of the piecewise continuous function $f(t)$ of Figure 4.2 may be expressed as:

$$\sum_{k=0}^{n-1} \int_{t_k}^{t_{k+1}} e^{-st} f_k(t) dt + \int_{t_n}^{\infty} e^{-st} f_n(t) dt = \int_0^{\infty} e^{-st} f(t) dt , \quad (4.17)$$

where:

$$f_k(t_k) = f(t_{k+}) ; \quad f_{k-1}(t_k) = f(t_{k-}) . \quad (4.18)$$

Equation (4.16) may be written as:

$$L[f'(t)] = s \bar{f}(s) - \sum_{k=1}^n e^{-st} [f(t_{k+}) - f(t_{k-})] - f(0_+) , \quad (4.19)$$

which provides an operational rule for the transform of the first derivative of sectionally continuous functions. Note that for a continuous function such that $f(k_+) = f(k_-)$, Eq. (4.19) reduces to the standard operational rule for derivatives of continuous functions, as described by Churchill (1944).

A summary of operational rules for the unit step function is presented in Table 4.1.

43. APPLICATION OF THE UNIT STEP FUNCTION METHOD

In order to establish a method of solution for transient flow problems with time-dependent boundary conditions, Laplace transformation and the unit step function were used to solve two important problems in well test analysis; pressure buildup following either constant-rate or constant-pressure production.

43.1. Pressure Buildup Following Constant-Rate Production

This problem considers pressure buildup in a well with skin and wellbore storage, follow-

ORIGINAL, FUNCTION	TRANSFORM
$f(t)$	$\bar{f}(s) = \int_0^{\infty} e^{-st} f(t) dt$
$S_k(t)$	$\frac{e^{-ks}}{s}$
$S_k f(t)$	$\bar{f}(s) - \int_0^k e^{-st} f(t) dt$
$[1 - S_k] f(t)$	$\int_0^k e^{-st} f(t) dt$
$f'(t)$	$s \bar{f}(s) - f(0_+)$
$S_k f'(t)$	$s \bar{f}(s) - f(k_-) e^{-ks} - s \int_0^k e^{-st} f(t) dt =$ $= s [S_k f(t)] - f(k_-) e^{-ks}$

TABLE 4.1 - Operational Rules for the Unit Step Function

ing constant-rate production at the wellhead. The problem for the production phase is discussed in detail in Appendix A. The shut-in, or pressure buildup phase, has usually been handled by superposition. In **this** treatment the unit step function is used to write an inner boundary condition which describes both production and shut-in by a single solution.

During the production phase the inner boundary condition for the constant rate problem, assuming both skin and wellbore storage effects, is given by:

$$C_D \frac{dp_{wD}}{dt_D} + q_{wD}(t_D) = q_D, \quad 0 < t_D < t_{pD}, \quad (4.20)$$

where:

$$q = \text{constant wellhead flow rate, } [L]^3[T]^{-1}.$$

Note that definitions of dimensionless variables commonly used in solutions of constant rate problems differ from the definitions employed in **this** study, which are described in Table 3.1. Equation (4.20) states that the wellhead flow rate, q_D , is given by the sum of the sandface flow rate, q_{wD} , and the rate of unloading of wellbore fluids, $C_D dp_{wD}/dt_D$. A more detailed discussion of **this** inner boundary condition is presented in Appendix A.

The wellbore pressure solution for the production phase may be expressed as:

$$\frac{p_{wD}(t_D)}{q_D} = \frac{2 \pi k h}{q \mu} \left[p_i - p_w(t) \right] = g_{wD}(S, C_D, t_D). \quad (4.21)$$

where $g_{wD}(S, C_D, t_D)$ is the dimensionless wellbore pressure response to a unit production at the wellhead. The notation for g_{wD} was chosen in order to avoid confusion with the actual dimensionless wellbore pressure p_{wD} . The function $g_{wD}(S, C_D, t_D)$ could represent the wellbore pressure response for a generic system, including linear, radial, spherical or other flow geometries. Usually $g_{wD}(S, C_D, t_D)$ has been obtained by inversion of Laplace transformed solutions. Appendix A describes the process employed to obtain the Laplace transformed pressure response for radial flow, which is given by Eq. (A.22). The real time inversion of **this** solution is presented graphically in Figure A. 1.

The solution described by Eq. (4.21) is valid as long the wellhead flow rate remains constant. Upon shut in, the surface flow rate becomes zero, and the new inner boundary condition is described by:

$$C_D \frac{dp_{wD}}{dt_D} + q_{wD}(t_D) = 0, \quad t_D > t_p . \quad (4.22)$$

Equations (4.20) and (4.22) may be combined into one expression using the unit step function S_k , as described in Eq. (4.3), resulting in:

$$\left[1 - S_k\right] \left[C_D \frac{dp_{wD}}{dt_D} + q_{wD}(t_D) - q_D\right] + S_k \left[C_D \frac{dp_{wD}}{dt_D} + q_{wD}(t_D)\right] = 0, \quad (4.23)$$

where k is equivalent to the production time t_p . Factoring and cancelling like terms, Eq. (4.23) yields:

$$C_D \frac{dp_{wD}}{dt_D} + q_{wD}(t_D) = \left[1 - S_k\right] q_D \quad (4.24)$$

For times less than k , Eq. (4.24) yields the usual constant rate condition. For times greater than k , the condition of Eq. (4.22) results. Equation (4.24) provides an inner boundary condition correct for all times, which can be transformed to provide a general solution for both production and buildup. Application of the Laplace transform to Eq. (4.24) yields:

$$C_D s \bar{p}_{wD}(s) + \bar{q}_{wD}(s) = \frac{1 - e^{-ks}}{s} q_D . \quad (4.25)$$

A relationship between the transforms of the sandface flow rate and the wellbore pressure is presented in Appendix A, Eq. (A.14). Substitution of Eq. (A.14) into Eq. (4.25), and observing the definition of $\bar{g}_{wD}(S, C_D, s)$ given in Eq. (A.22), yields the following Laplace space solution:

$$\frac{\bar{p}_{wD}(s)}{q_D} = \bar{g}_{wD}(S, C_D, s) = e^{-ks} \bar{g}_{wD}(S, C_D, s) . \quad (4.26)$$

The first transform is that of the storage-skin constant rate well for the total time t , while

the second transform is the same function evaluated for $(t - k)$. This is the familiar result obtained by superposition. Eq. (4.26) may be inverted as follows:

$$\frac{p_{WD}(t_D)}{q_D} = \frac{2 \pi k h}{q \mu} \left[p_i - p_w(t) \right] = g_{WD}(S, C_D, t_D + \Delta t_D) - g_{WD}(S, C_D, \Delta t_D), \quad (4.27)$$

where:

Δt = elapsed shut-in time, [T].

This example provides a demonstration of the essential difference between a conventional use of the unit step function, S_k , and the new use proposed here. The unit step function is normally used to provide a time translation of a function $f(t)$ by k time units. Churchill (1944) emphasizes this point by noting that S_k is simply the translation of $f(t) = 1$. This can be seen in Figure 4.3.1.

The product of S_k and $f(t)$ is essentially different in its behavior. The unit step function causes $f(t)$ to have the value zero between times 0 and k . At $t = k_+$, the product, $S_k f(t)$ has the value $f(t) = f(k_+)$. This is shown in Figure 4.3.2, and it does not represent a translation. It actually represents a truncation of $f(t)$ for times less than k .

43.2. Pressure Buildup Following Constant-Pressure Production

Although the analytical solution of the constant-pressure production problem has been studied in detail, the shut-in following a constant-pressure production has not been handled analytically in a complete manner. The shut in period has been conventionally expressed in terms of a superposition integral.

This section presents an analytical solution which combines both the constant-pressure production phase to time k and the following shut-in period to the total time t . The skin effect acts in both periods. The shut-in period requires all flow from the formation to be stored within the wellbore.

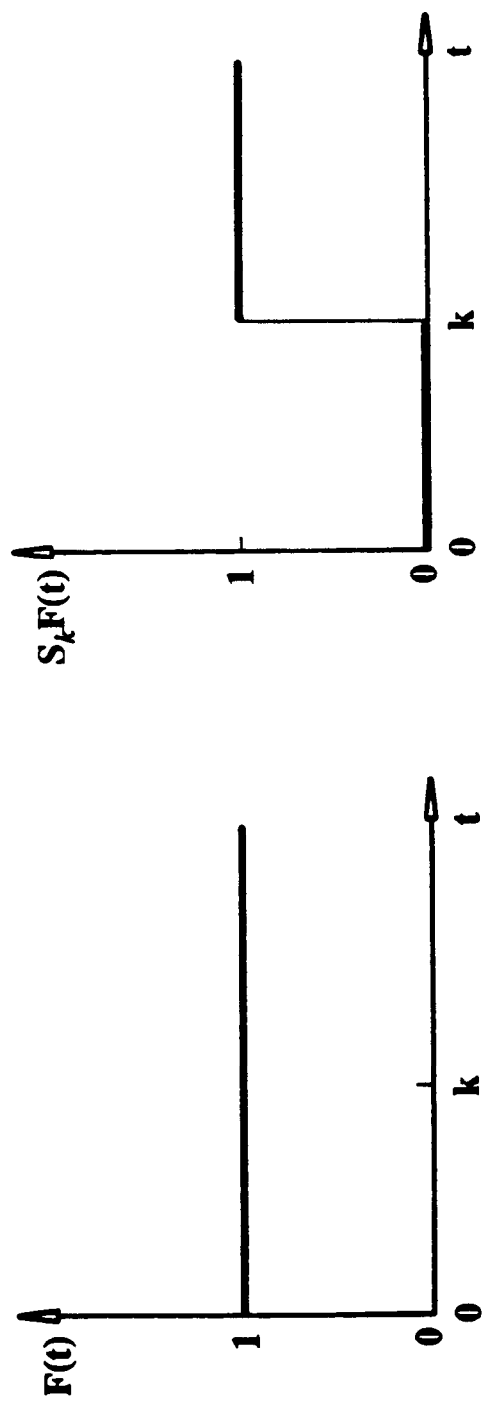


Figure 4.3.1 Use of the Unit Step Function to Provide a Translation in Time

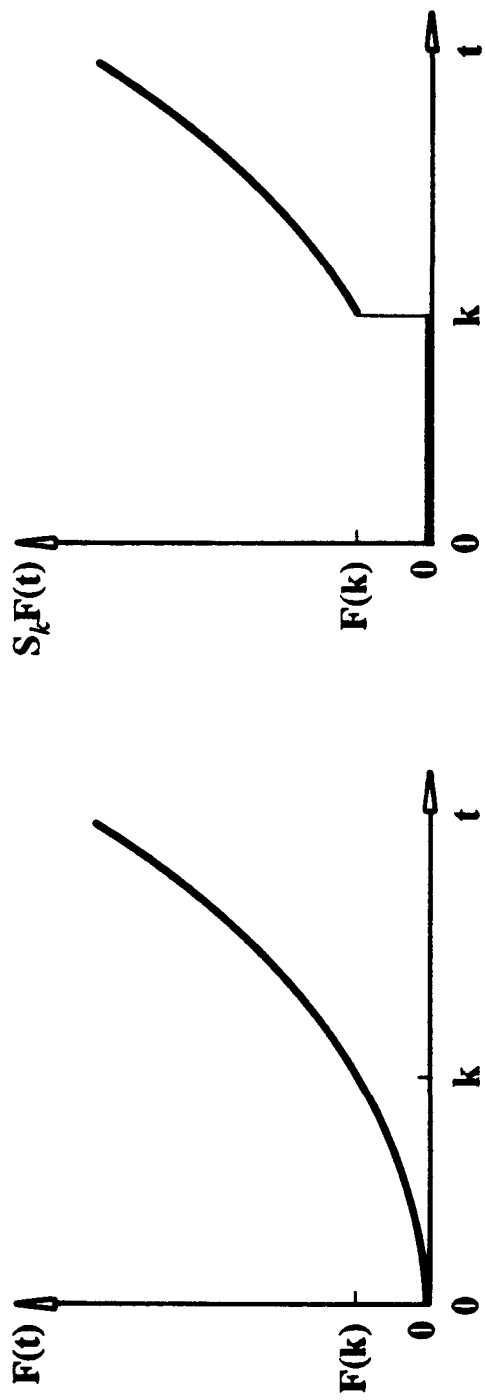


Figure 4.3.2 $F(t)$ and the product of $F(t)$ and the Unit Step Function

During the production phase, the wellbore pressure is described by:

$$p_{wD}(t_D) = 1 ; \quad 0 < t_D < t_{pD} , \quad (4.28)$$

with the following wellbore initial condition:

$$p_{wD}(0_+) = 1 . \quad (4.29)$$

After shutting the well in, the sandface flow rate must equal the rate of fluid accumulation inside the wellbore, which may be described by the following inner boundary condition:

$$C_D \frac{dp_{wD}}{dt_D} + q_{wD}(t_D) = 0 , \quad t_D > t_{pD} = k . \quad (4.30)$$

Conditions given by Eqs. (4.28) and (4.30) may be combined by means of the unit step function, Eq. (4.3), yielding:

$$\left[1 - S_k \right] \left[1 - p_{wD}(t_D) \right] + S_k \left[C_D \frac{dp_{wD}}{dt_D} + q_{wD}(t_D) \right] = 0 , \quad (4.31)$$

which may be rearranged to give:

$$S_k \left[C_D \frac{dp_{wD}}{dt_D} + q_{wD}(t_D) + p_{wD}(t_D) - 1 \right] = p_{wD}(t_D) - 1 . \quad (4.32)$$

Observing the operational rules for the unit step function given by Eqs. (4.6) and (4.10), and using the fact that $p_{wD}(k_-) = 1$, then Eq. (4.32) may be transformed to:

$$C_D \left[s \bar{p}_{wD}(s) - 1 \right] + \bar{q}_{wD}(s) = \int_0^k e^{-s\tau_D} q_{wD}(\tau_D) d\tau_D , \quad (4.33)$$

where:

τ = variable of integration, [T].

Substituting Eq. (A.14) into Eq. (4.33) and solving for \bar{p}_{wD} we obtain:

$$\bar{p}_{wD}(s) = \frac{C_D}{s C_D + \frac{1}{s \bar{g}_{wD}(S, s)}} + \frac{\int_0^k e^{-s\tau_D} q_{wD}(\tau_D) d\tau_D}{s C_D + \frac{1}{s \bar{g}_{wD}(S, s)}} \quad (4.34)$$

The first right hand term is the transform of the "slug test" solution. The second term is the product of the transformed "slug test" solution and an integral, which is a function of the Laplace variable only. Therefore, using the definition of $\bar{g}_{WD}(S, C_D, s)$ given in Eq. (A.22), the inverse transform of Eq. (4.34) may be found in terms of a convolution integral:

$$p_{WD}(t_D) = C_D g'_{WD}(S, C_D, t_D) + \int_0^{t_D} g'_{WD}(S, C_D, t_D - \tau_D) [1 - S_k] q_{WD}(\tau_D) d\tau_D . \quad (4.35)$$

The function $g'_{WD}(S, C_D, t_D)$ represents the derivative with respect to time of the constant-rate skin and wellbore storage solution. The product of C_D and $g'_{WD}(S, C_D, t_D)$ yields the "slug test" solution, as discussed in Appendix A. Because $[1 - S_k]$ is zero for times greater than k , Eq. (4.35) reduces to:

$$p_{WD}(t_D) = C_D g'_{WD}(S, C_D, t_D) + \int_0^k g'_{WD}(S, C_D, t_D - \tau_D) q_{WD}(\tau_D) d\tau_D . \quad (4.36)$$

Eq. (4.36) describes the solution for the pressure buildup phase following constant-pressure production. As the production time approaches zero, Eq. (4.36) converges to the "slug test" solution.

5. PRESSURE ANALYSIS OF DRILLSTEM TESTS

This section describes the use of the unit step function method to develop an analytical solution for the drill stem test problem which is correct for both flowing and shut-in periods. The effects of both skin and wellbore storage are considered.

The solution is used to generate new methods of interpretation of pressure-time data obtained from field cases. Application of these new methods to field data may provide the initial reservoir pressure, the formation permeability and the skin effect.

5.1. SOLUTION OF THE DRILLSTEM TEST PROBLEM

The drillstem test problem is described in Section 3 of this work. A summary of the normalized equations is presented in Section 3.4. Recall that the drill stem test may be viewed as a "slug test" with a step change in wellbore storage.

The internal boundary condition for the DST problem is described by Eqs. (3.17) and (3.18). The unit step function can be used to write an inner boundary condition which is valid for all times. Hence, Eqs. (3.17) and (3.18) may be combined as follows:

$$\left[(1 - S_k) C_{FD} + S_k C_{SD} \right] \frac{dp_{WD}}{dt_D} + q_{WD}(t_D) = 0, \quad t_D > 0, \quad (5.1)$$

where k is equivalent to the production time t_p . For times less than k , S_k is zero and the condition of the changing liquid level wellbore storage is obtained. For times greater than k , S_k is unity and the compressibility dominated wellbore storage period results. Observing the operational rule given in Eq. (4.10), Eq. (5.1) can be transformed to yield:

$$C_{SD} \left[s \bar{p}_{WD}(s) - p_{WD}(0_+) \right] + (C_{FD} - C_{SD}) \int_0^k e^{-st_D} p'_{WD}(\tau_D) d\tau_D + \bar{q}_{WD}(s) = 0. \quad (5.2)$$

Using the wellbore initial condition, Eq. (3.16), and recalling the relationship defined in Eq. (A.14), Eq. (5.2) becomes:

$$\bar{p}_{wD}(s) = \frac{C_{SD} - (C_{FD} - C_{SD}) \int_0^k e^{-st_D} p'_{wD}(\tau_D) d\tau_D}{s C_{SD} + \frac{1}{s \bar{g}_{wD}(S, s) + S}}. \quad (5.3)$$

Recalling the definition of $\bar{g}_{wD}(S, C_{SD}, s)$ described in Eq. (A.22), Eq. (5.3) may be written as:

$$\bar{p}_{wD}(s) = C_{SD} s \bar{g}_{wD}(S, C_{SD}, s) - (C_{FD} - C_{SD}) s \bar{g}_{wD}(S, C_{SD}, s) \int_0^k e^{-st_D} p'_{wD}(\tau_D) d\tau_D. \quad (5.4)$$

In order to invert Eq. (5.4), it is useful to recall the transform of the time derivative of $g_{wD}(S, C_{SD}, t_D)$. Because $g_{wD}(S, C_{SD}, 0) = 0$, it follows that:

$$L^{-1} \left[s \bar{g}_{wD}(S, C_{SD}, s) \right] = g'_{wD}(S, C_{SD}, t_D). \quad (5.5)$$

Also, from the operational rule described by Eq. (4.7), we obtain:

$$L^{-1} \left[\int_0^k e^{-st_D} p'_{wD}(\tau_D) d\tau_D \right] = [1 - S_k] p'_{wD}(t_D). \quad (5.6)$$

Finally, using the transforms given in Eqs. (5.5) and (5.6), Eq. (5.4) may be inverted to yield:

$$p_{wD}(t_D) = C_{SD} g'_{wD}(S, C_{SD}, t_D) + \\ (C_{SD} - C_{FD}) \int_0^{t_D} g'_{wD}(S, C_{SD}, t_D - \tau_D) [1 - S_k(\tau_D)] p'_{wD}(\tau_D) d\tau_D. \quad (5.7)$$

It should be emphasized that the unit step function presented in Eq. (5.7) is referenced to the dimensionless time described by the dummy variable of integration, τ_D . Eq. (5.7) is the wellbore pressure solution of the drillstem test problem, and is valid for all times. However, Eq. (5.7) may be expanded to represent the flowing and the shut-in phases separately by more simple expressions.

First consider the case where $t_D < t_{pD} = k$. Then, S_k is zero and Eq. (5.7) reduces to:

$$p_{wD}(t_D) = C_{SD} g'_{wD}(S, C_{SD}, t_D) + \\ (C_{SD} - C_{FD}) \int_0^k g'_{wD}(S, C_{SD}, t_D - \tau_D) p'_{wD}(\tau_D) d\tau_D, \quad t_D < k. \quad (5.8)$$

From physical considerations, Eq. (5.8) must be the "slug test" solution with a changing liquid level wellbore storage coefficient, $g_{wD}(S, C_{FD}, t_D)$. This may be demonstrated by assuming that Eq. (5.8) is valid for all times, so it can be Laplace transformed yielding:

$$\bar{p}_{wD}(s) = C_{SD} s \bar{g}_{wD}(S, C_{SD}, s) + \\ [C_{SD} - C_{FD}] s \bar{g}_{wD}(S, C_{SD}, s) [s \bar{p}_{wD} - p_{wD}(0_+)]. \quad (5.9)$$

Recalling that $p_{wD}(0_+) = 1$, and using the definition of $\bar{g}_{wD}(S, C_{SD}, s)$ given by Eq. (A.22), then Eq. (5.9) may be solved for $\bar{p}_{wD}(s)$ to yield:

$$\bar{p}_{wD}(s) = \frac{C_{FD}}{s C_{FD} + \frac{1}{s g_{wD}(S, s)}} = C_{FD} s \bar{g}_{wD}(S, C_{FD}, s), \quad (5.10)$$

which, using the fact that $g_{wD}(S, C_{FD}, 0) = 0$, may be inverted to real time space as:

$$p_{wD}(t_D) = C_{FD} g'_{wD}(S, C_{FD}, t_D); \quad t_D < k. \quad (5.11)$$

Eq. (5.11) describes the wellbore pressure response during the production phase of a drillstem test.

Another important component of the solution is the equation for the shut-in phase. Because for $t_D > k$ it follows that $S_k = 1$, then Eq. (5.7) becomes:

$$p_{wD}(t_D) = C_{SD} g'_{wD}(S, C_{SD}, t_D) + \\ (C_{SD} - C_{FD}) \int_0^k g'_{wD}(S, C_{SD}, t_D - \tau_D) p'_{wD}(\tau_D) d\tau_D, \quad t_D > k. \quad (5.12)$$

This solution has some interesting features. First, consider the case where the production time

approaches zero. Then, the integral term in *Eq. (5.12)* vanishes and the result converges to the "slug test" solution with a compressibility dominated wellbore storage.

Also, because for the production phase a relationship between the sandface rate and the wellbore pressure may be obtained from the wellbore condition given by *Eq. (3.17)*:

$$q_{wD}(t_D) = -C_{FD} \frac{dp_{wD}}{dt_D}, \quad 0 < t_D < k, \quad (5.13)$$

then, using this relationship, *Eq. (5.12)* may be expressed as:

$$p_{wD}(t_D) = C_{SD} g'_{wD}(S, C_{SD}, t_D) + C_{SD} \int_0^k g'_{wD}(S, C_{SD}, t_D - \tau_D) p'_{wD}(\tau_D) d\tau_D + \int_0^k g'_{wD}(S, C_{SD}, t_D - \tau_D) q_{wD}(\tau_D) d\tau_D. \quad (5.14)$$

Now, consider the case of pressure buildup following constant-pressure production. For $0 < t_D < k$, it follows that $p'_{wD}(t_D) = 1$ and then $p'_{wD}(t_D) = 0$. Therefore, in this case *Eq. (5.14)* simplifies to:

$$p_{wD}(t_D) = C_{SD} g'_{wD}(S, C_{SD}, t_D) + \int_0^k g'_{wD}(S, C_{SD}, t_D - \tau_D) q_{wD}(\tau_D) d\tau_D. \quad (5.15)$$

This result is identical to *Eq. (4.36)*. *Equation (5.15)* is a particular case of the drillstem test solution, which could have been obtained by assuming $C_{FD} \gg C_{SD}$ in *Eq. (5.12)*. In fact, *Eq. (5.15)* may be viewed as the limiting case of the drillstem test solution as $C_{FD} \rightarrow \infty$. This could be ideally represented by production of a weightless fluid.

5.1.1. Late-Time Approximation

During the shut-in phase of a drillstem test, the sandface flow rate rapidly approaches zero, yielding a smooth pressure recovery curve. Pressure-time data collected during this phase are ideal for engineering analysis and may be used with interpretation methods to obtain reli-

able estimates of reservoir parameters.

A practical method of analysis for **DST** pressure buildup data can be developed based upon a late-time approximation for the solution given in Eq. (5.12). Consider that the shut-in time is long enough so that the following approximation may be used:

$$\dot{g}_{wD}(S, C_{SD}, t_D - k) = \dot{g}_{wD}(S, C_{SD}, t_D). \quad (5.16)$$

Using this relationship, the integrand in Eq. (5.12) reduces to $\dot{p}_{wD}(\tau_D)$ and may be promptly integrated. Also, using the fact that $p_{wD}(0) = 1$, then Eq. (5.12) yields:

$$p_{wD}(t_D) = \left\{ C_{FD} [1 - p_{wD}(k)] + C_{SD} p_{wD}(k) \right\} \dot{g}_{wD}(S, C_{SD}, t_D). \quad (5.17)$$

Because the average production rate is given by:

$$q_w^* = \frac{Q_w(t_p)}{t_p} = \frac{1}{t_p} \int_0^{t_p} q_w(\tau) d\tau, \quad (5.18)$$

where:

q_w^* = average production rate, $[L]^3[T]^{-1}$,

$Q_w(t)$ = cumulative fluid recovery, $[L]^3$,

and recalling that during the flow period fluid accumulation in the drill string equals the cumulative sandface flow, or $Q_{wD}(k) = C_{FD} [1 - p_{wD}(k)]$, then Eq. (5.17) may be expressed as:

$$p_{wD}(t_D) = \left[1 + \frac{C_{SD} p_{wD}(k)}{Q_{wD}(k)} \right] q_w^* t_p \dot{g}_{wD}(S, C_{SD}, t_D). \quad (5.19)$$

Substituting the expression for the late-time approximation for $\dot{g}_{wD}(S, C_{SD}, t_D)$ given by Eq. (A.33) into Eq. (5.19), we obtain the late-time pressure response for the shut in phase, which becomes:

$$p_{wD}(t_D) = \left[1 + \frac{C_{SD} p_{wD}(k)}{Q_{wD}(k)} \right] \frac{q_w^*}{2} \frac{t_p}{t_p + \Delta t}. \quad (5.20)$$

Recalling the definitions of the dimensionless variables described in Table 3.1, Eq. (5.20) may

be expressed in terms of dimensional variables, resulting in a Cartesian straight line:

$$p_{ws}(t) = p_i - m_C \frac{t_p}{t_p + \Delta t}, \quad (5.21)$$

with slope:

$$m_C = \frac{q_w^* \mu}{4 \pi k h} \left[1 + \frac{C_s (p_i - p_{ff})}{q_w^* t_p} \right], \quad (5.22)$$

where the average production rate, q_w^* , is computed from:

$$q_w^* = \frac{C_F (p_{ff} - p_{fi})}{t_p}, \quad (5.23)$$

and where:

m_C = slope of the Cartesian straight line, $[M] [L]^{-1}[T]^{-2}$,

p_{fi} = initial flowing pressure, p_0 , $[M] [L]^{-1}[T]^{-2}$,

p_{ff} = final flowing pressure, $[M] [L]^{-1}[T]^{-2}$,

p_{ws} = wellbore shut-in pressure, $[M] [L]^{-1}[T]^{-2}$.

From Eqs. (5.21) and (5.22) it is apparent that a Cartesian plot of p_{ws} versus the ratio $t_p/(t_p + \Delta t)$ for field pressure buildup data may yield a straight line with slope proportional to the reciprocal of permeability. Extrapolation of the straight line to an infinite shut-in time, $t_p / (\Delta t) \rightarrow 0$, should yield the initial reservoir pressure.

The expression:

$$\alpha_w = \frac{C_s (p_i - p_{ff})}{q_w^* t_p}, \quad (5.24)$$

is a volumetric ratio, comparing the additional volume of fluid that could be compressed into the storage chamber during the pressure buildup phase to the fluid volume recovered during the production phase. For most DST's the factor α_w is negligible compared to unity, and the formation transmissivity may be determined from a simplified version of Eq. (5.22), which is:

$$\frac{k h}{\mu} = \frac{q_w^*}{4 \pi m_C} \quad (5.25)$$

5.1.2 Results

Another important aspect of the solution presented in Eq. (5.20) is that for long shut-in times, the pressure buildup data are not influenced by the skin effect. The skin effect may affect the time of the start of the Cartesian straight line, but not the slope. Hence, in order to determine the degree of formation damage (or stimulation) of the well, information from the previous flow period is required.

If wellbore storage effects have become negligible for the wellbore pressure response of a constant-rate well, then $g_{WD}(S, C_D, t_D)$ may be expressed by a logarithmic approximation. According to Ramey *et al* (1975), this is true when the production time meets the following criterion:

$$t_D > C_D (60 + 3.5 S), \quad S > 0. \quad (5.26)$$

Because the "slug test" solution may be expressed as the time derivative of the constant rate skin and wellbore storage solution, it may be expected that the start of the Cartesian "slug test" straight line may be defined by a similar criterion. However, additional work has yet to be done in order to verify this point. Furthermore, according to Eq. (5.26), both the skin effect and wellbore storage should affect the beginning of the straight line.

Fig. 5.1 presents the influence of skin effect on the pressure buildup response of a DST. The Cartesian straight line only exists for very small values of the ratio $t_p/(t_p + \Delta t)$, when skin is large. If the skin effect is expected to be large, the well should remain shut in for an extended period of time.

The influence of the compressibility-dominated wellbore storage coefficient on the pressure buildup is presented in Fig. 5.2. A more reliable pressure buildup analysis may be accomplished if the wellbore storage factor for the shut-in phase is minimized. A small wellbore storage coefficient during pressure buildup may be achieved by reducing the dead volume below the bottom-hole valve.

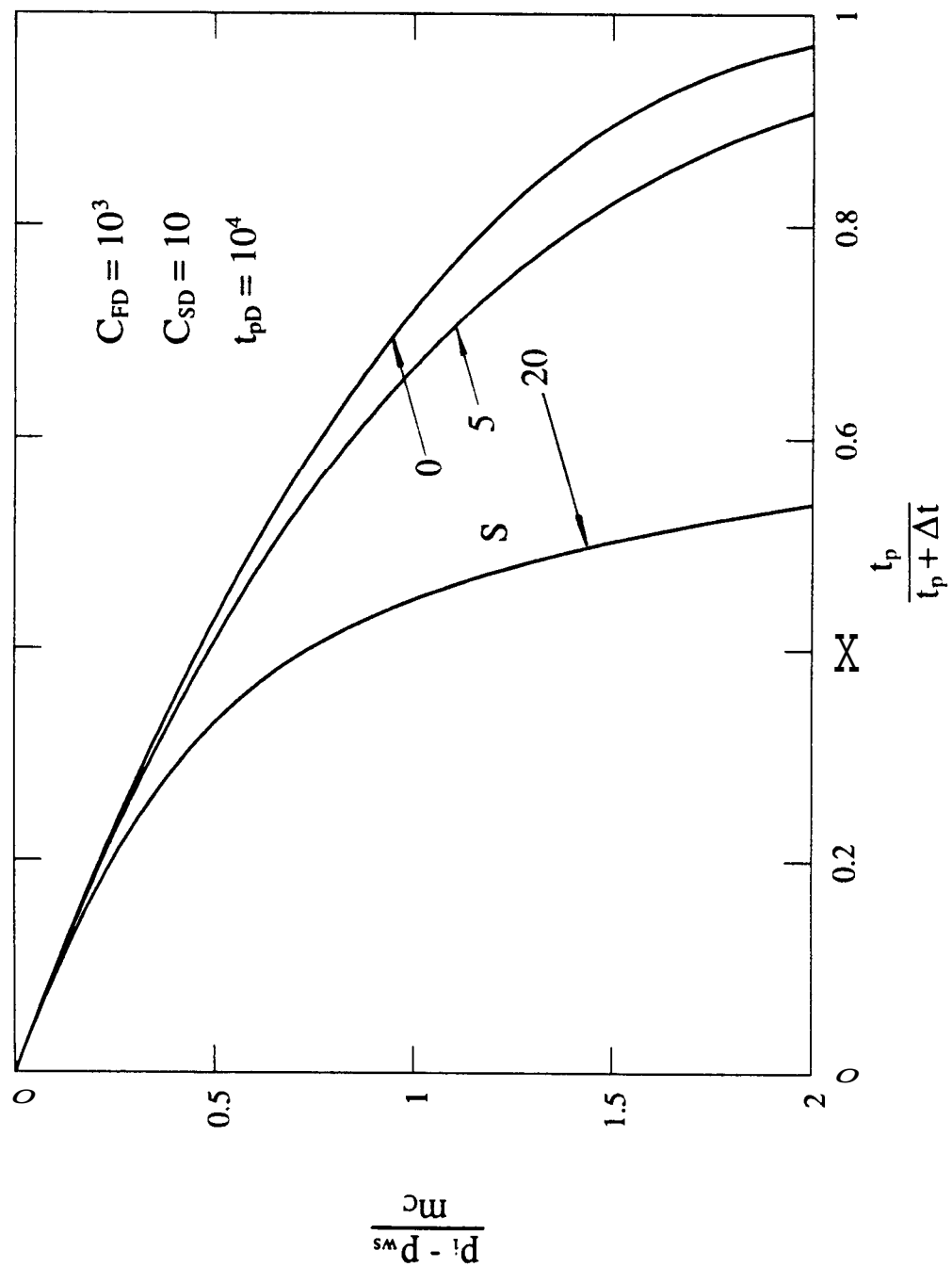


Figure 5.1 - Influence of Skin on Pressure Buildup

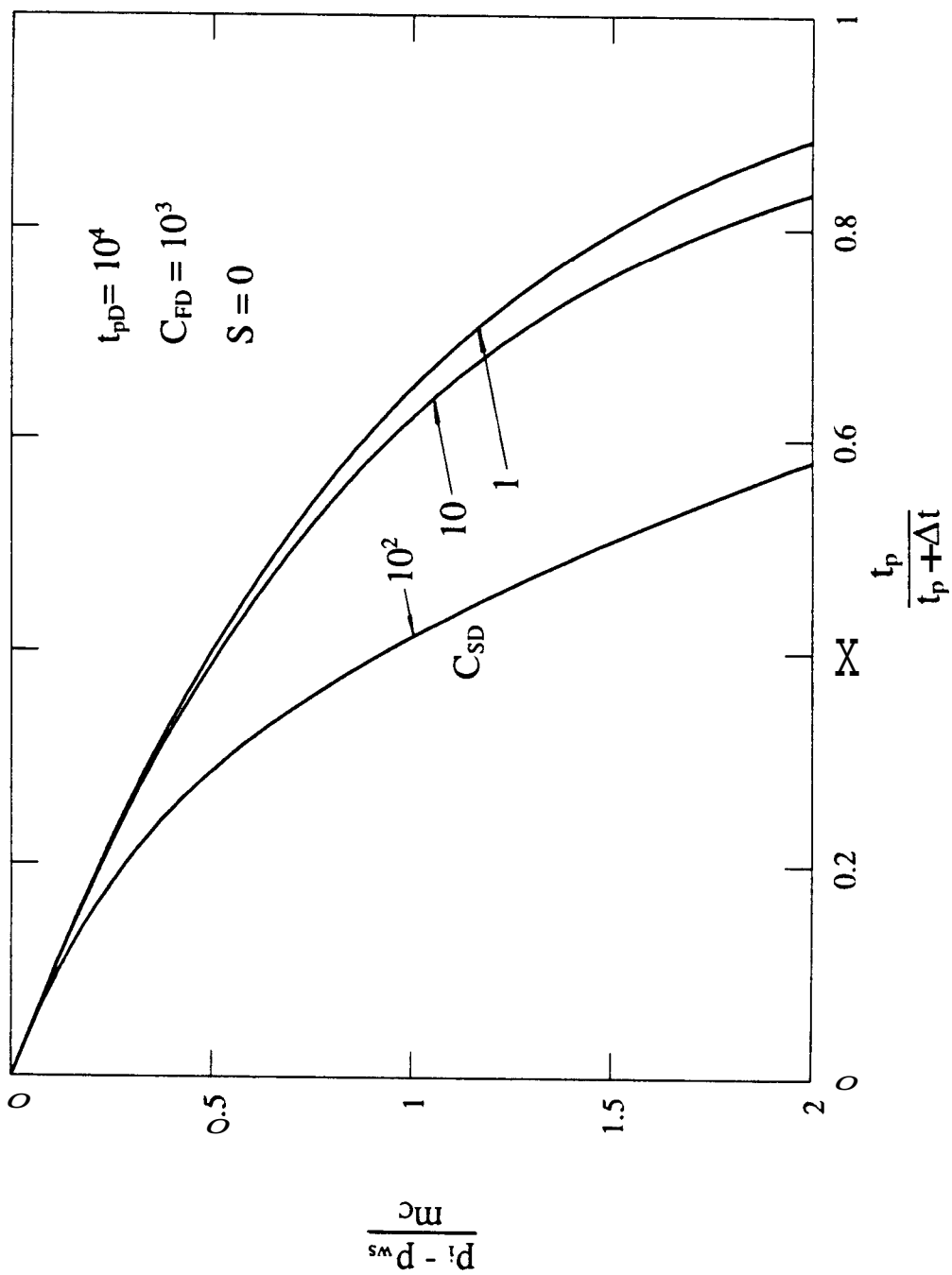


Figure 5.2 - Influence of Shut-in Storage Factor on Pressure Buildup

5.1.3. Damage Ratio

A common parameter used in well test analysis is the damage ratio, which is defined as the ratio of the theoretical flow rate that would be obtained if the well were not damaged (or stimulated), and the actual flow rate, assuming the same wellbore pressure drop is applied in both cases. According to this definition, the damage ratio for transient flow may be expressed as the ratio $[1/2 \ln(4t_D/\gamma) + S]/[1/2 \ln(4t_D/\gamma)]$. Therefore, the damage ratio changes with time, and a more general definition is required in order to quantify the degree of formation damage or stimulation.

In general, low productivity wells are more likely to be produced at a condition of constant bottom-hole pressure rather than at a constant flow rate. Considering the case of constant pressure production, the long-term response of a well in a closed drainage area may be characterized by an exponential rate decline, which according to Ehlig-Economides and Ramey (1979) is given by:

$$q_{wD}(t_D) = \frac{e^{-2\pi t_{DA} / (\beta + S)}}{\beta + S}, \quad (5.27)$$

with $t_{DA} = t_D r_w^2 / A$ and:

$$\beta = \frac{1}{2} \ln \left[\frac{4A}{\gamma C_A r_w^2} \right], \quad (5.28)$$

where:

A = drainage area, $[L]^2$,

β = geometric factor,

C_A = Dietz shape factor.

Assuming a well producing from the center of a closed square ($C_A = 30.88$), exponential rate decline starts at $t_{DA} = 0.1$. The damage ratio at the onset of exponential rate decline may be computed from the ratio between flow rates defined by Eq. (5.27) considering a finite and a zero skin effect. For an equivalent drainage radius of $\sqrt{A} / r_w = 2,000$ then $\beta = 6.29$, and the

expression for the damage ratio becomes:

$$DR = \left[1 + 0.1592 S \right] e^{-\frac{0.1 S}{6.29 + S}}. \quad (5.29)$$

Eq. (5.29) may be modified to consider any particular drainage shape or reservoir size, as well as to consider a steady-state flow regime.

5.2. SOLUTION OF THE GENERAL DST PROBLEM

In **this** section we consider the general case of the changing wellbore storage problem, including step changes in the wellbore pressure drop. Figure 5.3 presents a schematic of the general case of the **DST** problem.

So far we have studied the case where no discontinuity is present in the wellbore pressure, by the time the wellbore storage factor is changed. For instance, when the well is shut-in, the wellbore storage coefficient changes instantaneously from C_F to C_S , but the wellbore pressure remains continuous, $p_{WD}(k_-) = p_{WD}(k_+)$.

In most **DST**'s, after the first pressure buildup is completed, the bottom hole valve is opened again, and a new cycle of production and shut-in begins. When the valve is opened, wellbore storage changes sharply from C_S to C_F , and there is also a discontinuity in the wellbore pressure, which drops from p_{sf1} to p_{fi2} , as shown in Fig. 5.4. In view of Fig. 5.4, the following definitions apply:

- p_{fi1} = initial flowing pressure, first cycle, $[M] [L]^{-1} [T]^{-2}$,
- p_{fi2} = initial flowing pressure, second cycle, $[M] [L]^{-1} [T]^{-2}$,
- p_{ff1} = final flowing pressure, first cycle, $[M] [L]^{-1} [T]^{-2}$,
- p_{ff2} = final flowing pressure, second cycle, $[M] [L]^{-1} [T]^{-2}$,
- p_{sf1} = final shut-in pressure, first cycle, $[M] [L]^{-1} [T]^{-2}$,
- p_{sf2} = final shut-in pressure, second cycle, $[M] [L]^{-1} [T]^{-2}$.

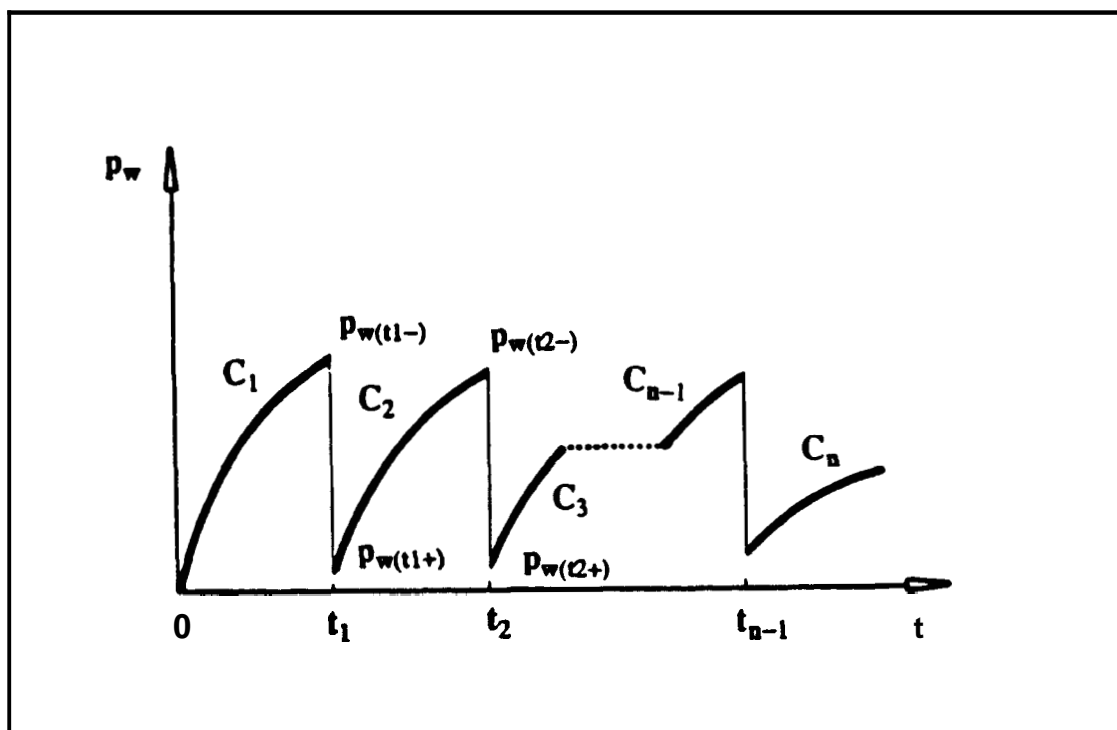


Figure 5.3 DST General Case

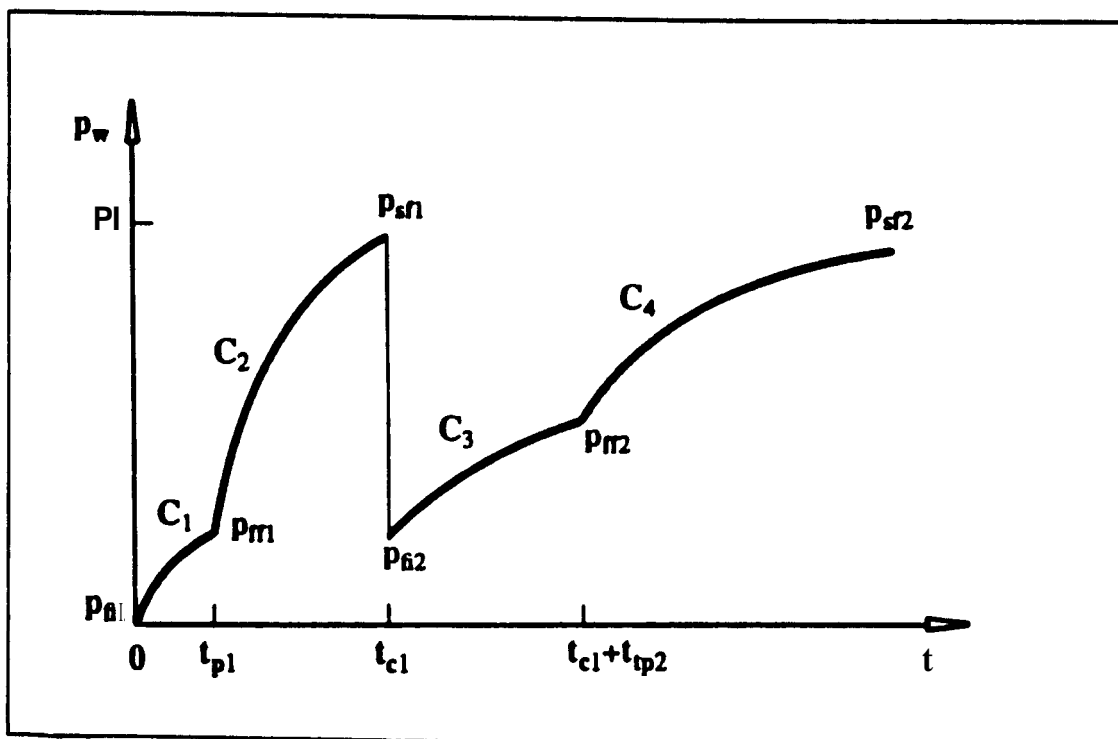


Figure 5.4 Pressure-Time Behavior for DST

As long as the wellbore storage coefficient remains constant during a given time interval, $t_{j-1} < t < t_j$, the general expression for the inner boundary condition of the DST problem is given by:

$$C_j \frac{dp_{wD}}{dt_D} + q_{wD}(t_D) = 0, \quad t_{j-1} < t < t_j ; \quad j = 1, n . \quad (5.30)$$

Considering the time interval $k-1 < t < k$, the function $(S_{k-1} - S_k)$ is unity in this interval and zero elsewhere. This is shown in Fig. 5.5, where $k = 0, 1, 2, \dots, n$ correspond to the elapsed time 0, t_1, t_2, \dots, t_n . Using this convention, each term of Eq. (5.30) may be expressed as:

$$[S_{k-1} - S_k] \left[C_k \frac{dp_{wD}}{dt_D} + q_{wD}(t_D) \right] = 0, \quad t > k . \quad (5.31)$$

For time greater than $n-1$, these expressions may be combined into a single equation, resulting in a general inner boundary condition which is valid for all times:

$$\sum_{k=1}^{n-1} (S_{k-1} - S_k) \left[C_k \frac{dp_{wD}}{dt_D} + q_{wD}(t_D) \right] + S_{n-1} \left[C_n \frac{dp_{wD}}{dt_D} + q_{wD}(t_D) \right] = 0 . \quad (5.32)$$

Equation (5.32) may also be written as:

$$\sum_{k=1}^{n-1} C_k (S_{k-1} - S_k) \frac{dp_{wD}}{dt_D} + S_{n-1} C_n \frac{dp_{wD}}{dt_D} + q_{wD}(t_D) = 0 . \quad (5.33)$$

Applying the definition of the Laplace transform, it can be shown that:

$$L \left[(S_{k-1} - S_k) F(t) \right] = \int_{k-1}^k e^{-st} F(t) dt , \quad (5.34)$$

and therefore the Laplace transform of Eq. (5.33) becomes:

$$\sum_{k=1}^{n-1} C_k \int_{k-1}^k e^{-st_D} \frac{dp_{wD}}{dt_D} dt_D + C_n \int_0^\infty e^{-st_D} S_{n-1} \frac{dp_{wD}}{dt_D} dt_D + \bar{q}_{wD}(s) = 0 . \quad (5.35)$$

Due to the nature of the unit step function, the second integral term in Eq. (5.35) may be expanded as:

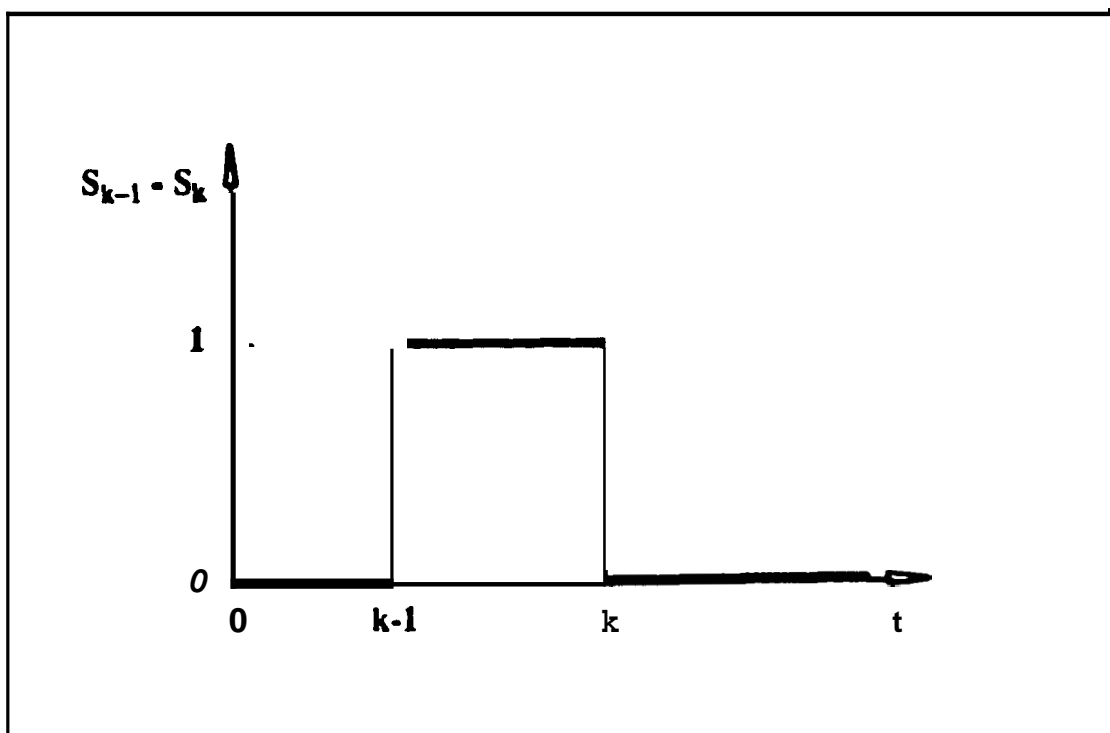


Figure 5.5 Combination of Unit Step Functions

$$\int_0^\infty e^{-st_D} S_{n-1} \frac{dp_{wD}}{dt_D} dt_D = \int_0^\infty e^{-st_D} \frac{dp_{wD}}{dt_D} dt_D - \int_0^{(n-1)} e^{-st_D} \frac{dp_{wD}}{dt_D} dt_D, \quad (5.36)$$

and because the function $p_{wD}(t_D)$ is only sectionally continuous, the Laplace transform of its derivative in Eq. (5.36) is given by the operational rule defined in Eq. (4.19). Therefore, using Eqs. (4.19) and (5.36), Eq. (5.35) reduces to:

$$\begin{aligned} \sum_{k=1}^{n-1} C_k \int_{k-1}^k e^{-st_D} p'_{wD}(t_D) dt_D &= C_n \int_0^{(n-1)} e^{-st_D} p'_{wD}(t_D) dt_D + C_n s \bar{p}_{wD} \\ &- C_n p_{wD}(0_+) - C_n \sum_{k=1}^{n-1} e^{-ks} \left[p_{wD}(k_+) - p_{wD}(k_-) \right] + \bar{q}_{wD}(s) = 0. \end{aligned} \quad (5.37)$$

Noting that $p_{wD}(0_+) = 1$ and using the relation between \bar{p}_{wD} and \bar{g}_{wD} defined in Eq. (A.14), Eq. (5.37) may be algebraically manipulated to yield:

$$\begin{aligned} \left[s C_n + \frac{1}{s \bar{g}_{wD}(S, s)} \right] \bar{p}_{wD}(s) &= C_n + C_n \sum_{k=1}^{n-1} e^{-ks} \left[p_{wD}(k_+) - p_{wD}(k_-) \right] + \\ &+ \sum_{k=1}^{n-1} (C_n - C_k) \int_{k-1}^k e^{-st_D} p'_{wD}(t_D) dt_D. \end{aligned} \quad (5.38)$$

This result is general and may be used to represent any reservoir model described by the diffusivity equation. Recalling the definition of $\bar{g}_{wD}(S, C_D, s)$ given in Eq. (A.22), and solving Eq. (5.38) for $\bar{p}_{wD}(s)$ we obtain:

$$\begin{aligned} \bar{p}_{wD}(s) &= C_n s \bar{g}_{wD}(S, C_n, s) \left\{ 1 + \sum_{k=1}^{n-1} e^{-ks} \left[p_{wD}(k_+) - p_{wD}(k_-) \right] \right\} + \\ &s \bar{g}_{wD}(S, C_n, s) \sum_{k=1}^{n-1} (C_n - C_k) \int_{k-1}^k e^{-st_D} p'_{wD}(t_D) dt_D. \end{aligned} \quad (5.39)$$

The wellbore pressure solution for the multi-cycle DST problem is then obtained by inverting Eq. (5.39) from Laplace space, which yields:

$$p_{wD}(t_D) = C_n g'_{wD}(S, C_n, t_D) + C_n \sum_{k=1}^{n-1} \left[p_{wD}(k_+) - p_{wD}(k_-) \right] g'_{wD}(S, C_n, t_D - k) +$$

$$\sum_{k=1}^{n-1} (C_n - C_k) \int_{k-1}^k g'_{WD}(S, C_n, t_D - \tau_D) p'_{WD}(\tau_D) d\tau_D . \quad (5.40)$$

This solution can be applied to interesting practical cases.

5.2.1. Change in Pipe Diameter

In some DST's the **flow** period is characterized by a change in the wellbore storage coefficient due to different drill collar and drill string internal diameters. Figure 5.6 shows a typical wellbore pressure response for **this** case. Notice the change in slope as the liquid level reaches the interface between the drill collars and the drill pipe at time t_l .

Because **for this** case the wellbore pressure is continuous, Eq. (5.40) is simplified, and the equation for the pressure buildup period becomes:

$$p_{WD}(t_D) = C_{SD} g'_{WD}(S, C_{SD}, t_D) + (C_{SD} - C_{ID}) \int_0^{t_{ID}} g'_{WD}(S, C_{SD}, t_D - \tau_D) p'_{WD}(\tau_D) d\tau_D + \\ (C_{SD} - C_{2D}) \int_{t_{ID}}^{t_p} g'_{WD}(S, C_{SD}, t_D - \tau_D) p'_{WD}(\tau_D) d\tau_D . \quad (5.41)$$

If the shut-in time is large, so that $g'_{WD}(S, C_{SD}, t_D - t_p) \approx g'_{WD}(S, C_{SD}, t_D)$, then the integrands in Eq. (5.41) become $p'_{WD}(\tau_D)$. Performing the integrals and using a long time approximation for the "slug test" solution described in Appendix A, which is given by $g'_{WD}(S, C_{SD}, t_D) = C_{SD}/(2 t_D)$, Eq. (5.41) reduces to:

$$p_{ws}(\Delta t) = p_i - \frac{q_w^* \mu}{4\pi k h} \left[1 + \frac{C_S (p_i - p_{ff})}{q_w^* t_p} \right] \frac{t_p}{t_p + \Delta t} , \quad (5.42)$$

where the average flow rate is given by:

$$q_w^* = \frac{C_{F1} (p_{w1} - p_{fi}) + C_{F2} (p_{ff} - p_{w1})}{t_p} . \quad (5.43)$$

The long time behavior of the shut-in pressure is not influenced by the change in storage dur-

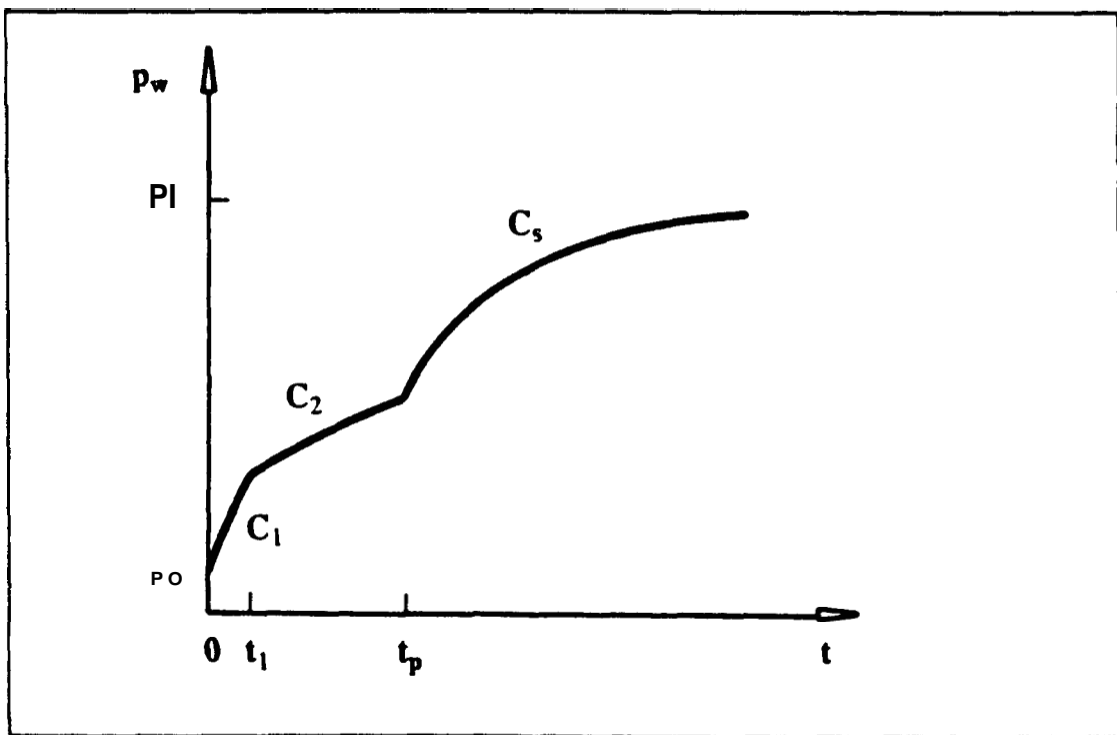


Figure 5.6 DST with Change in Pipe Diameter

ing production. An important consequence of this equation is that even for large changes in the wellbore storage coefficient during the flow period, the average flow rate should be used for computing the permeability from analysis of pressure buildup data. This fact may be useful in the analysis of pressure data obtained from closed chamber tests.

5.22 Second DST Cycle

A pressure response for a double-cycle DST is presented in Fig. 5.4. For the general case of a double cycle where the storage coefficients are unequal, Eq. (5.40) becomes:

$$\begin{aligned}
 p_{WD}(t_D) = & C_4 g'_{WD}(S, C_4, t_D) + \left[p_{WD}(t_{2D+}) - p_{WD}(t_{2D-}) \right] C_4 g'_{WD}(S, C_4, t_D - t_{2D}) + \\
 & (C_4 - C_1) \int_0^{t_{1D}} g'_{WD}(S, C_4, t_D - \tau_D) p'_{WD}(\tau_D) d\tau_D + (C_4 - C_2) \int_{t_{1D}}^{t_{2D}} g'_{WD}(S, C_4, t_D - \tau_D) p'_{WD}(\tau_D) d\tau_D + \\
 & (C_4 - C_3) \int_{t_{2D}}^{t_{3D}} g'_{WD}(S, C_4, t_D - \tau_D) p'_{WD}(\tau_D) d\tau_D. \tag{5.44}
 \end{aligned}$$

For the case where $C_1 = C_3 = C_F$ and $C_2 = C_4 = C_S$, Eq. (5.44) reduces to:

$$\begin{aligned}
 p_{WD}(t_D) = & C_{SD} g'_{WD}(S, C_{SD}, t_D) + \left[p_{WD}(t_{2D+}) - p_{WD}(t_{2D-}) \right] C_{SD} g'_{WD}(S, C_{SD}, t_D - t_{2D}) + \\
 & (C_{SD} - C_{FD}) \int_0^{t_{1D}} g'_{WD}(S, C_{SD}, t_D - \tau_D) p'_{WD}(\tau_D) d\tau_D + \\
 & (C_{SD} - C_{FD}) \int_{t_{2D}}^{t_{3D}} g'_{WD}(S, C_{SD}, t_D - \tau_D) p'_{WD}(\tau_D) d\tau_D. \tag{5.45}
 \end{aligned}$$

Making the assumptions that each shut-in time is large compared to its corresponding flowing time, the terms inside the first and second integrals of Eq. (5.45) can be approximated by $g'_{WD}(S, C_{SD}, t_D)$ and $g'_{WD}(S, C_{SD}, t_D - t_{2D})$ respectively. Using the fact that at late time $g'_{WD}(S, C_{SD}, t_D) = C_{SD}/(2 t_D)$, Eq. (5.45) becomes:

$$p_{WD}(t_D) = \frac{[p_{WD}(t_{3D}) - p_{WD}(t_{2D-})] + C_{FD} [p_{WD}(t_{2D+}) - p_{WD}(t_{3D})]}{2(t_D - t_{2D})} + \frac{C_{SD} p_{WD}(t_{1D}) + C_{FD} [1 - p_{WD}(t_{1D})]}{2 t_D} \quad (5.46)$$

Applying the nomenclature defined in Fig. 5.4, Eq. (5.46) results in:

$$p_{ws}(\Delta t) = p_i - \frac{q_{w2}^* \mu}{4\pi k h} \left[1 + \alpha_{w2} \right] R_C(\Delta t_2), \quad (5.47)$$

where the dimensionless time ratio R_C is given by:

$$R_C(\Delta t_2) = \frac{t_{p2}}{t_{p2} + \Delta t_2} + \frac{q_{w1}^*}{q_{w2}^*} \frac{1 + \alpha_{w1}}{1 + \alpha_{w2}} \frac{t_{p1}}{t_{c1} + t_{p2} + \Delta t_2}, \quad (5.48)$$

and the coefficients α_w 's are given by:

$$\alpha_{w1} = \frac{C_S (p_i - p_{ff1})}{q_{w1}^* t_{p1}}, \quad (5.49)$$

and:

$$\alpha_{w2} = \frac{C_S (p_{sf1} - p_{ff2})}{q_{w2}^* t_{p2}} \quad (5.50)$$

5.3. FIELD CASES

So far we have discussed the use of an analytical solution to the **DST** problem only for the purpose of analyzing pressure buildup data. However, a **DST** flow period is an extra source of data that may be used to gather information on the reservoir parameters. Although the solution described in Eq. (5.7) may be used to automatically match **DST** data with a non-linear regression process, **this** will not be discussed here. Nevertheless, we will consider an integrated approach to analysis of **DST** pressure data which uses information from both flowing and shut-in phases separately.

53.1. High Productivity Well

This field test is related to an open hole DST performed in an oil well, which fully penetrates a conglomerate reservoir. The DST pressure-time chart is presented in Fig. 5.7. Detailed pressure-time data and additional well and reservoir data are presented in Table 5.1.

Pressure buildup data are plotted against the Cartesian time ratio, $RC = t_p/(t_p + \Delta t)$, as shown in Fig. 5.8. A representative straight line may be traced through the last 15 points, indicating a fairly homogeneous behavior of the reservoir during pressure recovery. Extrapolation of the data to an infinite shut-in time such that $t_p/(t_p + \Delta t) \rightarrow 0$, gives the initial reservoir pressure, $p_i = 892$ psi. The slope of the Cartesian straight line is found to be $m_C = 45.8$ psi.

An estimate of the formation permeability is found by means of Eq. (5.25), which yields:

$$k = 70.6 \frac{q_w^* B \mu}{m_C h} = \frac{70.6 (539) (1.055) (60)}{(45.8) (38)} = 1.38 \times 10^3 \text{ md} \quad (5.51)$$

The conversion factor **70.6** in Eq. (5.51) is required when oilfield units, as given in Table 5.1, are used in Eq. (5.25). Note the introduction of the oil formation volume factor **B** to correct the flow rate to bottom-hole condition.

The skin effect should be determined from the analysis of flow period data. The shape of the flowing pressure curve in Fig. 5.7 suggests a stimulated well. A plot of flowing wellbore pressure versus square root of flowing time is displayed in Fig. 5.9. A straight line may be drawn using the first 15 points, excluding the very first one ($t = 0$). In fact, it seems that the reported initial flowing pressure, $p_0 = 142.4$ psi, is in error. An estimate of the initial flowing pressure from Fig. 5.9 gives $p_0 = 86$ psi. The early time behavior of the test may be represented by:

$$p_{wf}(t) = p_0 + m_F \sqrt{t}, \quad (5.52)$$

where the slope of the straight line is found from the early time approximation for the zero skin "slug test" solution, $p_{wD}(t_D) = 1 - (2/C_D) (\sqrt{C_D/\pi})$, described in Appendix A, Eq. (A.30),

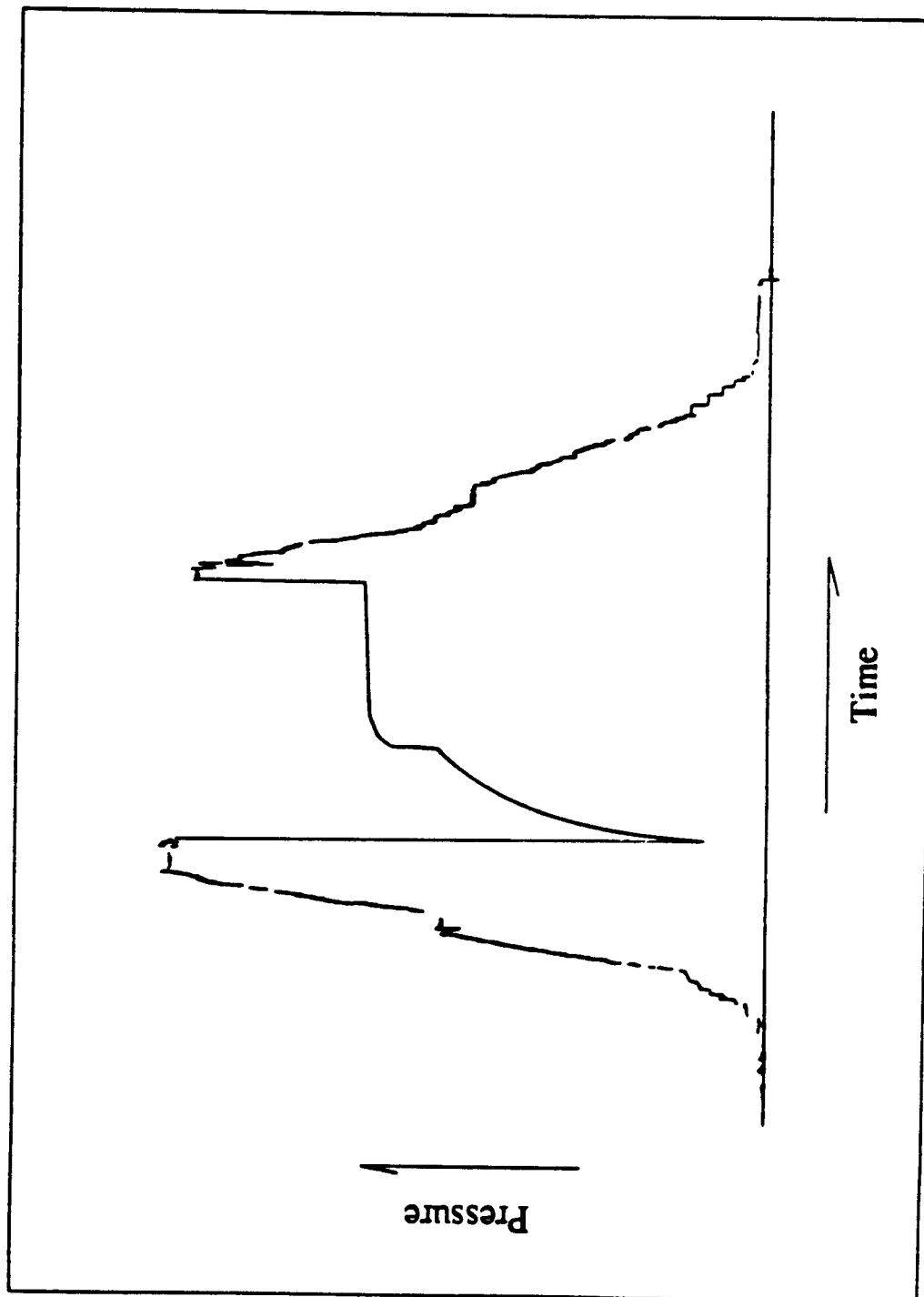


Figure 5.7 DST Chart for Well A

Rock and Fluid Data											
$\phi = 0.062$		$h = 38 \text{ ft}$		$c_t = 10.2 \times 10^{-6} \text{ psi}^{-1}$		$r_w = 0.354 \text{ ft}$					
$B_o = 1.055 \text{ RB/STB}$		$\mu_o = 60 \text{ cp}$		$q_w^* = 539 \text{ STBID}$		$C_F = 0.0365 \text{ RB/psi}$					
Pressure Data											
Flow Period				Shut-in Period							
t, hr	p_{wf}, psi	t, hr	p_{wf}, psi	At, hr	p_{ws}, psi	At, hr	p_{ws}, psi				
0.000	142.4	0.264	430.3	0.000	712.2	0.372	856.6				
0.022	186.2	0.295	449.6	0.022	766.9	0.418	858.2				
0.026	195.1	0.334	470.9	0.026	798.7	0.470	859.4				
0.034	209.9	0.372	491.0	0.034	816.4	0.528	861.0				
0.041	221.6	0.418	511.1	0.041	824.0	0.590	862.2				
0.053	239.3	0.470	537.7	0.053	830.9	0.662	863.4				
0.067	261.8	0.528	561.0	0.067	835.7	0.774	864.6				
0.084	282.3	0.590	583.9	0.084	838.9	0.835	865.8				
0.106	310.5	0.662	607.3	0.106	841.3	0.938	867.4				
0.132	333.4	0.774	630.2	0.132	844.1	1.051	868.7				
0.166	364.0	0.835	655.1	0.166	846.9	1.181	870.3				
0.187	380.0	0.938	677.2	0.187	848.5	1.325	871.5				
0.209	394.9	1.051	698.9	0.209	849.8	1.486	872.3				
0.235	412.2	1.126	712.2	0.235	851.4	1.666	873.5				
				0.264	852.6	1.870	874.7				
				0.295	853.8	2.098	876.3				
				0.334	855.4	2.189	876.3				

TABLE 5.1 - DST Data for Well A

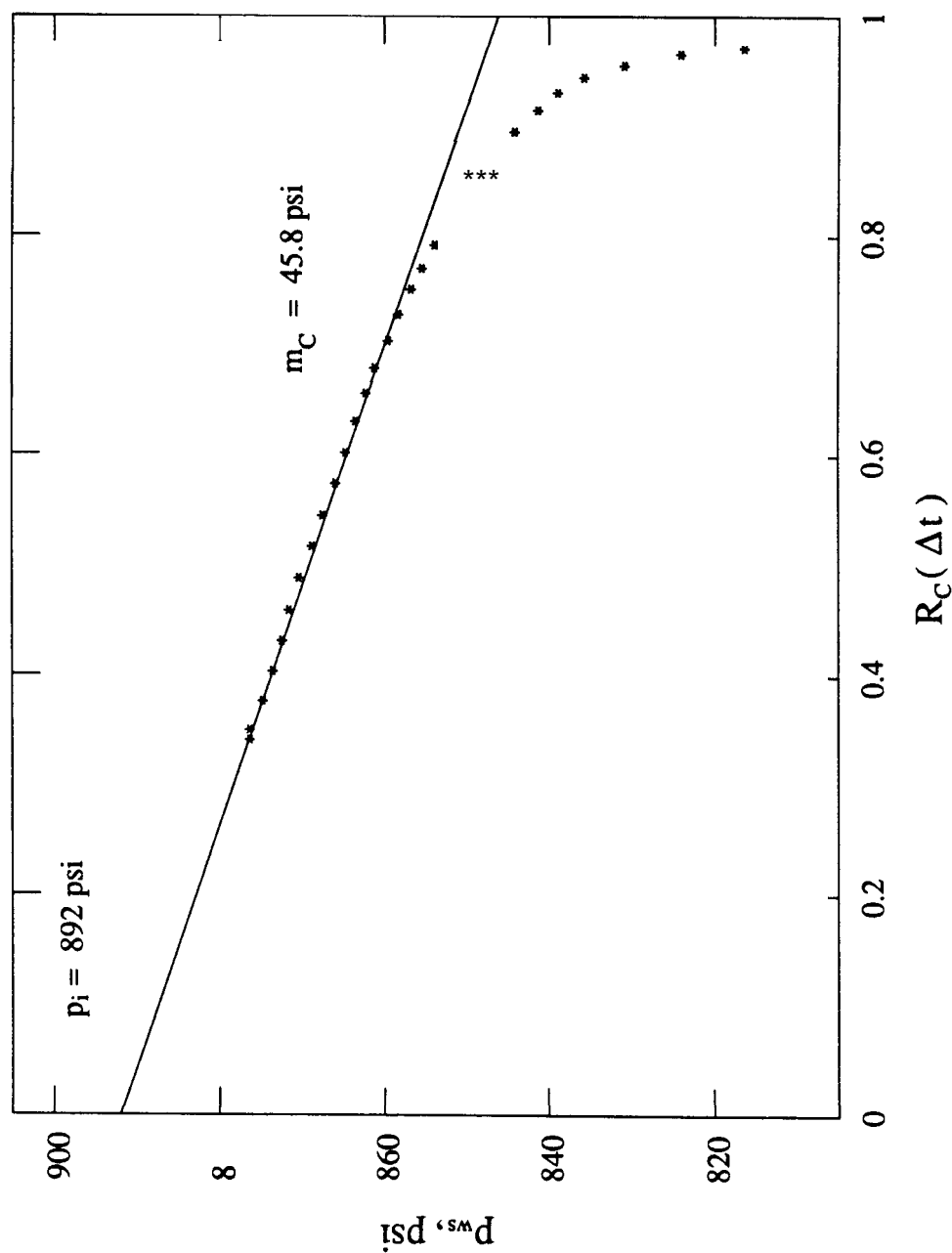


Figure 5.8 - Pressure Buildup Analysis for Well A

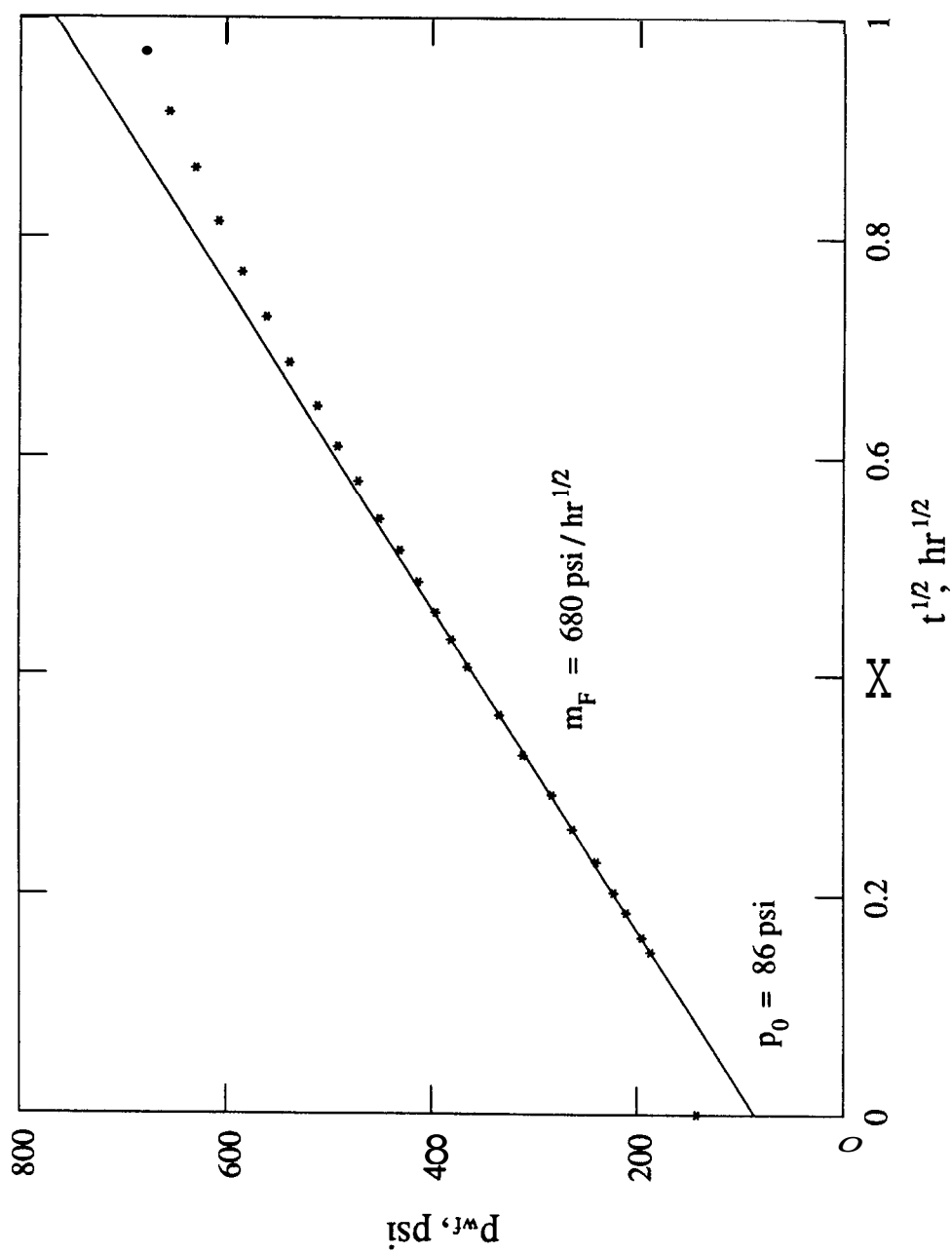


Figure 5.9 - Flow Analysis for Well A

resulting in:

$$m_F = \frac{4 \sqrt{\pi} (p_i - p_0) r_w \sqrt{(k h / \mu)} (\phi h c_t)}{C_F} \quad (5.53)$$

Assuming that stimulated wells present an effective wellbore radius given by $r'_w = r_w e^{-S}$, then Eq. (5.53) may be solved for the skin effect, yielding:

$$S = \ln \left[\frac{0.0205 (p_i - p_0) r_w \sqrt{(k h / \mu)} (\phi h c_t)}{m_F C_F} \right], \quad (5.54)$$

where the constant 0.0205 used in Eq. (5.54) is required when the oilfield units defined in Table 5.1 are used.

Using the available data, the skin effect for well this is computed from Eq. (5.54) as follows:

$$S = \ln \left[\frac{0.0205 (892 - 86) (0.354) \sqrt{(877)} (2.4x)}{(680)(0.0365)} \right] = -3.4. \quad (5.55)$$

The damage ratio may be determined by using this result for the skin effect in Eq. (5.29), yielding:

$$DR = \left[1 + 0.1592(-3.4) \right] \exp \left[\frac{0.1(-3.4)}{6.29 + (-3.4)} \right] = 0.41, \quad (5.56)$$

and the productivity ratio, which is defined as the reciprocal of the damage ratio, can be found to be $PR = 2.5$.

Although the well has not been artificially stimulated, the figures have shown that production has improved on the order of 150%. This fact has been systematically observed from the analysis of DST's performed in open hole wells, and it is believed to be related to the stimulation effect of the sudden initial pressure drop imposed on the formation.

53.2. Low Productivity Well

This example discusses the case of DST in a low productivity well. Figure 5.10 displays a pressure-time chart obtained from a DST performed in the oil well producer, 7-APR-10-BA, located at the Reconcavo Basin in Brazil. Rock, fluid and detailed pressure-time data are presented in Table 5.2. Figure 5.11 presents a Cartesian graph of the wellbore pressure versus the time ratio $R_C(\Delta t)$ for both shut-in periods. For the final pressure buildup phase, $R_C(\Delta t)$ is given by Eq. (5.48), while for the initial shut-in, $R_C(\Delta t) = t_p/(t_p + \Delta t)$.

Extrapolation of the shut-in pressure to $R_C = 0$ in Fig. 5.11 indicates an initial reservoir pressure of $p_i = 2,405$ psi. The Cartesian straight lines for both shut-in phases extrapolate to the same pressure value, indicating that no major anomaly was detected during the test period, and that homogeneous reservoir behavior was obtained.

The slopes of the straight lines representing the initial and final pressure buildup phases were computed from Fig. 5.11 to be $m_{C1} = 1,105$ psi and $m_{C2} = 850$ psi respectively. The reservoir permeability may be determined by applying Eq. (5.51) independently to both the initial and final shut-in periods. It may be anticipated that the poor fluid recovery indicates a low permeability zone. The computed reservoir permeability from the initial pressure buildup period is:

$$k_1 = 70.6 \frac{q_w^* B \mu}{m_{C1} h} = \frac{70.6 (214) (1.27) (0.8)}{(1,105) (49)} = 0.28 \text{ md} , \quad (5.57)$$

and for the final shut-in the permeability is computed as:

$$k_2 = 70.6 \frac{q_w^* B \mu}{m_{C2} h} = \frac{70.6 (140) (1.27) (0.8)}{(850) (49)} = 0.24 \text{ md} . \quad (5.58)$$

Although the DST chart in Fig. 5.10 could be read, let us consider the case in which pressure-time data for both production periods were not available. In that case, the integrated approach to calculate the **skin** effect, based on early time solutions to the production phase, would not be appropriate. However, it is possible to estimate the **skin** effect using the

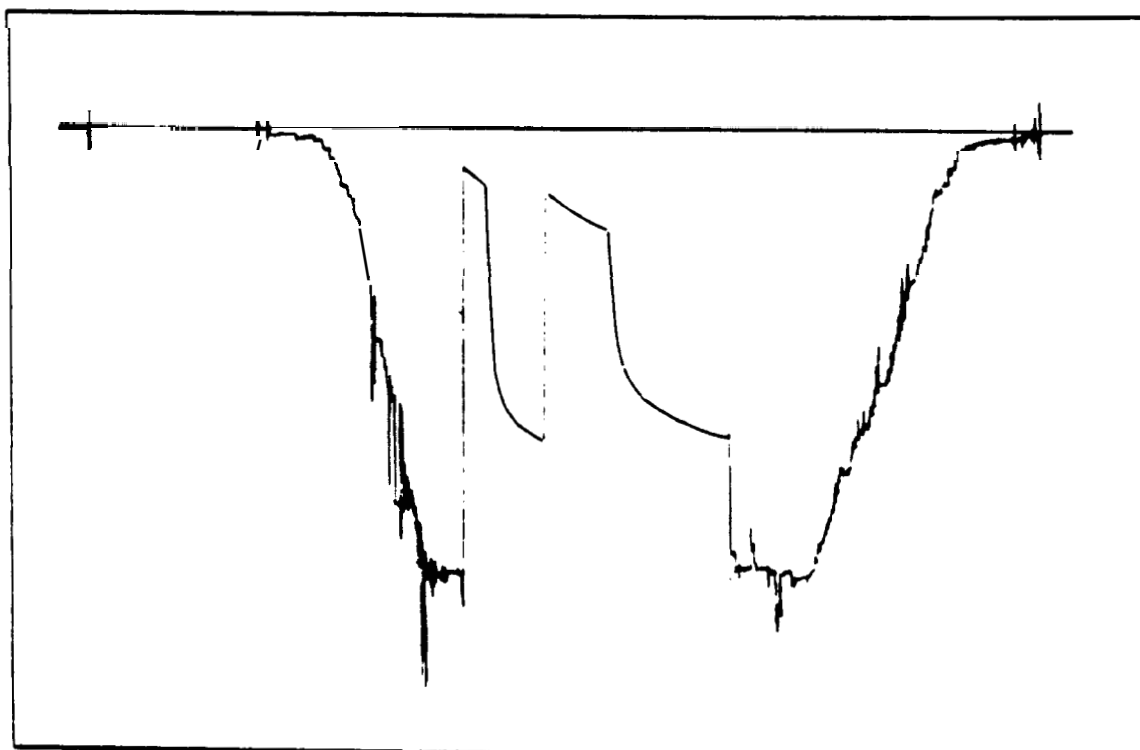


Figure 5.10 DST Chart for Well 7-APR-I O-BA

Rock and Fluid Data					
$\phi = 0.15$	$h = 49 \text{ ft}$	$c_t = 10 \times 10^{-6} \text{ psi}^{-1}$	$r_w = 0.40 \text{ ft}$		
$B_o = 1.27 \text{ RBISTB}$	$\mu_o = 0.8 \text{ cp}$	$q_{w1}^* = 214 \text{ STBID}$	$q_{w2}^* = 140 \text{ STBID}$		
$C_F = 0.0403 \text{ RBpsi}$		$C_S = 0.1 \times 10^{-3} \text{ RBpsi}$			
$t_{p1} = 0.538 \text{ h}$		$t_{s1} = 1.435 \text{ h}$	$p_{fi1} = 265 \text{ psi}$	$p_{ff1} = 384 \text{ psi}$	
$t_{p2} = 1.555 \text{ h}$		$t_{s2} = 2.947 \text{ h}$	$p_{fi2} = 439 \text{ psi}$	$p_{ff2} = 664 \text{ psi}$	
Pressure Buildup Data					
First Shut-in Period			Second Shut-in Period		
$\Delta t, \text{ h}$	$R_C(\Delta t)$	$p_{ws}, \text{ psi}$	$\Delta t, \text{ h}$	$R_C(\Delta t)$	$p_{ws}, \text{ psi}$
0.000	1.000	384	0.000	1.083	664
0.101	0.842	944	0.264	0.932	1472
0.115	0.824	1013	0.302	0.914	1527
0.134	0.800	1129	0.346	0.893	1555
0.154	0.778	1198	0.394	0.872	1596
0.182	0.747	1335	0.451	0.849	1637
0.211	0.718	1438	0.523	0.820	1678
0.250	0.683	1561	0.605	0.791	1712
0.269	0.667	1589	0.701	0.758	1747
0.298	0.644	1644	0.821	0.722	1785
0.322	0.626	1678	0.970	0.681	1822
0.355	0.602	1719	1.056	0.659	1839
0.394	0.577	1754	1.152	0.637	1863
0.432	0.554	1788	1.262	0.613	1884
0.485	0.526	1819	1.382	0.589	1904
0.542	0.498	1852	1.526	0.562	1925
0.610	0.469	1891	1.690	0.535	1951
0.691	0.438	1925	1.882	0.506	1973
0.792	0.404	1959	2.102	0.477	2001
0.917	0.370	2001	2.366	0.446	2028
1.095	0.331	2035	2.688	0.413	2055
1.301	0.292	2076	2.947	0.390	2079
1.435	0.273	2095			

TABLE 5.2 - DST Data for Well 7-APR-IO-BA

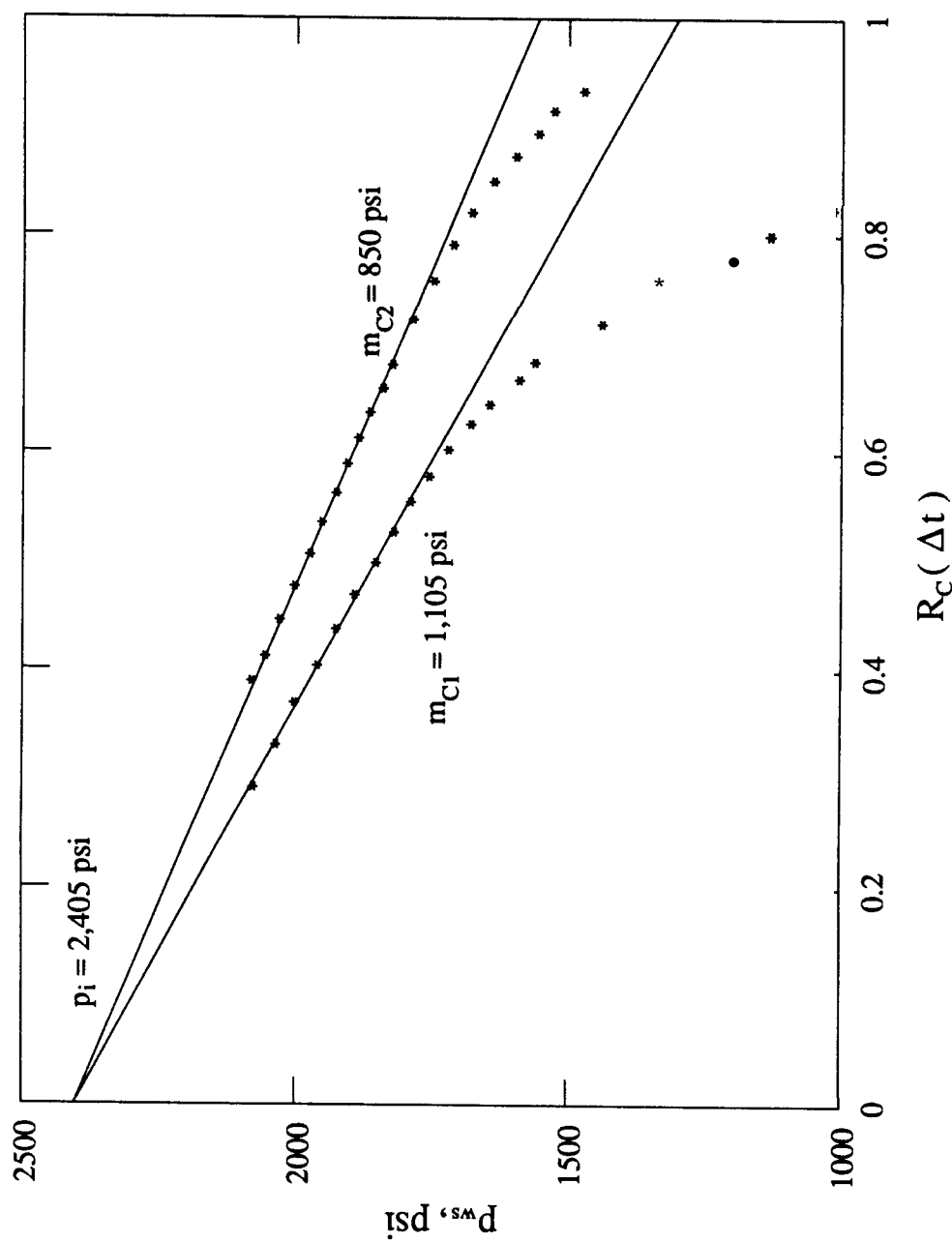


Figure 5.11 - Pressure Buildup Analysis for Well 7-APR-10-BA

following procedure.

For the first flow period, compute both the dimensionless time **and** pressure at the end of the flow period as follows:

$$\frac{t_{pD}}{C_{FD}} = 0.000295 \frac{k h}{\mu} \frac{t_p}{C_F} = \frac{0.000295 (0.28) (49) (0.538)}{(0.8) (0.0403)} = 0.068 , \quad (5.59)$$

and:

$$1 - p_{wD}(t_{pD}) = \frac{p_{ff1} - p_{fi1}}{p_i - p_{ff1}} = \frac{(384) - (265)}{(2,405) - (265)} = 0.056 . \quad (5.60)$$

With these intermediate results interpolate with the "slug test" type curve given by Ramey *et al* (1973), which yields $C_D e^{2S} = 10^2$. The skin effect can then be computed as:

$$S_1 = \frac{1}{2} \ln \left[\frac{C_D e^{2S}}{C_{FD}} \right] = \frac{1}{2} \ln \left[\frac{(10^2)}{(3,060)} \right] = -1.7 . \quad (5.61)$$

If the wellbore pressure at the end of the first pressure buildup phase **is** close to the initial reservoir pressure, then a similar procedure may be applied to compute the **skin** effect for the final cycle. The dimensionless variables at the end of the second flow period are:

$$\frac{t_{pD}}{C_{FD}} = 0.000295 \frac{k h}{\mu} \frac{t_p}{C_F} = \frac{0.000295 (0.24) (49) (1.555)}{(0.8) (0.0403)} = 0.167 , \quad (5.62)$$

and:

$$1 - p_{wD}(t_{pD}) = \frac{p_{ff2} - p_{fi2}}{p_{sf1} - p_{ff2}} = \frac{(664) - (439)}{(2,095) - (439)} = 0.136 . \quad (5.63)$$

Interpolation with the "slug test" type curve in Ramey *et al* (1975), yields $C_D e^{2S} = 35$, and the skin effect is:

$$S_2 = \frac{1}{2} \ln \left[\frac{C_D e^{2S}}{C_{FD}} \right] = \frac{1}{2} \ln \left[\frac{(35)}{(3,060)} \right] = -2.2 . \quad (5.64)$$

In both cases the well shows a stimulation condition.

As discussed by Sageev (1986), there is not a unique correlation for the slug test solution

with respect to the dimensionless group $C_D \epsilon^{2S}$, and therefore this procedure may produce uncertain results for the skin effect. However, because the permeability and the initial reservoir pressure may be obtained from pressure buildup analysis, customized type curves where the only unknown is the skin effect may be generated easily. The skin effect may be found by interpolation with these appropriate type curves.

6. DISCUSSION

The initial objective of this study was to evaluate the significance of a new approach to drillstem test analysis. This approach is to consider the shut-in portion of a DST as a continuation of the production phase in which wellbore storage changes abruptly to a smaller value. These abrupt changes were handled through the use of the unit step function. This concept is original and probably the most important result of this study.

This section discusses the implications of this new analysis technique for drillstem test pressure data as compared to previous methods of interpretation available in the literature.

6.1. INTEGRATED MATERIAL BALANCE METHOD

Initially it appeared that a solution to the problem of a "slug test" with changing wellbore storage was already available. Agarwal and Ramey (1972) presented a solution for a problem with an abrupt change in wellbore storage for a constant flow rate and a constant skin. The time derivative of that solution should have been appropriate as a solution to the "slug test". Time derivatives are readily obtained by multiplying the transformed solution by the Laplace parameter, s . Correa (1982) applied this concept to produce a solution to the DST problem. Although the pressure solution seemed to match the latter portion of pressure buildup curves, poor results were obtained for times immediately following well shut-in.

The method proposed by Agarwal and Ramey (1972) is reviewed briefly. To be consistent with the previous nomenclature, let us assume a well producing at a constant wellhead flow rate in which wellbore storage changes from C_F to C_S at time $t_p = k$. The inner boundary condition for this problem becomes:

$$C_D \frac{dp_{WD}}{dt_D} + q_{WD}(t_D) = q_D, \quad t_D > 0, \quad (6.1)$$

where:

$$C_D = C_{FD}; \quad 0 < t_D < t_{pD} = k, \quad (6.2a)$$

$$= C_{SD}; \quad t_D > t_{pD} = k. \quad (6.2b)$$

Agarwal and Ramey (1972) proposed the use of an integrated material balance technique to handle the boundary condition of Eqs. (6.1), (6.2a) and (6.2b). The method consists of integration of Eq. (6.1) with respect to time, and then Laplace transformation of the resulting equation. The authors have shown that the integrated material balance technique provides the following solution to the proposed problem:

$$\frac{p_{wD}(t_D)}{q_D} = g_{wD}(S, C_D, t_D) + [C_{SD} - C_{FD}] p_{wD}'(k) g_{wD}'(S, C_{SD}, t_D). \quad (6.3)$$

Due to the nature of the method used, Eq. (6.3) is only valid for times greater than k . The first component of the solution is the constant-rate skin and wellbore storage solution. The second component is the "slug test" solution, which approaches zero at late times.

Although the integrated material balance technique appears to be rigorously correct, it is in fact only a good approximation to the exact solution. Laplace transformation involves integration over the entire time domain, which implies that information from all times is mapped into Laplace space. The integrated version of Eq. (6.1) does not contain chronological information about the production process before the step change in wellbore storage. Therefore, the Laplace transform of the integrated equation does not reflect the correct boundary condition. At times far from the change, transients due to early production effects have little influence on the wellbore pressure response, and Eq. (6.3) becomes a very good approximate solution for the problem.

The step function method may be applied to the proposed changing wellbore storage problem. The key point is to rewrite Eqs. (6.1), (6.2a) and (6.2b) as:

$$\left[(1 - S_k) C_{FD} + S_k C_{SD} \right] \frac{dp_{wD}}{dt_D} + q_{wD}(t_D) = q_D, \quad t_D > 0. \quad (6.4)$$

Applying the procedure described in Section 4 of this study, the following solution may be obtained:

$$\begin{aligned}
 \frac{p_{WD}(t_D)}{q_D} &= g_{WD}(S, C_{SD}, t_D) + (C_{SD} - C_{FD}) g'_{WD}(S, C_{SD}, t_D - k) + \\
 &(C_{SD} - C_{FD}) \int_0^{t_D} g''_{WD}(S, C_{SD}, t_D - \tau_D) [1 - S_k] p_{WD}(\tau_D) d\tau_D + \\
 &\frac{C_{SD} - C_{FD}}{C_{SD}} [1 - S_k] p_{WD}(t_D). \tag{6.5}
 \end{aligned}$$

Equation (6.5) is valid for all times. For times greater than k , it follows that $(1 - S_k)$ is zero, and Eq. (6.5) may be simplified to:

$$\begin{aligned}
 \frac{p_{WD}(t_D)}{q_D} &= g_{WD}(S, C_{SD}, t_D) + (C_{SD} - C_{FD}) g'_{WD}(S, C_{SD}, t_D - k) + \\
 &(C_{SD} - C_{FD}) \int_0^k g''_{WD}(S, C_{SD}, t_D - \tau_D) p_{WD}(\tau_D) d\tau_D. \tag{6.6}
 \end{aligned}$$

The integral term in Eq. (6.6) may be evaluated by parts, and the solution takes the form:

$$\frac{p_{WD}(t_D)}{q_D} = g_{WD}(S, C_{SD}, t_D) + (C_{SD} - C_{FD}) \int_0^{t_D} g'_{WD}(S, C_{SD}, t_D - \tau_D) p'_{WD}(\tau_D) d\tau_D. \tag{6.7}$$

At late time such that $g'_{WD}(S, C_{SD}, t_D - k) \approx g'_{WD}(S, C_{SD}, t_D)$, Eq. (6.7) reduces to the integrated material balance solution, Eq. (6.3). Figure 6.1 displays results obtained from evaluation of both the integrated material balance and the step function solutions for an increase in wellbore storage. The values used in this figure were $C_{FD} = 1,000$, $C_{SD} = 100,000$, $S = 0$. Although results seem to agree, this is not true for all cases. Despite the fact that both solutions present similar forms, it may be shown that the wellbore pressure response given by Eq. (6.3) is discontinuous at time k . This led to the conclusion that the Agarwal and Ramey (1972) solution was approximate, and the step function solution was accurate. Figure 6.2 presents both solutions for a case where there is a decreasing wellbore storage coefficient ($C_{FD} = 1,000$, $C_{SD} = 10$, $S = 0$). In this case there is a significant difference between the two solutions at small shut-in times. This explains why the

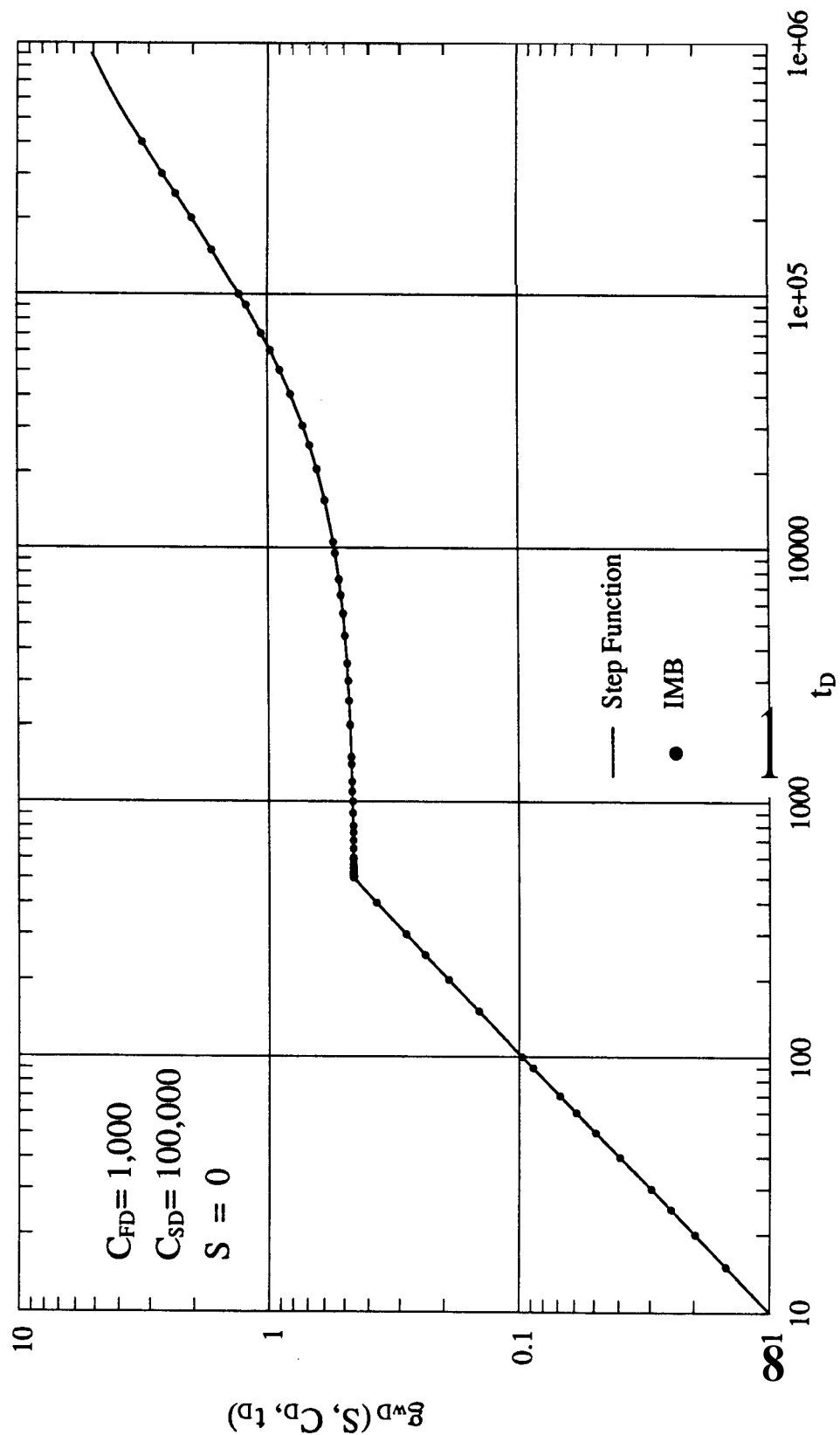


Figure 6.1 - Increasing Wellbore Storage Constant-Rate Solution

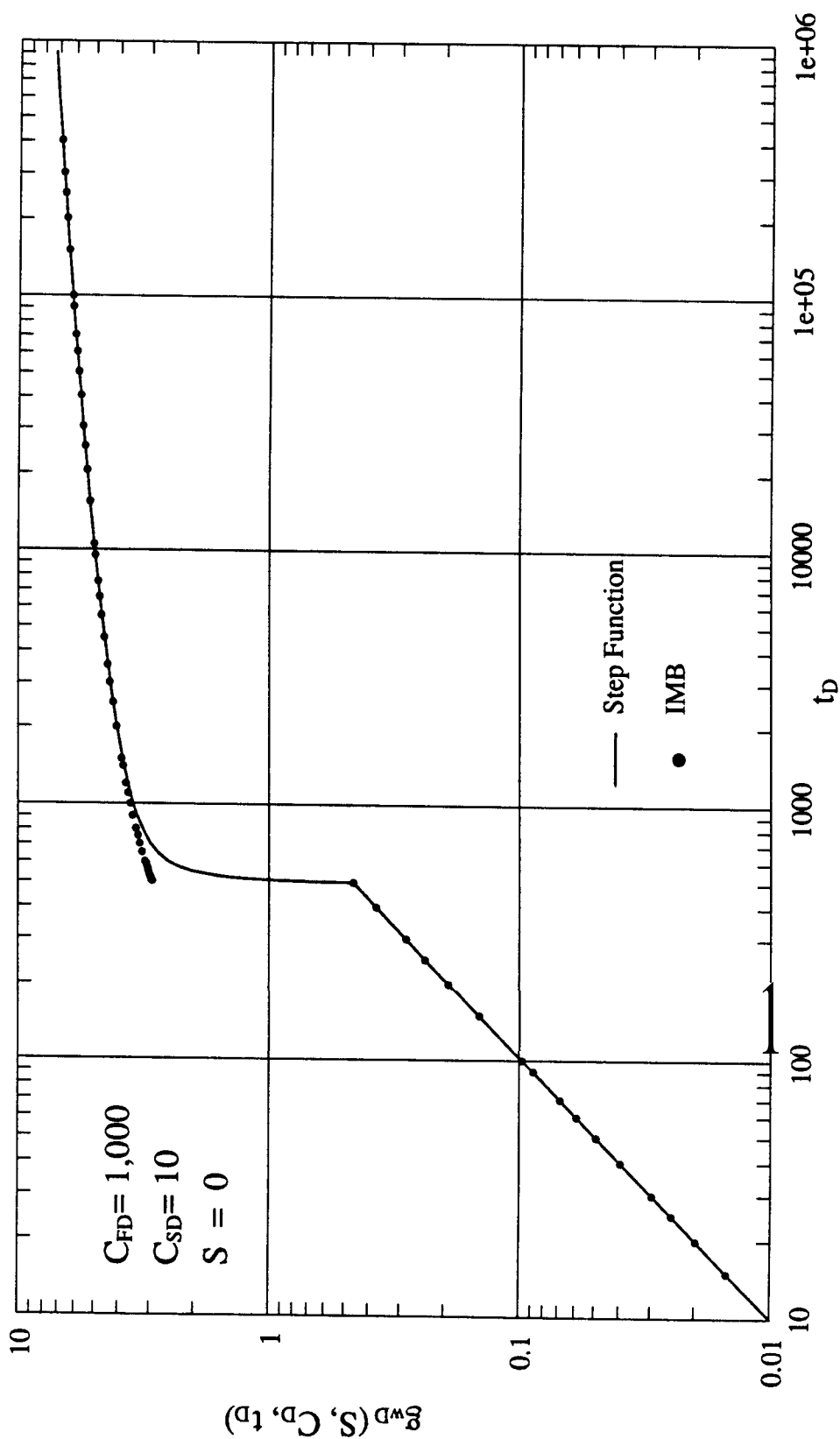


Figure 6.2 - Decreasing Wellbore Storage Constant-Rate Solution

derivative of the Agarwal and Ramey (1972) solution failed to match short time pressure buildup of drillstem tests.

In the course of **this** study, it became apparent that the use of the unit step function should offer a new method to derive solutions for problems in which the boundary conditions depend upon time. Investigation of **this** method indicated that new operational rules would be necessary to handle other interesting problems. After the development of the step function mathematics, it was discovered that solutions of many problems with mixed boundary conditions could be obtained promptly. One such example is the problem of pressure buildup following constant-pressure production. This often arises in drillstem testing of gas wells.

6.2. DST WITH CONSTANT-PRESSURE FLOW

Although the step function method is applicable to solutions of linear partial differential equations only, the theory presented in **this** study may be extended to pressure analysis of gas wells. This requires the near linearization of the gas equation through the real gas potential theory, as presented by Al-Hussainy *et al* (1966) and Al-Hussainy and Ramey (1966). In many cases the real gas potential is directly proportional either to pressure or to pressure squared.

It has been observed that most **DST's** performed in gas wells lead to constant-pressure flow. A solution of the problem of pressure buildup following constant-pressure production has been presented in Section 4 of **this** study. Solution for the pressure buildup phase **is** given by Eq. (4.36). It has also been shown in Section 5 that **this** solution may be considered a particular case of the changing storage "slug test" solution, in which the first wellbore storage coefficient is assumed to approach infinity. Therefore, the use of a long time approximation for the pressure buildup phase as discussed in Section 4.1 is appropriate. Figure 6.3 presents the effect of production time on shut-in pressure, while Fig. 6.4 presents the effect of wellbore storage and Fig. 6.5 shows the effect of skin. In all three cases pressure buildup follows constant pressure production. At late time, the results converge to a unit slope log-log straight line.

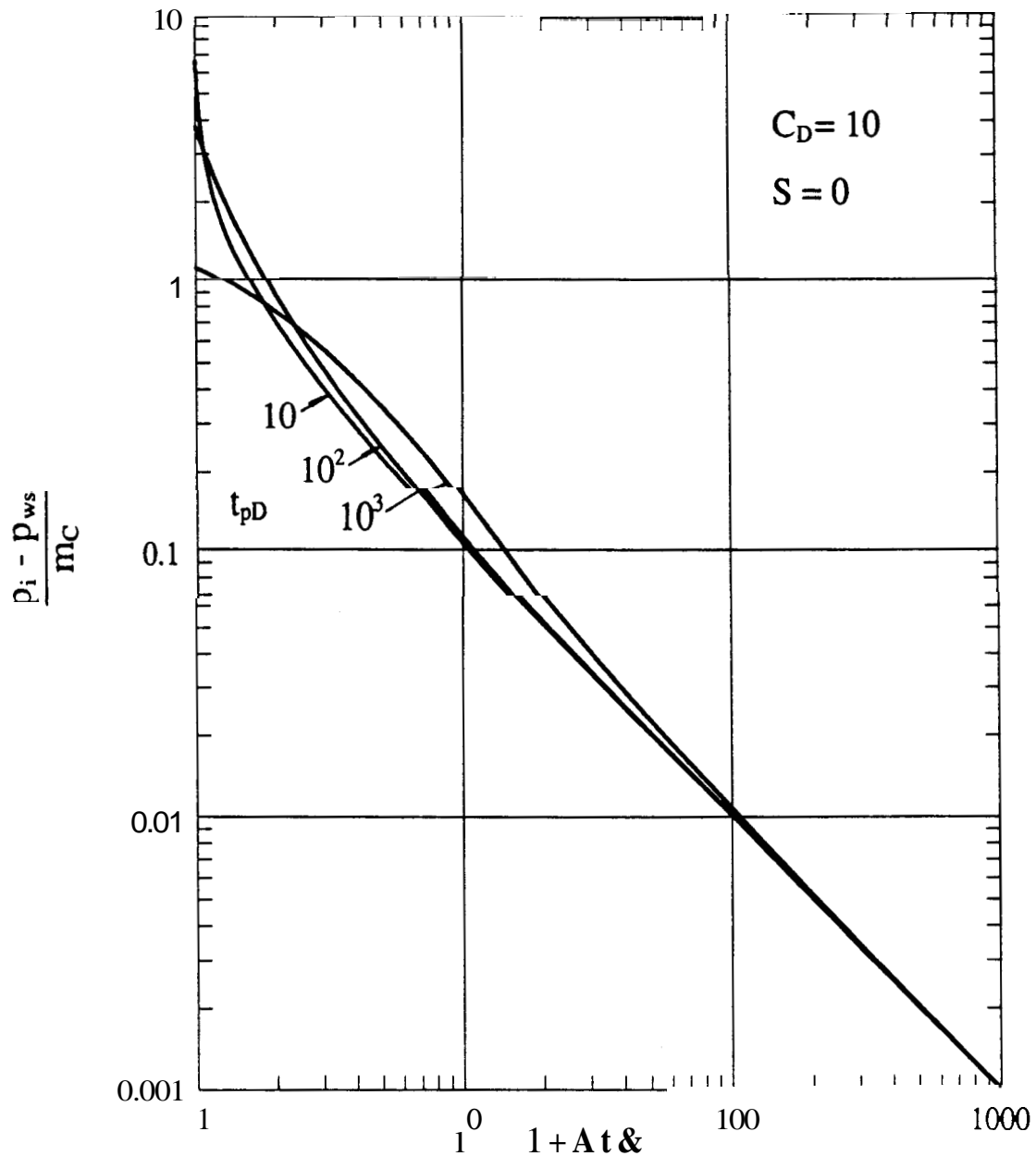


Figure 6.3 - Influence of Production Time on Pressure Buildup

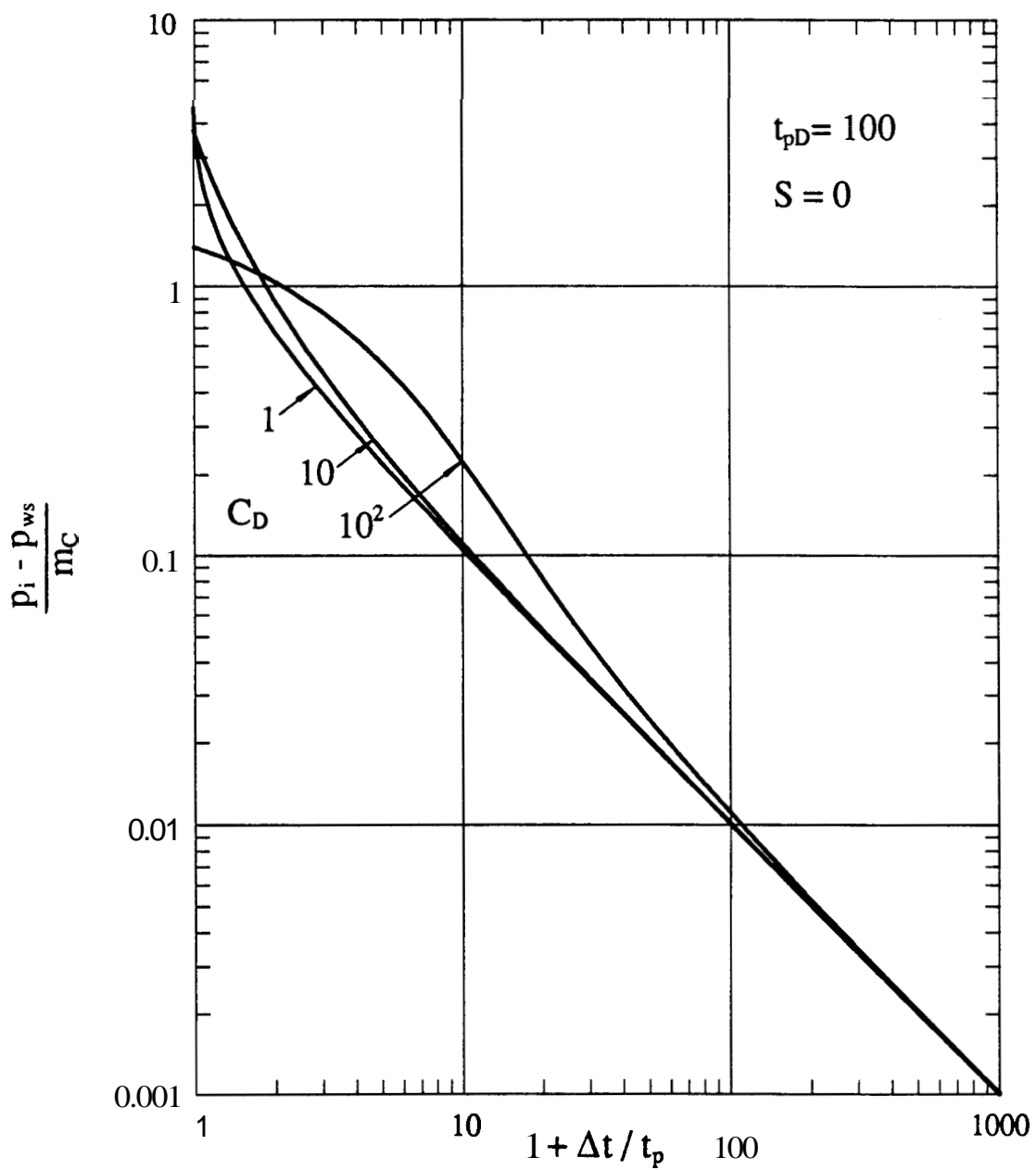


Figure 6.4 - Influence of Wellbore Storage on Pressure Buildup

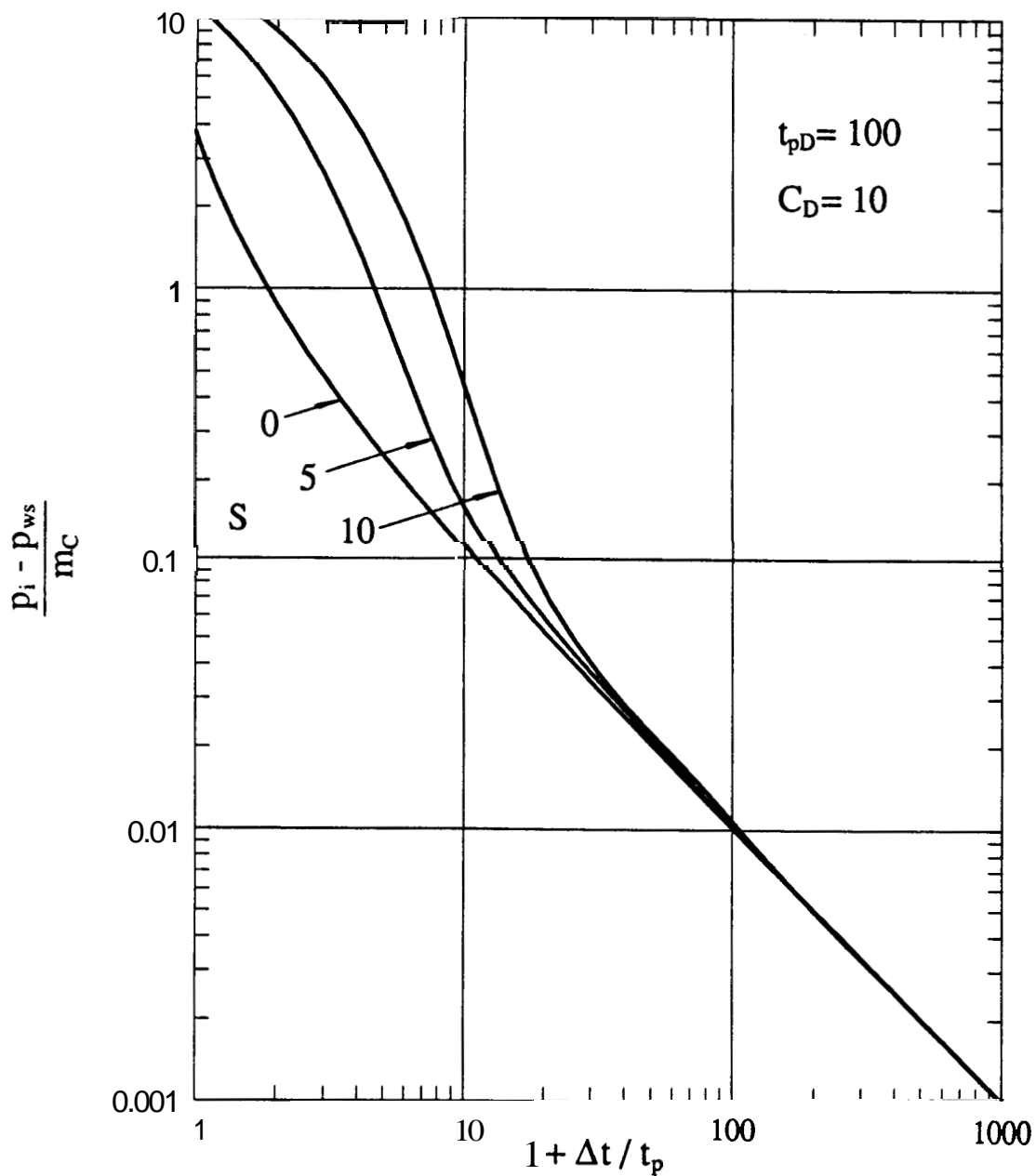


Figure 6.5 - Influence of Skin Effect on Pressure Buildup

Hence, at late time, a graph of p_{ws} versus $t_p/(t_p + \Delta t)$ may yield a straight line which extrapolates to the initial reservoir pressure. The slope of that straight line may provide an estimate of the formation permeability.

The skin effect may be obtained from information collected during the previous flow period. Because flow is held at constant-pressure, information other than pressure should be used. Jacob and Lohman (1952) described an expression for the flow rate in a well produced at constant pressure. Earlougher (1977) included a skin effect in the original formula, resulting in:

$$\frac{1}{q_{wD}(t_D)} = \frac{1}{2} \ln \frac{4 t_D}{\gamma} + S . \quad (6.8)$$

If the flow rate at shut-in is known, then Eq. (6.8) may be coupled with the expression for the pressure buildup straight line to yield the skin effect:

$$S = \frac{1}{2} \left[\frac{p_i - p_0}{m_C} \frac{q_w^*}{q_w(t_p)} - \ln \frac{4 k t_p}{\gamma \phi \mu c_t r_w^2} \right] . \quad (6.9)$$

Jacob and **Lohman** (1952) used the Theis (1935) method to analyze a recovery curve in a water well operated at constant-pressure. Recall that **both** the Theis (1935) and Horner (1951) equations are based on superposition of constant-rate solutions. Ehlig-Economides and Ramey (1979) and Uraiet and Raghavan (1979) have studied the implication of constant-pressure production in the Horner analysis. Uraiet and Raghavan concluded that in the presence of wellbore storage, the Agarwal *et al* (1970) type curve could be used to analyze pressure buildup data if $t_{pD} \geq 200 C_D$ and $S \geq 0$. These criteria are usually not satisfied for short-time drillstem tests in low productivity wells.

It is possible to show that Eq. (4.36) may be expanded to yield:

$$p_{wD}(t_D) = 1 - \int_0^{\Delta t_D} g'_{wD}(S, C_{SD}, \tau_D) q_{wD}(t_{pD} + \Delta t_D - \tau_D) d\tau_D . \quad (6.10)$$

If the shut-in time is small compared to the production time such that $t_p + \Delta t \approx t_p$, then Eq.

(6.10) may be integrated to yield:

$$\frac{p_{wD}(t_D)}{q_{wD}(t_{pD})} = g_{wD}(S, C_{SD}, \Delta t_D), \quad t_{pD} \gg \Delta t_D. \quad (6.11)$$

This result was first obtained by Ehlig-Economides and Ramey (1979). For early shut-in times, pressure buildup behavior should match the standard constant-rate drawdown type curves. As the shut-in time increases, pressure buildup behavior will deviate from the constant-rate **type** curve, however.

It would be helpful to apply a desuperposition technique in order to eliminate the effect of production from the pressure buildup data. Desuperposition methods for other problems have been presented by Slider (1971) and Agarwal (1980). Because production is held at constant pressure, a method to desuperpose the transients caused during the previous flow period is not evident.

In order to develop a desuperposition technique for **this** case, we seek a relation between terminal constant-rate and constant-pressure solutions. A common basis to correlate these solutions may be found in the cumulative production. Figure 6.6 presents the pressure drop distribution in the reservoir for both constant-rate and constant-pressure production. **Notice that** the pressure drop is normalized with respect to the sandface flow rate. For that for $t_D > 10^4$ the two distributions are in good agreement. For a given cumulative production, constant-rate and the constant-pressure production cause a similar normalized pressure drop in a reservoir. Hence, if a well produced at constant-pressure is shut-in at time t_p , then the following pressure buildup phase may be described by the **use** of superposition, which yields:

$$\frac{p_{wD}(t_D)}{q_{wD}(t_{pD})} = \frac{2 \pi k h (p_i - p_{ws})}{q_w(t_p) \mu} = g_{wD}(S, C_{SD}, t_{pD}^* + \Delta t_D) - g_{wD}(S, C_{SD}, \Delta t_D), \quad (6.12)$$

where:

$$t_p^* = \text{equivalent production time, [T].}$$

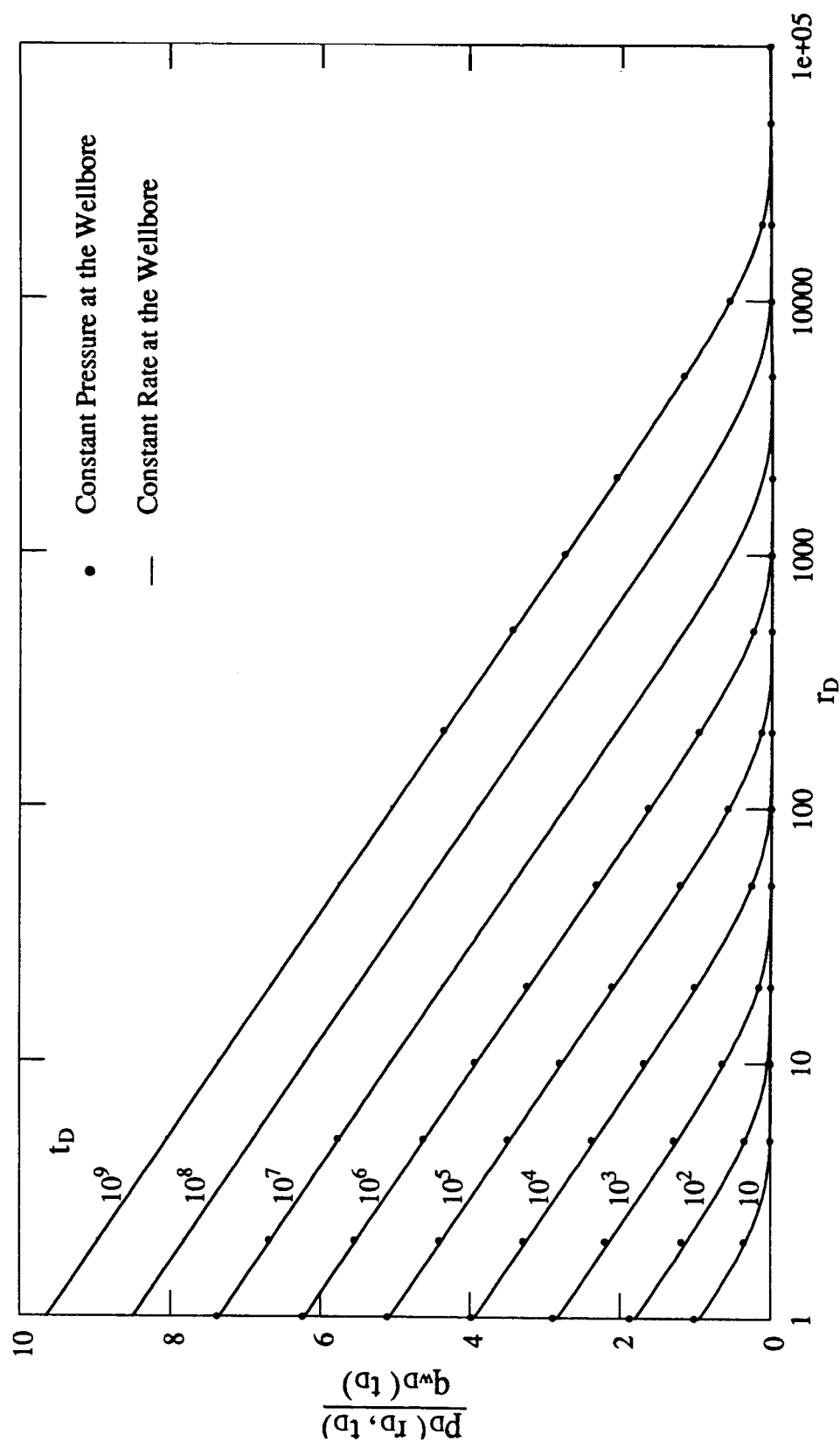


Figure 6.6 - Normalized Pressure Drop in the Reservoir

The equivalent production time is given by the ratio between the cumulative production and the sandface flow rate at the time of shut-in of the well, yielding:

$$t_{pD}^* = \frac{Q_{wD}(t_{pD})}{q_{wD}(t_{pD})} = \frac{k t_p^*}{\phi \mu c_t r_w^2}. \quad (6.13)$$

This approach indicates that, at least for the infinite acting period, desuperposed pressure buildup data may be analyzed using standard constant-rate drawdown type curves. It also suggests that application of the Homer method to constant pressure flow problems may be correct, provided the equivalent production time and the flow rate at shut-in are used. This is identical to the results obtained by Ehlig-Economides and Ramey (1979). The ideas presented in this study may also be useful in the development of methods for pressure buildup analysis in wells produced at constant pressure from either constant-pressure or no-flow external reservoir boundaries. These boundary conditions have not been studied herein.

63. HOMER ANALYSIS

So far the discussion of the use of the Homer method has been restricted to the case of constant pressure production. However, in practice, most DST pressure buildups are analyzed by the Homer method.

The internal boundary condition for a drillstem test flow period, Eq. (3.2), deserves some comments. In a drillstem test, production follows a finite wellbore pressure drop at time zero. If the flow rate is assumed to be constant, from Eq. (3.2) it follows that wellbore pressure must increase linearly with time. Hence, for any type, shape or size reservoir, fluid must be supplied to the wellbore in order to maintain a steady increase in the wellbore pressure. This is not feasible practically, and to study constant-rate production a more complex wellbore model should be considered. Frictional losses, inertial effects and critical flow are among the factors that may affect wellbore performance. These factors do not usually affect production at low flow rates however, and flow rate naturally decreases with time. There are cases when the rate

of decrease in the flow rate is slow, and production seems to be held at constant flow rate. This effect may be better observed in wells with high values of the skin effect. The main point is that in a DST with an increasing liquid level, flow rates change faster than in constant-pressure production, and the Homer method may not be applicable.

63.1. High Productivity Well

The following discussion is referred to Well A of Section 6.3.1. of this study. Figure 6.7 displays a Horner graph in which the pressure buildup data of Table 5.1 has been used. The Horner ratio in Fig. 6.7 was computed using the actual production time. Examination of the Homer graph suggests the possible existence of a linear flow barrier near the well. Recall that the same pressure buildup data was graphed in Figure 5.8, in which the time function is given by $t_p/(t_p + At)$. An analysis of Figures 5.8 and 6.7 indicates that there may be an important difference between results from the two methods. The apparent sealing fault evident in the Homer display on Figure 6.6 appears erroneous in view of Figure 5.8. Also differences in buildup extrapolated formation pressures often attributed to depletion (or supercharge by mud pressure) may be an artifact of the conventional Homer graphing. The "slug test" solution appears to be a better description of DST conditions.

Although this type of Horner analysis has been widely used in the industry, there have been methods available to correct for variations in the flow rate. Odeh and Selig (1963) proposed a correction for both production time and flow rate to be used in a conventional Horner graph. A better result from a Horner analysis for well A may be obtained if the fast decrease in the flow rate is considered. The flow rate at the shut-in time may be computed from the "slug test" condition:

$$q_w(t_p) = 24 C_F \left[\frac{dp_{wf}}{dt} \right]_{t=t_p} = 24 (0.0365) \frac{(712.2) - (698.9)}{(1.126) - (1.051)} = 155 \text{ STB/D} . \quad (6.14)$$

The equivalent production time is computed as:

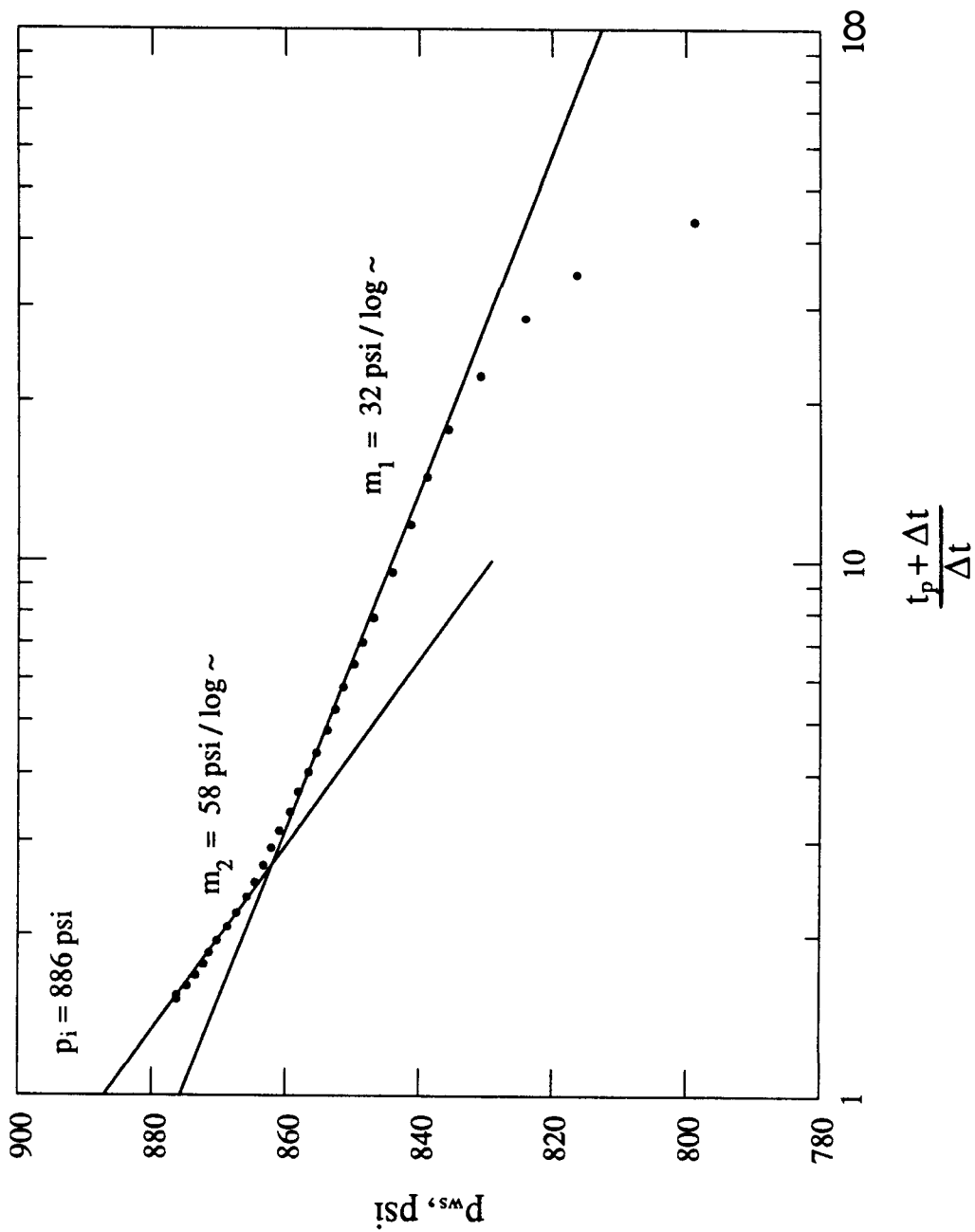


Figure 6.7 - Horner Graph for Well A with Actual Production Time

$$t_p^* = \frac{q_w^* t_p}{q_w(t_p)} = \frac{(539)(1.126)}{(155)} = 3.92 \text{ hr} . \quad (6.15)$$

Figure 6.8 presents another Homer graph for the same pressure buildup data of well A. The Homer time ratio has now been computed with the equivalent production time t_p^* . The shape of the pressure recovery curve indicates a homogeneous reservoir. The extrapolated buildup pressure yields $p_i = 890$ psi. The formation permeability may be found from the equation for the slope of the semilog straight line, which yields:

$$k = \frac{162.6 q_w(t_p) B \mu}{m_H h} = \frac{162.2(115)(1.055)(60)}{(31.0)(38)} = 1.00 \times 10^3 \text{ mD} , \quad (6.16)$$

where:

$$m_H = \text{slope of the Homer graph, } [M]^{-1} [L]^{-1} [T]^{-2}/\log \cdot$$

These results are in good agreement with the interpretation described in Section 5.3.1., which give $k = 1.035 \times 10^3$ mD and $p_i = 892$ psi. Although the Homer straight line in Fig. 6.8 starts earlier than the Cartesian straight line in Fig. 5.8, this is not always the case for comparisons with other DST data. Both graphs present no indication of discontinuities or reservoir heterogeneities during the period of the test.

The skin effect may be computed from:

$$S = 1.151 \left[\frac{p_i - p_{ff}}{m_H} - \log \frac{k t_p^*}{\phi \mu c_1 r_w^2} + 3.23 \right] = \\ 1.151 \left[\frac{(890) - (712.2)}{(31.0)} - \log \frac{(1.00 \times 10^3)(4.92)}{(0.062)(60)(10.2 \times 10^{-6})(0.354)^2} + 3.23 \right] = -0.1 . \quad (6.17)$$

There is a considerable difference between this value of the skin effect, and the value $S = -3.4$ computed in section 5.3.1. of this work. This difference deserves comments. In the derivation of Eq. (6.16) it was implicitly assumed that the constant-rate solution could be applied to compute the flowing wellbore pressure at the shut-in time. Although this solution may be used to correlate the constant-pressure production case, there is no evidence that it may

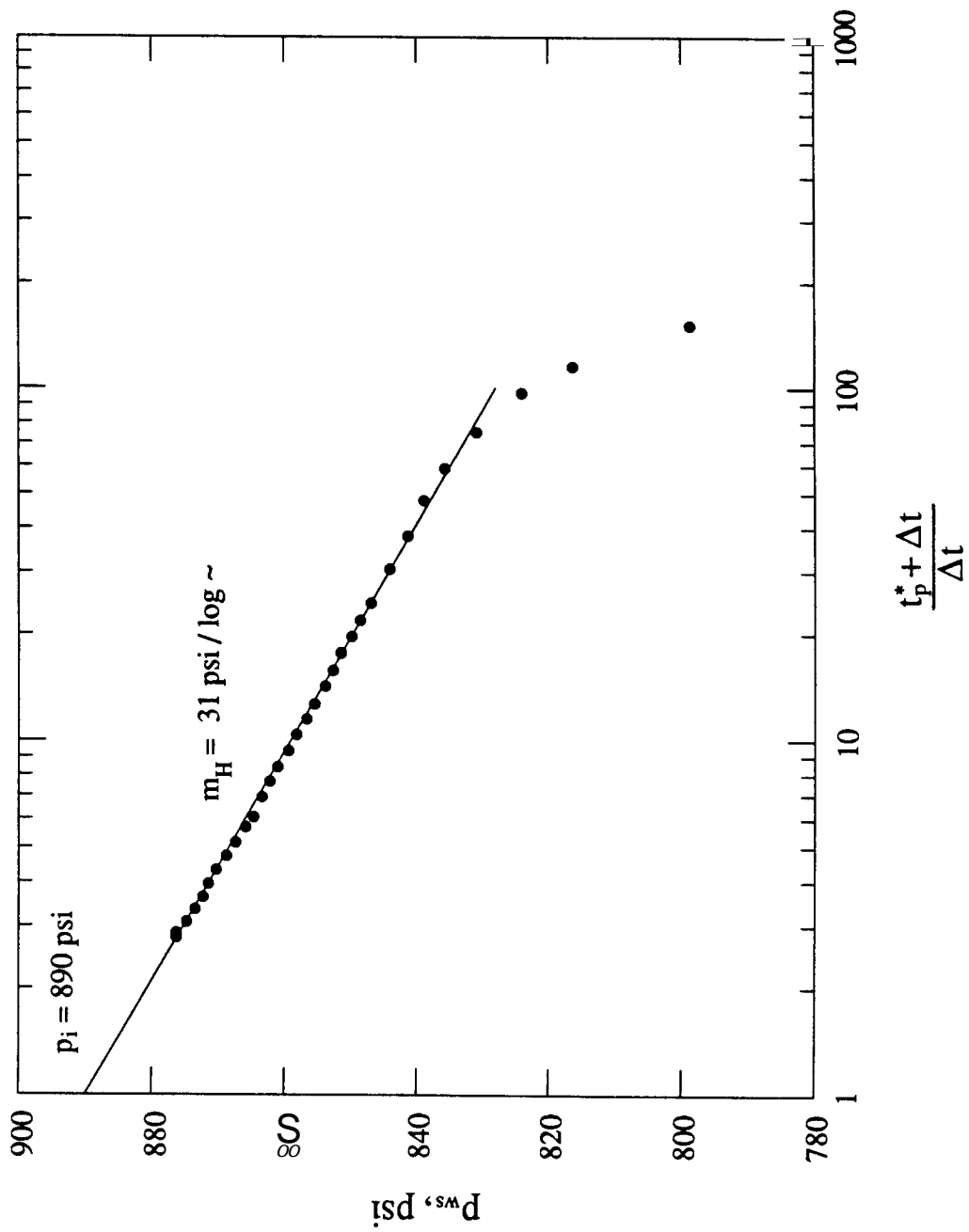


Figure 6.8 - Horner Graph for Well A with Equivalent Production Time

$$\frac{t_p^* + \Delta t}{\Delta t}$$

be used for the case of a liquid DST, which presents an increasing flowing pressure with time. On the other hand, determination of the skin effect in Section 5.3.1. used a short time approximation for the "slug test" solution, which did not consider important factors such as frictional losses in the drill pipe or inertial effects in the fluid column. Also, the fact that the diffusivity equation does not include large pressure gradients in the reservoir, which always occur during the early phase of a "slug test", may impose a serious restriction on the determination of the skin factor by means of the early time "slug test" solution. This last remark is valid whether an analytical form of the solution or a graphical type curve is used.

63.2. Low Productivity Well

Another example of application of the Homer method to pressure buildup analysis of drillstem tests may be developed with the data for the low productivity well 7-APR-10-BA described in section 5.3.2. Pressure buildup and well data are given in Table 5.2. The shape of the DST curve in Fig. 5.10 indicates that the flow rates in both production phases were approximately constant. A Homer plot for this well is presented in Figure 6.9. Because the flow rates were almost constant, the Homer time ratio of Fig. 6.9 were computed with the actual production times. From the slopes of the semilog straight lines, the formation permeabilities for the initial and final pressure buildups may be found to be 0.51 mD and 0.41 mD respectively. These values differ almost 100% from the permeabilities found in Section 5.3.2., which are 0.28 mD and 0.24 mD, respectively. The extrapolated buildup pressure may be found to be 2,280 psi from the Homer plot of Fig. 6.9, which gives a much lower value than the 2,405 psi obtained from the Cartesian analysis of Fig. 5.11. A close inspection of the Horner display in Fig. 6.9 shows a doubling of slope during the second pressure buildup phase. This apparent heterogeneity was not observed in the Cartesian analysis of Fig. 5.11. Also it seems that the last few points of the final buildup in Fig. 6.9 are still bending upwards, indicating that a stabilized growth of the shut-in pressure was not achieved.

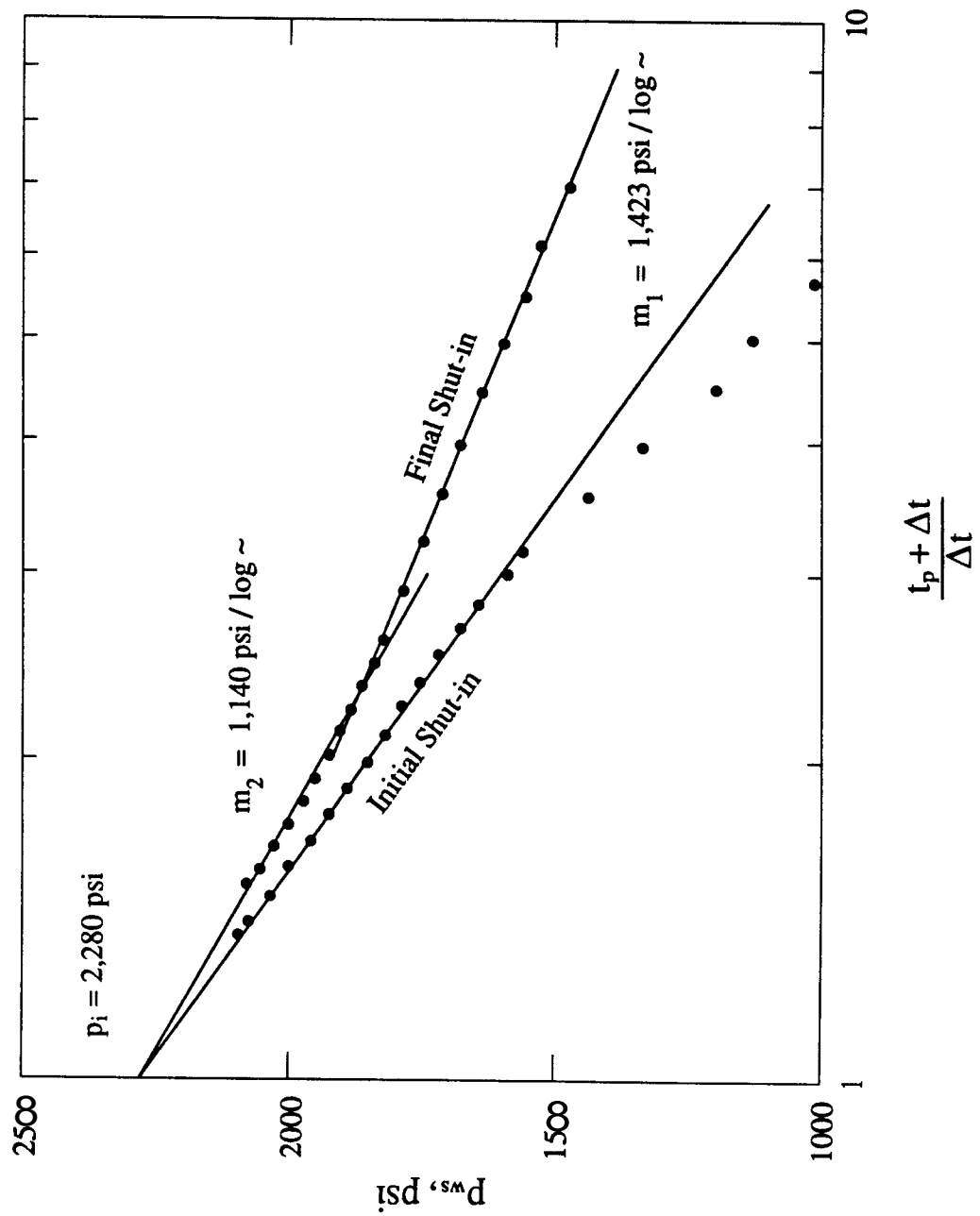


Figure 6.9 - Horner Graph for Well 7-APR-10-BA

6.4. RADIUS OF INVESTIGATION

A question that often arises in well test analysis is: How far into the formation has the test investigated. Kohlhass (1972) suggested that the distance investigated by a "slug test" may be on the order of a few wellbore radii. Ramey *et al* (1975) have shown that a "slug test" may cause measurable pressure drops at appreciable distances from the wellbore. In order to be detected by a single well transient pressure test, a reservoir anomaly should cause a measurable effect in the wellbore pressure response. The effect of flow barriers may be handled by superposition of image wells. Linear faults are often recognized by the characteristic doubling of slope on a Homer graph.

The duration of a test is the main factor in the detection of flow barriers. Because a **DST** may be viewed as a changing wellbore storage "slug test", the total time of the test should be considered in the computation of the radius of investigation. In the analysis method described in Section 5, the Cartesian straight line observed in **DST** pressure buildup data may be function of the total testing time. Intrinsic reservoir heterogeneities also affect the wellbore pressure response. Complex models such as double porosity systems often present a homogeneous behavior at late times, and anomalies detected during the latter part of a Cartesian straight line may be attributed to areal discontinuities. However, the amount of fluid withdrawn during the production phase should control the magnitude of the effect of a reservoir anomaly on the following pressure buildup. If only a small amount of fluid is produced, the pressure recovery in the well is relatively fast, and the effect of flow barriers may not be detected with the equipment available.

6.5. HOMER GRAPHS FOR SLUG TEST SOLUTIONS

Perhaps the best way to demonstrate the weakness of Horner analysis of **DST** data is by Horner graphing simulated data with the "slug test" changing storage model. Figures 6.10 to 6.12 present such results for dimensionless parameters typical of **DST** tests. The straight line

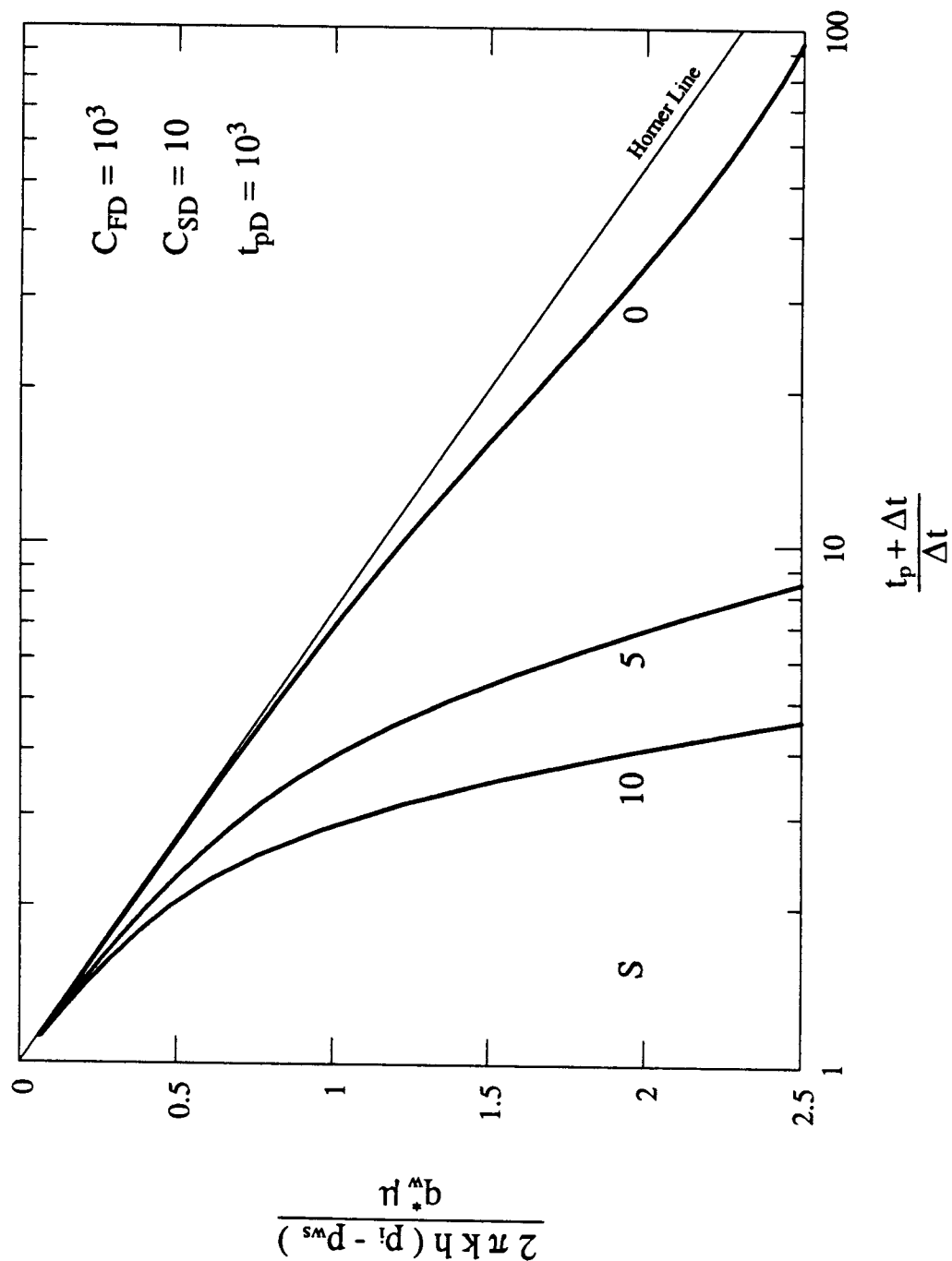


Figure 6.10 - Homer Graph for DST Model - Influence of Skin

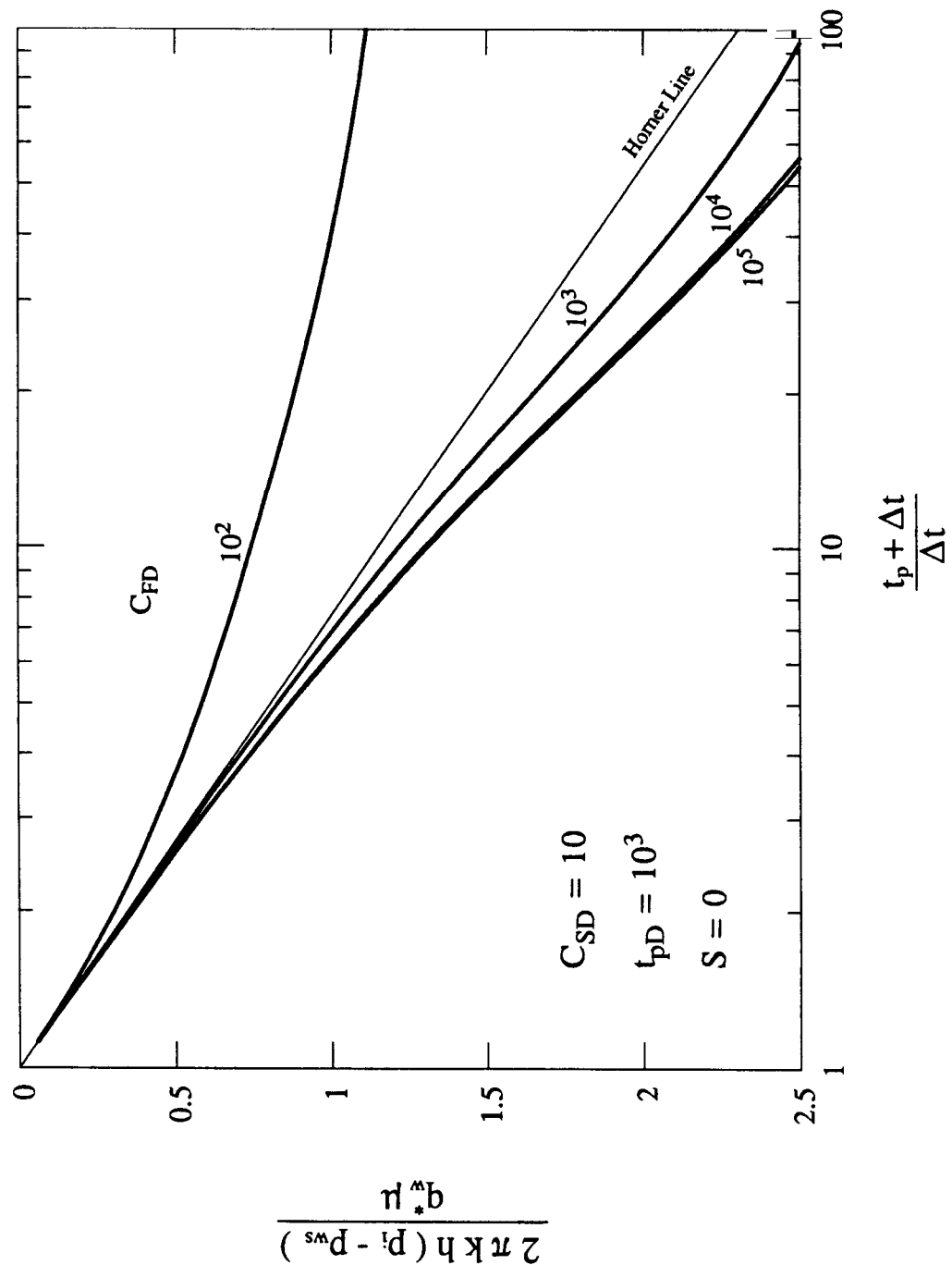


Figure 6.11 - Homer Graph for DST Model - Effect of Flowing Wellbore Storage

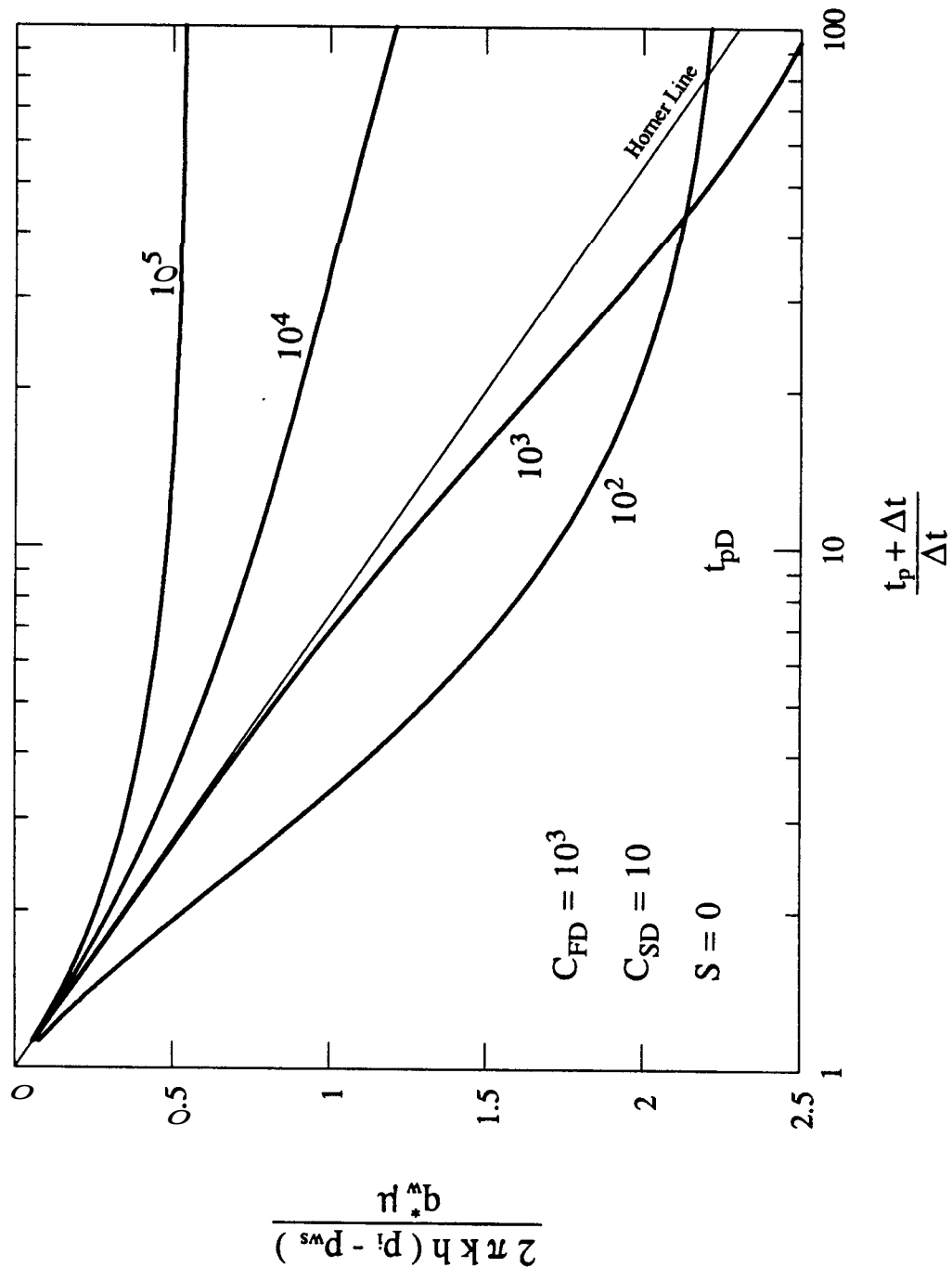


Figure 6.12 - Horner Graph for DST Model - Influence of Production Time

with a slope of 1.15/cycle **is** the correct Horner line. As can be seen from Figures 6.10 to 6.12, the simulated data do appear to form approximate straight lines, but neither the slope nor the extrapolated pressure at infinite shut in appear correct. At very long shut-in times however, the simulated data approach the apparent Horner straight line. **This** may be due **to** the fact that for large At , the Cartesian relation, $t_p/(t^p + At)$, and the Horner time ratio, $\frac{1}{2} \ln [(t_p + \Delta t)/\Delta t]$, have approximately the same numerical value.

These shows that Horner analysis results are approximate, at best.

Application of the results of **this** study to drillstem test analysis should be important in this field. The constant rate Horner type analysis appears to have been an improper application to the **DST** problem. The abrupt change in the wellbore storage concept appears much closer to actual **DST** testing conditions. In view of the large number of **DST**'s run throughout the world yearly, **this** finding should have a significant impact on the oil industry. In the cases studied *so* far, the Horner analysis often indicates either a nearby fault, or a decline in formation pressure. The new analysis indicates neither the presence of a fault, nor the apparent depletion between two shut-in periods. Results of the new analysis should lead **to** a decrease in loss of oil caused by rejection of formations for which the two shutins indicated a rapid pressure depletion -- or a very small reservoir. Review of geological maps which have been constructed with indications of nearby faults from well tests, should incorporate additional reserves and provide a better understanding of reservoir behavior. **The** changing wellbore storage concept is a new direction for models for **DST** analysis.

As a result **of this** study, several conclusions and recommendations appear warranted. They are presented in the next section.

7. CONCLUSIONS AND RECOMMENDATIONS

A general procedure to solve transient flow problems with time-dependent boundary conditions has been described. The method does not involve superposition and is not restricted to solution of the diffusivity equation. New transform and operational rules developed in this work are essential for application of the solution method to a variety of problems.

An analytical solution to the problem of pressure buildup following constant-pressure production is presented. Both a skin effect and wellbore storage are included. Pressure buildup response may be considered as a particular case of a drillstem test. A rigorous analytical solution to the drillstem test problem, which is valid for both production and shut-in phases, is obtained by modeling the DST inner boundary condition with a step change in the wellbore storage coefficient. A solution to the generalized drillstem test is also present. The solutions are used to develop practical methods for interpretation of DST pressure data. Application of the proposed methods to analysis of field data may provide estimates of the initial reservoir pressure, formation permeability and skin effect.

Although the derivations carried out in this worked assumed an arbitrary reservoir model, practical applications have been limited to radial flow. However, the theory presented here may be extended to include several features usually found in more complex flow models. Among others, we recommend that the effect of the following factors on the DST pressure response be studied:

1. Linear, spherical and elliptical flow patterns,
2. Double porosity, double permeability and composite reservoir systems,
3. Constant pressure and no-flow external boundaries.

Because the drillstem test equation may be expressed as combinations of both time derivative and integral of the constant-rate skin and wellbore storage solution, previous solutions for the constant-rate problem available in the literature may be used to produce new DST solutions for other flow models.

8. NOMENCLATURE

A	=	drainage area, [L] ²
B	=	oil formation volume factor
C	=	wellbore storage constant, [M] ⁻¹ [L] ⁴ [T] ²
C_A	=	Dietz shape factor
c_t	=	total compressibility, [M] ⁻¹ [L] [T] ²
c_w	=	compressibility of the wellbore fluid, [M] ⁻¹ [L] [T] ²
d	=	differential operator
DR	=	damage ratio
g	=	gravity acceleration constant
g_D	=	pressure response to a unit flow rate
g_{wD}	=	wellbore pressure response to a unit flow rate
h	=	formation thickness, [L]
I₀	=	modified Bessel function of first kind and zero order
k	=	formation permeability, [L] ²
k	=	dimensionless production time
K₀	=	modified Bessel function of second kind and zero order
K₁	=	modified Bessel function of second kind and first order
L	=	Laplace transform operator
m_C	=	slope of p _{ws} vs R _C (Δt) graph, [M] [L] ⁻¹ [T] ⁻²
m_F	=	slope of p _{wf} vs \sqrt{t} graph, [M] [L] ⁻¹ [T] ^{-2.5}
P	=	pressure, [M] [L] ⁻¹ [T] ⁻²
p_i	=	initial reservoir pressure, [M] [L] ⁻¹ [T] ⁻²
P_o	=	initial flowing pressure, [M] [L] ⁻¹ [T] ⁻²
P_{fi}	=	initial flowing pressure, [M] [L] ⁻¹ [T] ⁻²
P_{ff}	=	final flowing pressure, [M] [L] ⁻¹ [T] ⁻²

P_f	=	final shut-in pressure, $[M] [L]^{-1} [T]^{-2}$
P_w	=	wellbore pressure, $[M] [L]^{-1} [T]^{-2}$
p_{wf}	=	wellbore flowing pressure, $[M] [L]^{-1} [T]^{-2}$
P_{ws}	=	wellbore shut-in pressure, $[M] [L]^{-1} [T]^{-2}$
PR	=	productivity ratio
q	=	wellhead flow rate, $[L]^3 [T]^{-1}$
q_w	=	variable production rate, $[L]^3 [T]^{-1}$
q_w^*	=	average volumetric production rate, $[L]^3 [T]^{-1}$
Q_w	=	cumulative fluid recovery, $[L]^3$
r	=	radial distance from wellbore, $[L]$
r_p	=	internal radius of the production pipe, $[L]$
r_w	=	wellbore radius, $[L]$
r_e	=	effective wellbore radius, $[L]$
R_C	=	function of the shut-in time
s	=	Laplace space variable
S	=	skin factor
S_k	=	unit step function
t	=	time, $[T]$
t_c	=	cycle time, $[T]$
t_p	=	production time, $[T]$
V_w	=	volume of the bottom-hole storage chamber, $[L]^3$
α_w	=	volume ratio
β	=	reservoir shape and size factor
At	=	shut-in time, $[T]$
a	=	partial differential operator
ϕ	=	porosity, fraction of bulk volume
μ	=	viscosity, $[M] [L]^{-1} [T]^{-1}$

ρ = average density of liquid in the wellbore, [M] $[L]^{-3}$

z = variable of integration

Subscript

D = dimensionless

F = flow

S = shut-in

1 = first cycle

2 = second cycle

Physical Units

[L] = length

[M] = mass

[T] = time

9. REFERENCES

Abramovitz, M. and Stegun, I. A. (ed.): *Handbook of Mathematical Functions With Formulas Graphs and Mathematical Tables*, National Bureau of Standards Applied Mathematics Series-**55** (June 1964) 227-253.

Agarwal, R. G.: "A New Method to Account for Producing Time Effects When Drawdown Type Curves Are Used to Analyze Pressure Buildup and Other Test Data", paper presented at the SPE-AIME 55th Annual Fall Technical Conference and Exhibition, Dallas, Texas, (Sept. 21-24, 1980).

Agarwal, R. G., Al-Hussainy, R., and Ramey, H. J., Jr.: "An Investigation of Wellbore Storage and Skin Effect in Unsteady Liquid flow: I. Analytical Treatment," *Soc. Pet. Eng. J.* (Sept., 1970) 279-290.

Carslaw H. S. and Jaeger, J. C.: *Operational Methods in Applied Mathematics*, Oxford University Press, London (1941)

Carslaw H. S. and Jaeger, J. C.: *Conduction of Heat in Solids*, 1st ed., Oxford at the Clarendon Press, London (1947); 2nd ed., Oxford University Press, London (1959).

Churchill, R. V.: *Operational Mathematics*, McGraw-Hill, New York (1944)

Cooper, H. H., Jr., Bredehoeft, J. D. and Papadopoulos, I. S.: "Response to a Finite-Diameter Well to an Instantaneous Charge of Water," *Water Resour. Res.*, (1967)3(1), 263-269.

Correa, A. C.: "Well Test Analysis in Wells Produced at Constant Pressure," (in Portuguese) paper presented at the 2nd Brazilian Petroleum Congress, Rio de Janeiro, Brazil, (Oct. 3-7, 1982)

Dolan, J. P., Einarsen, C. A., and Hill, G. A.: "Special Application of Drill-Stem Test Pressure Data," *Trans., AIME* (1957) 210, 318-324.

Earlougher, R. C., Jr.: *Advances in Well Test Analysis*, Monograph Series, Society of Petroleum Engineers, Dallas (1977) 5.

Earlougher, R. C., Jr., Kersch, K. M., and Ramey, H. J., Jr.: "Wellbore Effects in Injection Well Testing," *J. Pet. Tech.* (Nov. 1973) 1244-1250.

Ehlig-Economides, C. and Ramey, H. J., Jr.: "Pressure Buildup for Wells Produced at a Constant Pressure," *Soc. Pet. Eng. J.* (Dec., 1981) 104-114.

Ehlig-Economides, C. and Ramey, H. J., Jr.: "Transient Rate Decline Analysis For Wells Produced at Constant Pressure," paper SPE 8387 presented at the SPE-AIME 54th Annual Fall Technical Conference and Exhibition, Las Vegas, Nevada, (Sept. 23-26, 1979).

Fems, J. G. and Knowles, D. B.: "The Slug Test for Estimating Transmissibility," *U. S. Geol. Survey Ground Water Note* 26, (1954) 1-17.

Gringarten, A. C., Bourdet, D., Landel, P. A., and Kniazeff, W.: "A Comparison Between Different Skin and Wellbore Storage Type Curves for Early Time Transient Analysis," Paper SPE 8205 presented at the SPE 54th Annual Fall Meeting held in Las Vegas, Nevada, (Sept. 23-26, 1979).

Horner, D. R.: "Pressure Buildup in Wells," *Proc.*, Third World Pet. Cong., The Hague (1951) Sec. 11, 503-523.

Hurst, W.: "Establishment of the Skin Effect and Its Impediment to Fluid-Flow into a Well Bore," *Per. Eng.* (Oct., 1953) Vol. 25, B-6.

Jacob, C. E. and Lohman, S. W.: "Nonsteady Flow to a Well of Constant Drawdown in an Extensive Aquifer," *Trans., AGU* (AUG. 1952) 559-569

Jaeger, J. C.: "Heat Flow in the Region Bounded Internally by a Circular Cylinder," *Proc. Roy. Soc. Edinburgh*, A, (1942) 61, 223.

Jaeger, J. C.: "Numerical Values for the Temperature in Radial Heat Flow," *J. Math. Phys.* (1955) 34.

Jaeger, J. C.: "Conduction of Heat in an Infinite Region Bounded Internally by a Circular Cylinder of a Perfect Conductor," *Aust. J. Phys.*, (1956) 9(2), 167.

Kohlhaas, C. A.: "A Method for Analyzing Pressures Measured During Drillstem-Test Flow Periods," *J. Pet. Tech.*, (Oct., 1972) 1278-1282, *Trans.. AIME*, 253

Matthews, C. S., and Russell, D. G.: *Pressure Buildup and Flow Tests in Wells*, Monograph Series, Society of Petroleum Engineers, Dallas (1967) 1.

Moore, T. V., Schilthuis, R. J. and Hurst, W.: "The Determination of Permeability from Field Data," *Proc.*, API Meeting, Tulsa, Okla. (May 17-19, 1933) 4.

Muskat, M.: "Use of Data on the Build-Up of Bottom-Hole Pressures," *Trans., AIME* (1937) 123, 44-48.

Odeh, A. S., and Selig, F.: "Pressure Buildup Analysis, Variable-Rate Case," *J. Pet. Tech.* (July, 1963) 790-794, *Trans., AIME*, 228.

Olson, C. C.: "Technical Advancement - Four Decades of DST," paper presented at the Eight Annual Logging Symposium of the SPWLA, Denver, Colorado (June 12-14, 1967).

Ramey, H. J., Jr.: "Short-Time Well Test Data Interpretation in the Presence of Skin and

Wellbore Storage," *J. Pet. Tech.* (Jan. 1970) 97-104

Ramey, H. J., Jr. and Agarwal, R.: "Annulus Unloading Rates as Influenced by Wellbore Storage and Skin Effect," *Soc. Pet. Eng. J.* (Oct. 1972) 453-462; *Trans.*, AIME, 253.

Ramey, H. J., Jr., Kumar, Anil, and Gulati, Mohinder S.: *Gus Well Test Analysis Under Water-Drive Conditions*, AGA, Arlington, Va. (1973).

Ramey, H. J., Jr., Agarwal, R. and Martin, I.: "Analysis of 'Slug Test' or DST Flow Period Data," *J. Cdn. Pet. Tech.* (July-Sept. 1975) 37-47.

Sageev, A.: "Slug Test Analysis," *Water Resour. Res.*, (1986)22(8), 1323-1333.

Saldana-C., M. A.: "Flow Phenomenon of Drill Stem Test With Inertial and Frictional Wellbore Storage Effects," Ph.D. Dissertation, Stanford University, 1983.

Soliman, M. Y.: "Analysis of Pressure Buildup Tests with Short Producing Time," paper presented at the SPE-AIME 57th Annual Fall Technical Conference and Exhibition, New Orleans, LA, (Sept. 26-29, 1982).

Stehfest, H.: "Numerical Inversion of Laplace Transforms", *Communications of the ACM* (Jan., 1970) Vol. 13, No. 1, 47-49.

Theis, C. V.: "The Relation Between the Lowering of the Piezometric Surface and the Rate and Duration of Discharge of a Well Using Ground-Water Storage," *Trans.*, AGU (1935)519-524.

Uraiet, A. A. and Raghavan, R.: "Pressure Buildup Analysis for a Well Produced at Constant Bottom-Hole Pressure," paper SPE 7984 presented at the SPE-AIME California Regional Meeting, Ventura, California, (April 18-20, 1979).

Van Everdingen, A. F. and Hurst, W.: "The Application of the Laplace Transformation to Flow Problems in Reservoirs," *Trans. AIME* (1949) Vol. 186, 305-324.

Van Everdingen, A. F.: "The Skin Effect and Its Influence on the Productive Capacity of a Well," *Trans. AIME* (1953) Vol. 198, 171-176.

APPENDIX A

FUNDAMENTAL SOLUTIONS OF THE DIFFUSIVITY EQUATION

Due to the linear character of the diffusivity equation, solutions to complex problems may be simplified when expressed as combinations of basic solutions. A review of some useful fundamental solutions of the diffusivity equation is presented in this section.

A.I. SPECIFIED SANDFACE FLOW RATE

Let us consider the case of radial flow with an arbitrarily specified sandface flow rate. For simplicity let the reservoir be considered to be **of** infinite extent in the radial direction. The partial differential equation with initial **and** outer boundary conditions are given by **Eqs.** (3.13), (3.14) and (3.15) in the main text.

Solution of this problem may be obtained by Laplace transformation. Taking the Laplace transform of the partial differential equation in dimensionless variables, **Eq.** (3.13), and using the initial condition, **Eq.** (3.14), we obtain:

$$\frac{d^2\bar{p}_D}{dr_D^2} + \frac{1}{r_D} \frac{d\bar{p}_D}{dr_D} = s \bar{p}_D, \quad (A.1)$$

where:

$\bar{p}_D(r_D, s)$ = Laplace-transformed dimensionless reservoir pressure

Equation (A.1) is the modified Bessel differential equation with the general solution:

$$\bar{p}_D(r_D, s) = A K_0(r_D \sqrt{s}) + B I_0(r_D \sqrt{s}), \quad (A.2)$$

where:

I_0 = modified Bessel function of 1st kind and zero order,

K_0 = modified Bessel function of 2nd kind and zero order,

and **A** and **B** are parameters to be determined. Laplace transforming the outer boundary

condition, Eq. (3.15), yields:

$$\lim_{r_D \rightarrow \infty} \bar{p}_D(r_D, s) = 0 . \quad (\text{A.3})$$

The function I_0 is unbounded as its argument approaches infinity. Hence inspection of Eq. (A.2) with respect to the constraint given by Eq. (A.3) yields, $B = 0$. Therefore Eq. (A.2) simplifies to:

$$\bar{p}_D(r_D, s) = A K_0(r_D \sqrt{s}) , \quad (\text{A.4})$$

which gives the Laplace-transformed solution to the diffusivity equation with an arbitrary inner boundary condition, considering radial flow and the infinite reservoir. Specification of the internal boundary condition provides means to determine the parameter A .

Taking the Laplace transform of the dimensionless sandface flow rate, Eq. (3.19), we obtain:

$$\bar{q}_{wD}(s) = - \left[r_D \frac{d\bar{p}_D}{dr_D} \right]_{r_D=1} . \quad (\text{A.5})$$

Observing the rule for derivatives of Bessel functions given in Abramovitz and Stegun (1972), from Eq. (A.4) it follows that:

$$\frac{d\bar{p}_D}{dr_D} = - A \sqrt{s} K_1(r_D \sqrt{s}) , \quad (\text{A.6})$$

where:

K_1 = modified Bessel function of 2nd kind and first order.

Substituting Eq. (A.6) into Eq. (A.5) and evaluating the result at $r_D = 1$, we obtain:

$$A = \frac{\bar{q}_{wD}(s)}{\sqrt{s} K_1(\sqrt{s})} . \quad (\text{A.7})$$

Now, substituting Eq. (A.7) into Eq. (A.4), it follows that:

$$\bar{p}_D(r_D, s) = \bar{q}_{wD}(s) \frac{K_0(r_D \sqrt{s})}{\sqrt{s} K_1(\sqrt{s})} . \quad (\text{A.8})$$

Defining:

$$\bar{g}_D(r_D, s) = \frac{K_0(r_D\sqrt{s})}{s\sqrt{s} K_1(\sqrt{s})}, \quad (A.9)$$

Eq. (A.8) may be written as:

$$\bar{p}_D(r_D, s) = s \bar{q}_{wD}(s) \bar{g}_D(r_D, s). \quad (A.10)$$

The function $\bar{g}_{wD}(S, s)$ given in Eq. (A.9) is the Laplace-transformed reservoir pressure response to a continuous unit production rate at the sandface. Carslaw and Jaeger (1959) present an expression for the real time inversion of Eq. (A.9) in terms of a Mellin integral. Using the fact that $g_D(r_D, 0) = 0$, the solution for the variable rate case may be obtained by means of the convolution property of Laplace transforms:

$$p_D(r_D, t_D) = q_{wD}(t_D) * \dot{g}_D(r_D, t_D), \quad (A.11)$$

where the notation, $*$, in Eq. (A.11) represents the convolution integral given by:

$$p_D(r_D, t_D) = \int_0^{t_D} q_{wD}(\tau_D) \dot{g}_D(r_D, t_D - \tau_D) d\tau_D, \quad (A.12)$$

and $\dot{g}_D(r_D, t_D)$ is the time derivative of the function $g_D(r_D, t_D)$.

The relationship given in Eq. (A.12) is known as the superposition theorem and is not restricted to radial flow nor to the infinite reservoir case. Table A.1 presents the Laplace-transformed reservoir pressure response to a unit sandface production rate for several systems. The wellbore pressure considering a *positive* skin effect may be found from the condition given by Eq. (3.20), yielding:

$$p_{wD}(t_D) = \int_0^{t_D} q_{wD}(\tau_D) \dot{g}_D(1, t_D - \tau_D) d\tau_D + S q_{wD}(t_D), \quad S > 0. \quad (A.13)$$

In Laplace space Eq. (A.13) becomes:

$$\bar{p}_{wD}(s) = s \bar{q}_{wD}(s) \bar{g}_{wD}(S, s), \quad (A.14)$$

where the function $\bar{g}_{wD}(S, s)$ is given by:

CONSTANT RATE AT THE SANDFACE	
TYPE OF SYSTEM	TRANSFORMED SOLUTION, $\bar{g}_D(r_D, s)$
Infinite Reservoir - Line Source Well	$\frac{K_0(r_D\sqrt{s})}{s}$
Infinite Reservoir - Cylindrical Source	$\frac{K_0(r_D\sqrt{s})}{s\sqrt{s} K_1(\sqrt{s})}$
No-Flow Outer Boundary	$\frac{1}{s\sqrt{s}} \frac{K_0(r_D\sqrt{s}) I_1(r_{eD}\sqrt{s}) + K_1(r_{eD}\sqrt{s}) I_0(r_D\sqrt{s})}{K_1(\sqrt{s}) I_1(r_{eD}\sqrt{s}) - K_1(r_{eD}\sqrt{s}) I_0(\sqrt{s})}$
Constant-Pressure Outer Boundary	$\frac{1}{s\sqrt{s}} \frac{K_0(r_D\sqrt{s}) I_0(r_{eD}\sqrt{s}) - K_0(r_{eD}\sqrt{s}) I_0(r_D\sqrt{s})}{K_1(\sqrt{s}) I_0(r_{eD}\sqrt{s}) + K_0(r_{eD}\sqrt{s}) I_1(\sqrt{s})}$

TABLE A.1 - Laplace Transformed Solutions for Radial Flow

$$\bar{g}_{wD}(S, s) = \bar{g}_D(1, s) + \frac{S}{s}, \quad S > 0. \quad (\text{A.15})$$

For a *negative* skin effect, Eq. (A.14) may be obtained by Laplace transforming Eq. (3.21) and setting:

$$\bar{g}_{wD}(S, s) = \bar{g}_D(e^{-S}, s), \quad S \leq 0. \quad (\text{A.16})$$

These relationships are general and may be used in connection with other reservoir models. However, they are restricted to non rate-dependent skin effect problems.

A.2. CONSTANT-RATE PRODUCTION WITH SKIN AND WELLBORE STORAGE

This problem considers constant-rate production at the wellhead, as introduced by van Everdingen and Hurst (1949). Both skin effect and wellbore storage are considered. A review of the literature on similar heat conduction problems was presented by Agarwal *et al* (1970).

The inner boundary condition may be determined by performing a material balance on the wellbore, yielding:

$$C_D \frac{dp_{wD}}{dt_D} + q_{wD}(t_D) = q_D, \quad (\text{A.17})$$

where the *constant* dimensionless wellhead flow rate q_D is defined as:

$$q_D = \frac{q \mu}{2 \pi k h (p_i - p_0)}. \quad (\text{A.18})$$

The reason for the introduction of a dimensionless wellhead flow rate is because the dimensionless pressure definitions used in this work are different from the definitions for the dimensionless pressure used in constant rate problems. However, final solutions are independent of the choices for the dimensionless variables.

For this problem the initial wellbore pressure is assumed to be:

$$p_{wD}(0) = 0, \quad (\text{A.19})$$

which makes the choice for p_0 in Eq. (A.18) to be arbitrary. The Laplace transform of the internal boundary condition, Eq. (A.17), yields:

$$C_D [s \bar{p}_{wD}(s) - p_{wD}(0)] + \bar{q}_{wD} = \frac{q_D}{s}. \quad (\text{A.20})$$

Substitution of Eqs. (A.14) and (A.19) into Eq. (A.20) and solution for $\bar{p}_{wD}(s)$ gives:

$$\bar{p}_{wD}(s) = \frac{q_D}{s \left[s C_D + \frac{1}{s \bar{g}_{wD}(S, s)} \right]}. \quad (\text{A.21})$$

$$\bar{g}_{wD}(S, C_D, s) = \frac{1}{s \left[s C_D + \frac{1}{s \bar{g}_{wD}(S, s)} \right]}, \quad (\text{A.22})$$

Eq. (A.21) reduces to:

$$\bar{p}_{wD}(s) = q_D \bar{g}_{wD}(S, C_D, s). \quad (\text{A.23})$$

Eq. (A.22) describes the Laplace-transformed wellbore pressure response due to production with a unit dimensionless surface flow rate, including both skin effect and wellbore storage. Solution in real time space may be obtained by inverting Eq. (A.23), which may be expressed as:

$$\frac{p_{wD}(t_D)}{q_D} = \frac{2 \pi k h}{q \mu} [p_i - p_w(t)] = g_{wD}(S, C_D, t_D). \quad (\text{A.24})$$

The function $g_{wD}(S, C_D, t_D)$ has been computed by Agarwal *et al* (1970) and presented both in the form of tables and graphically as families of **type** curves. Fig. A.1 presents the solution to this problem as computed from Eq. (A.22) by means of the Stehfest (1970) algorithm. This form of the type curves was first presented by Gringarten *et al* (1979). Solutions for other flow models, such as linear or spherical flow patterns, may be obtained similarly, if the function $\bar{g}_{wD}(S, s)$ is chosen properly.

This solution deserves some comment. At early time the wellbore pressure response is primarily affected by wellbore storage, and the following approximation holds:

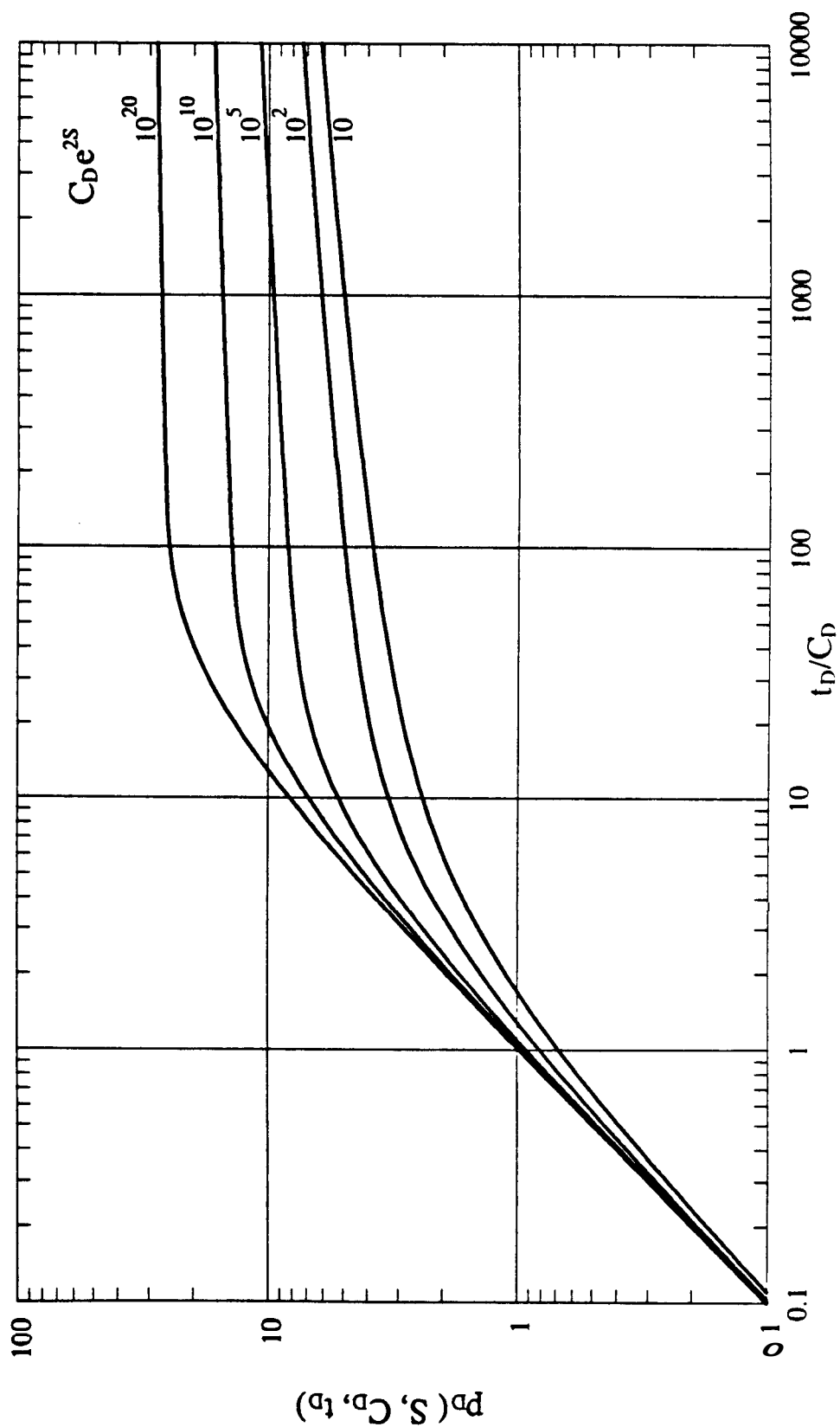


Figure A.1 Constant-Rate Drawdown Type Curve

$$\frac{p_{WD}(t_D)}{q_D} = \frac{t_D}{C_D}, \quad (A.25)$$

which describes the equation for the unit slope log-log straight line. As time increases, the solution departs **from** the log-log straight line. At late time the radial flow solution may be correlated with the semi-log approximation, which is given by:

$$\frac{p_{WD}(t_D)}{q_D} = g_{WD}(S, C_D, t_D) = \frac{1}{2} \ln \left[\frac{4 t_D}{\gamma} \right] + S, \quad (A.26)$$

where $\gamma = 1.781\dots$ is the exponential of Euler's constant.

For intermediate times, there is no simple analytical expression to represent the wellbore pressure response. Furthermore, as reviewed by Agarwal *et al* (1970), asymptotic short-time forms for positive and zero skin effects are differ from each other, although the Laplace solution forms do not. The zero skin solution may also describe the wellbore pressure for stimulated wells (negative skin effect), provided the concept of effective wellbore radius applies.

A.3. SLUG TEST SOLUTION

The "slug test" was defined by Ferris and Knowles (1954); it consists of an instantaneous withdrawal or injection of a "slug" of fluid from/into a well. The "slug test" has become popular in ground water testing because of **the** ease of testing and short duration of the test.

The flowing period of a drill stem test performed in liquid producing wells may also be described by the slug test conditions. The reservoir equation with the initial and outer boundary conditions are represented by Eqs. (3.13), (3.14) and (3.15) in the main text. The initial condition and wellbore equation are described by Eqs. (3.16) and (3.17).

Taking the Laplace transform of the wellbore condition, Eq. (3.17), and using the initial condition, Eq. (3.16), we obtain:

$$C_D s \bar{p}_{WD}(s) + \bar{q}_{WD}(s) = 0. \quad (A.27)$$

Substitution of Eq. (A.14) into Eq. (A.27) and solving for $p_{WD}(s)$ yields:

$$\bar{p}_{wD}(s) = \frac{C_D}{s C_D + \frac{1}{s \bar{g}_{wD}(S, s)}} \quad (A.28)$$

As discussed by Agarwal and Ramey (1972), Eq. (A.28) may be written in terms of the constant-rate solution, Eq. (A.23), resulting in:

$$\bar{p}_{wD}(s) = C_D s \bar{g}_{wD}(S, C_D, s), \quad (A.29)$$

which may be inverted to real time space to yield:

$$p_{wD}(t_D) = C_D g'_{wD}(S, C_D, t_D), \quad (A.30)$$

where $g'_{wD}(S, C_D, t_D)$ represents the time derivative of $g_{wD}(S, C_D, t_D)$.

Although Agarwal and Ramey (1972) evaluated the Mellin inversion integral, the Stehfest (1970) algorithm has also been used here to evaluate the "slug test" solution, Eq. (A.30), and the results for the zero skin case are presented in Figure A.2. Evaluation of Mellin inversion integrals is often difficult. Jaeger (1942) frequently qualified his tabulated results with a comment that calculations were carried out to five places and it was hoped that results were good to four places. It is significant that the Agarwal and Ramey (1972) Mellin integral values and the results from the Stehfest inversion agree almost exactly. This sort of agreement was not often obtained by various groups using Mellin integral evaluation only. Use of the Stehfest algorithm has provided an alternate method to check previous Mellin integral evaluations, and has greatly aided the use of Laplace transformation in solving modern problems.

Jaeger (1956) discussed the case of an equivalent heat transfer problem and showed that the early time approximations obtained from Eq. (A.30) differ for the zero and finite skin effect cases. According to Jaeger (1956), these short-time limiting forms are:

$$1 - p_{wD}(t_D) = \frac{t_D}{C_D S}, \quad S > 0, \quad (A.31)$$

and:

$$1 - p_{wD}(t_D) = \frac{2}{C_D} \sqrt{\frac{t_D}{\pi}} + \frac{t_D}{C_D}, \quad S = 0. \quad (A.32)$$

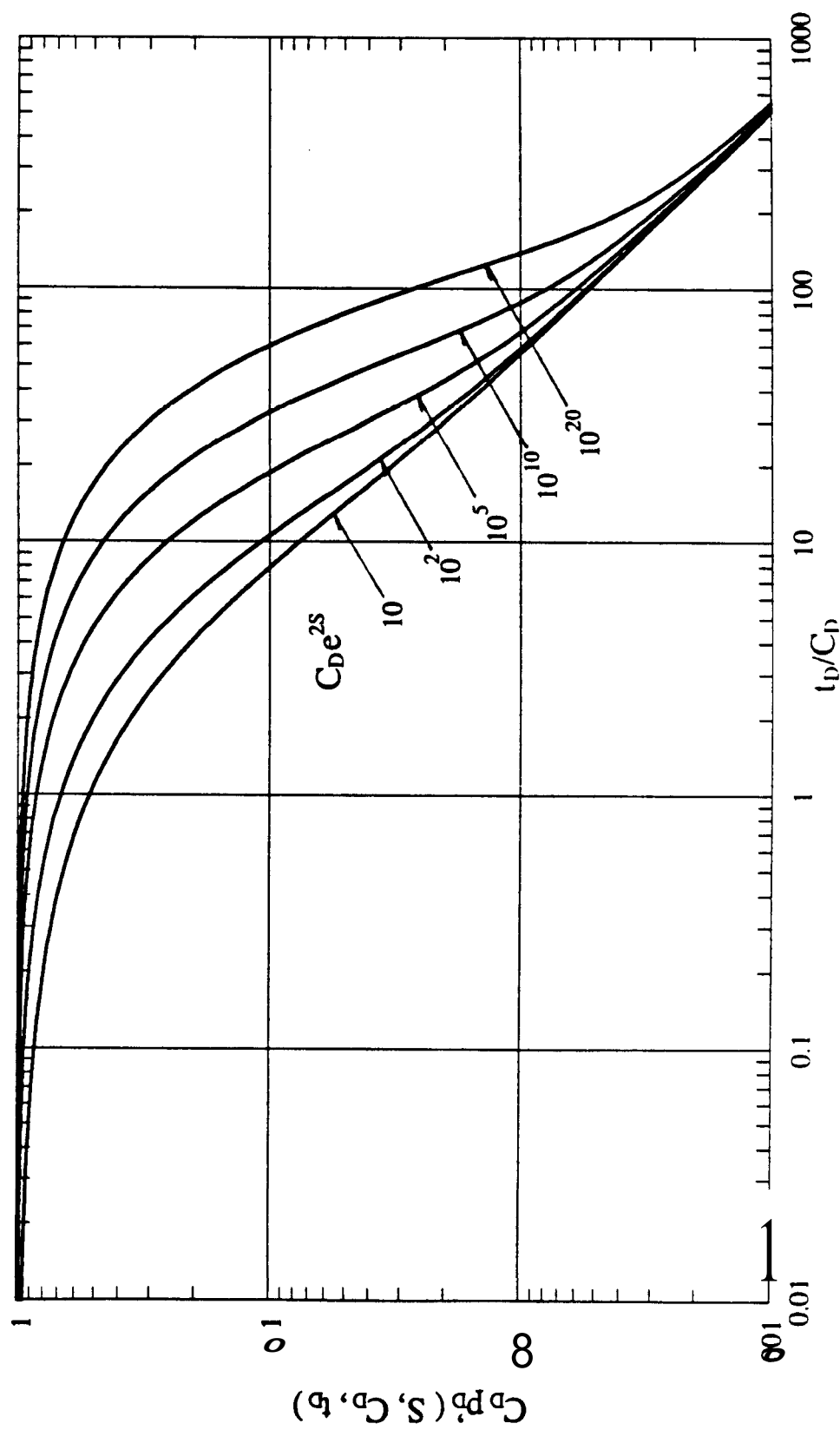


Figure A.2 "Slug Test" Type Curve

These relationships are useful for analyzing pressure data obtained from the production period of a drill stem test.

An analytical expression for the wellbore pressure at late time may be obtained for the "slug test" problem by using the logarithmic approximation, Eq. (A.26). Differentiation of Eq. (A.26) with respect to time and substitution into Eq. (A.30), yields the following late time approximation for the "slug test":

$$p_{wD}(t_D) = \frac{C_D}{2 t_D} . \quad (A.33)$$

APPENDIX B

COMPUTER PROGRAM

```
C
C This program calculates the DST wellbore pressure for
C the pressure buildup period.
C
IMPLICIT REAL*8 (A-H,O-Z)
DIMENSION TD(50),PWD(50)
READ(5,*) S
READ(5,*) CFD
READ(5,*) CSD
READ(5,*) TPD
C
C Compute the dimensionless average flow rate
C
pwDk = PDPRIME ( tpD , CFD, S )
qwDstar = CFD * ( 1.0 - pwDk ) / tpD
C
C Compute the equivalent time
C
qwDtPd = RATESL ( tpD, CFD, S )
tpDtStar = qwDstar * tpD / qwDtPd
C
CTR = 0.0
WRITE(6,*)
DO 50 I = 1, 49
  CTR = CTR + 0.02
  TD(I) = TPD/CTR
  DTD = TD(I) * TPD
C
C Compute the Cartesian graph
C
PWD(I) = PDST(DTD,TPD,CFD,CSD,S)
write(7,101) CTR, PWD(I)
C
C Compute the Generalized Horner graph
C
HTR = TD(I) / DTD
PDH = PWD(I) / qwDtPd
write(8,101) HTR, PDH
C
C Compute the Generalized Modified Horner graph
C
HTRM = ( tpDtStar + DTD ) / DTD
PDHM = PWD(I) / qwDtPd
write(9,101) HTRM, PDHM
      WRITE(6,102) TD(I),DTD,PWD(I),HTR,PDH,HTRM,PDHM
50 CONTINUE
101 FORMAT(2x,F10.4,2x,f10.6)
102 FORMAT(2x,f8.0,2x,f8.0,2x,f8.4,2(2x,f8.2,2x,f8.4))
      STOP
      END

REAL*8 FUNCTION PDST(DTD,TPD,CFD,CSD,S)
IMPLICIT REAL*8 (A-H,O-Z)
```

```
COMMON/FPRD/DTDC,TPDC,CFDC,CSDC,SC
EXTERNAL FPROD
IF (DTD .EQ. 0.0) THEN
    PWDCP = 1.0
    RETURN
ENDIF
DTDC = DTD
TPDC = TPD
CFDC = CFD
CSDC = CSD
SC = S
C
C   NUMERICAL INTEGRATION OF THE CONVOLUTION TERM
C   USING AN ADPTIVE QUADRATURE BASED ON A 9-POINT NEWTON-COTES
C   RULE (ROUTINE QUANC8)
C
C
RELERR = 0.0D0
ABSERR = 1.0D-8
TUP = TPDC
CALL QUANC8(FPROD,0.0,TUP,ABSERR,RELERR,RESULT,ERREST,NOFUN,F4)
C
IDBUG = 0
IF (IDBUG .NE. 0) THEN
    WRITE(6,1003) RESULT
    WRITE(6,1004) ERREST
    WRITE(6,1006) NOFUN
ENDIF
IF (FLAG .NE. 0.0D0) WRITE(6,1005) FLAG
1003 FORMAT(/5x,'RESULT = ',F14.10)
1004 FORMAT(5x,'ERROR ESTIMATE FROM QUANC8 = ',E13.6)
1005 FORMAT(44H WARNING..RESULT MAY BE UNRELIABLE. FLAG = ,F6.2)
1006 FORMAT(4x,40H NUMBER OF FUNCTION EVALUATIONS NOFUN =,I6/)
C
PDST = CSD * PDPRIME(TPD+DTD,CSD,S) + (1.0D0-CSD/CFD) * RESULT
C
RETURN
END

REAL*8 FUNCTION FPROD(TAUD)
IMPLICIT REAL*8 (A-H,O-Z)
COMMON/FPRD/DTD,TPD,CFD,CSD,S
TD = TPD + DTD
FPROD = PDPRIME(TAUD,CSD,S) * RATESL(TD-TAUD,CFD,S)
RETURN
END

REAL*8 FUNCTION PDPRIME(TD,CD,S)
IMPLICIT REAL*8 (A-H,M,O-Z)
DIMENSION V(20)
N = 16
IF (ICALL .NE. 1) THEN
    CALL COEFF(N,V)
ELSE
```

```
ICALL = 1
ENDIF
IF (TD .EQ. 0.0) THEN
  PDPRIME = 1.0D0/CD
  RETURN
ENDIF
DLOGTW = 0.6931471805599453
  SUM = 0.0D0
    ARG = DLOGTW / TD
  DO 20 J = 1, N
    Z = J * ARG
    X = DSQRT(Z)
    IF (X .LE. 85.D0) THEN
      BK0 = MMBSK0(1,X,ierr)
      BK1 = MMBSK1(1,X,ierr)
    ELSE
      BK0 = MMBSK0(2,X,ierr)
      BK1 = MMBSK1(2,X,ierr)
    ENDIF
    FUNC = BK0/BK1/X + S
    PLAP = 1.0D0/(Z*CD + 1.0D0/FUNC)
20  SUM = SUM + V(J) * PLAP
  PDPRIME = SUM * ARG
  RETURN
END

REAL*8 FUNCTION RATESL(TD,CD,S)
C
C This function computes the dimensionless sandface flow rate
C during a slug test.
C
IMPLICIT REAL*8 (A-H,M,O-Z)
DIMENSION V(20)
N = 16
IF (ICALL .NE. 1) THEN
  CALL COEFF(N,V)
ELSE
  ICALL = 1
ENDIF
DLOGTW = 0.6931471805599453
  SUM = 0.0D0
    ARG = DLOGTW / TD
  DO 20 J = 1, N
    Z = J * ARG
    X = DSQRT(Z)
    IF (X .LE. 85.D0) THEN
      BK0 = MMBSK0(1,X,ierr)
      BK1 = MMBSK1(1,X,ierr)
    ELSE
      BK0 = MMBSK0(2,X,ierr)
      BK1 = MMBSK1(2,X,ierr)
    ENDIF
    FUNC = BK0/BK1/X + S
    QWDLAP = 1.0D0/(Z*FUNC+1.0/CD)
```

```
20  SUM = SUM + V(J) * QWDLAF
    RATESL = SUM * ARG
    RETURN
    END

SUBROUTINE COEFF(N,V)
IMPLICIT REAL*8 (A-H,O-Z)
DIMENSION H(10),G(20),V(20)
C   CALCULATE V-ARRAY
M = N
G(1) = 1.
NH = N/2
DO 5 I = 2, N
5 G(I) = G(I-1)*I
H(1) = 2./G(NH-1)
DO 10 I = 2, NH
FI = I
IF (I .EQ. NH) GO TO 8
H(I) = FI**NH * G(2*I)/(G(NH-I) * G(I) * G(I-1))
GO TO 10
8 H(I) = FI**NH * G(2*I)/(G(I) * G(I-1))
10 CONTINUE
SN = 2 * (NH - NH/2*2) + 1
DO 50 I = 1, N
V(I) = 0.D0
K1 = (I+1)/2
K2 = I
IF (K2 .GT. NH) K2 = NH
DO 40 K = K1, K2
    IF (2*K-I .EQ. 0) GO TO 37
    IF (I .EQ. K) GO TO 38
    V(I) = V(I) + H(K)/(G(I-K) * G(2*K-I))
    GO TO 40
37    V(I) = V(I) + H(K)/G(I-K)
    GO TO 40
38    V(I) = V(I) + H(K)/G(2*K-I)
40    CONTINUE
    V(I) = SN * V(I)
    SN = -SN
50 CONTINUE
100 CONTINUE
    RETURN
    END
```